Interference management in cooperative multi-cell networks

Le, Tuan

Awarding institution:
King's College London

INTERFERENCE MANAGEMENT IN COOPERATIVE MULTI-CELL NETWORKS

Tuan Anh Le

Institute of Telecommunications
School of Natural & Mathematical Sciences

King's College London

Submitted to the King's College London
for the degree of Doctor of Philosophy

September 2012

To my loving parents, my beloved wife and my daughter.

Acknowledgements

This thesis would not have been possible without the guidance and the help of several individuals who in one way or another contributed and extended their valuable assistance in the preparation and completion of this study.

Foremost, I would like to express my sincere gratitude to my supervisor Dr. Mohammad Reza Nakhai for the continuous support during my Ph.D study, for his patience, motivation, enthusiasm, and immense knowledge. His guidance helped me in all the time of research and writing of this thesis. I could not have imagined having a better advisor and mentor for my Ph.D study.

I wish to thank Professor Hamid Aghvami for providing a stimulating research environment in CTR. I also wish to thank Dr. Oliver Holland and Dr. Vasilis Friderikos for the encouragement and support they provided during my study at King's. I am especially grateful to my colleagues at CTR, including Nur, Auon, Aimal, Vahid, Azar, Saba, Laura, Adnan, Diogo, Panayiotis, Mati, Alexandre, Mojdeh, Ana and many others, who gave me hours of enjoyable company.

I owe my deepest gratitude to Dr. Truong Trong Nguyen, Dr. Ashley Mill, Mr. Dang Xuan Do, Mr. Nghia Manh Nguyen, Mr. Dzung Manh Nguyen, Mr. Walter Lowe, and Mrs. Jennifer Potter. Without their support, I could not have been completed my research. I would like to thank Mr. Neil Bridger and Ms. Azar Zarrebini-Eshahani for their valuable suggestions to improve the presentation of this thesis.

I wish to thank my parents for educating me with good moral, for unconditional support and encouragement to pursue my interest. I am grateful to my beloved wife, Hien Thi Thu Nguyen, for her love, support and being wonderful mother to our daughter, Linh Khanh Le. To them I dedicate this thesis.

Last but not least, I would like to acknowledge the financial support of the UK's Virtual Center of Excellence in Mobile and Personal Communications

(Mobile VCE) and the UK Government's Engineering & Physical Sciences Research Council (EPSRC).

Abstract

In multi-cell networks where resources are aggressively reused, eliminating interference is the key factor to reduce the system energy consumption. This thesis proposes interference management techniques based on beamforming with different levels of cooperation amongst base stations (BSs). First, a multi-cell beamforming (MBF) technique is introduced to design beamformers as if geographically distributed BSs were a single BS. The aim is to minimise the total transmit power across the network while maintaining the required signal-to-interference-plus-noise ratio (SINR) for every user. An iterative algorithm is proposed to solve the optimisation problem of MBF. Since the MBF scheme requires the circulation of all users' data amongst coordinating BSs, a user position aware (UPA) algorithm is developed for MBF to reduce the backhaul overhead by allocating each user to nearby BSs only. To completely avoid user data circulation, a semi definite programming (SDP) algorithm, named as coordinated beamforming (CBF), is introduced to jointly calculate beamformers for all coordinating BSs in a manner that each BS transmits to its local users only. Taking into account errors in channel estimations, robust beamforming designs are developed for CBF. Next, fast wireless backhaul protocols, i.e., Star and Ring, are proposed using network coding to enable links amongst coordinating BSs. The maximum achievable throughput of each protocol is analysed. The power consumption of the Ring protocol is characterised and used to compare and evaluate the performance of the proposed beamforming schemes. The deployments of MBF, UPA-MBF and CBF schemes require a central unit for a group of coordinating BSs as well as backhaul links amongst them. In fact, a central unit may not always be available, e.g., in femtocell and self-organising networks, while backhaul links may be limited. Hence, distributed beamforming (DBF) is proposed to independently design beamformers for the local users of each BS. In DBF, the combination of each BS's total transmit power and its resulting interference power toward other BSs' users is minimised while the required SINRs for

its local users are maintained. SDP and iterative algorithms are introduced to solve the optimisation problem of DBF.

Abbreviations

AoD	angle of departure
BS	base station
CBF	coordinated beamforming
CSI	channel state information
CSIT	channel state information at transmitter
DAS	distributed antenna system
DBF	decentralised beamforming
DDA	distributed-array antenna
FDD	frequency division duplexing
ICI	inter-cell interference
IMT	international mobile telecommunications
KKT	Karush-Kuhn-Tucker
LMI	linear matrix inequality
LTE	long term evolution
MAC	multiple access channel
MS	mobile station
MBF	multi-cell beamforming
MCP	multi-cell proccessing
MIMO	multiple input multiple output
MISO	multiple input single output
MMSE	minimum mean squared error
NC	network coding
QoS	quality of service
RS	relay station
SDP	semidefinite programming
SDR	semidefinite relaxation
SINR	signal-to-interference-plus-noise ratio
SNR	signal-to-noise ratio

SOC	second order cone
SOCP	second order cone programming
TDD	time division duplexing
UPA	user position aware
UHF	ultra high frequency
ZF	zero forcing
ZMCSCG	zero mean circularly symmetric complex Gaussian

Symbols

a	scaler a
$\mathbf{a}$	vector $\mathbf{a}$
$\mathbf{A}$	matrix $\mathbf{A}$
$\|a\|$	magnitude of a
$\Re\{a\}, \Im\{a\}$	real and imaginary parts of a, respectively
$\|\mathbf{a}\|$	Euclidean norm of $\mathbf{a}$
$\|\mathbf{A}\|_F$	Frobenius norm of $\mathbf{A}$
$\mathbf{A}^*$	complex conjugate of $\mathbf{A}$
$\mathbf{A}^T$	transpose of $\mathbf{A}$
$\mathbf{A}^H$	complex conjugate transpose of $\mathbf{A}$
$[\mathbf{A}]_{i,j}$	(i,j)th entry of $\mathbf{A}$
$\mathrm{Tr}\,(\mathbf{A})$	trace of $\mathbf{A}$
$\mathrm{vec}\,(\mathbf{A})$	stacks $\mathbf{A}$ into a vector columnwise[1]
$\mathbb{E}\,(\cdot)$	expectation operator
$\mathbf{A} \succeq 0$	$\mathbf{A}$ is a positive semidefinite matrix
$\mathbf{A} \succeq \mathbf{B}$	$\mathbf{A} - \mathbf{B}$ is a positive semidefinite matrix
$\mathbf{a} \succ 0$	all elements of $\mathbf{a}$ are positive
$\mathbf{a} \succeq 0$	all elements of $\mathbf{a}$ are nonnegative
$\mathbf{a} \succ \mathbf{b}$	element-wise greater than
$\mathbf{a} \succeq \mathbf{b}$	element-wise greater than or equal to
$\begin{bmatrix} a \\ \mathbf{a} \end{bmatrix} \succeq_K 0$	$a \geq \|\mathbf{a}\|$
$\mathbf{I}$	identity matrix with a suitable size
$\mathbf{e}_i$	column unit vector with a suitable size which contains all zeros except a one at the ith element
$\approx$	approximately equal to

[1] If $\mathbf{A} = \begin{bmatrix} \mathbf{a}_1 & \mathbf{a}_2 & \cdots & \mathbf{a}_n \end{bmatrix}$ is $m \times n$, then $\mathrm{vec}\,(\mathbf{A}) = \begin{bmatrix} \mathbf{a}_1^T & \mathbf{a}_2^T & \cdots & \mathbf{a}_n^T \end{bmatrix}^T$ is $mn \times 1$.

$\oplus$	bitwise XOR
$[a]^+$	$\max(0, a)$

Contents

List of Figures

Chapter 1

Introduction

1.1 Motivation

Increasing fuel prices and predicted long-term resource scarcity have brought the field of green communications to the forefront in recent times. Rigorous efforts are being made to cut down power consumption, particularly in wireless communications, whilst at the same time maintaining an acceptable quality of service. It is believed that more than 75% of total energy consumption in cellular networks are dissipated on radio parts, i.e. base stations (BSs) [1]. In particular, cooling systems alone comsume 40% to 60% of the BS's energy consumption[1]. Recent analysis by network operators and manufacturers has indicated that current wireless networks are not very energy efficient, particularly the BSs by which user terminals access service from the network [2]. Reducing transmit power at BSs will lead to substantial energy savings for the entire network.

Applications of mobile internet in different areas such as education, health care, smart grids and security have been growing very fast. As a result of increasing dependency on these applications in our day to day activities, demand for a significant increase in user data rate per area and the spectral efficiency are inevitable over the next 10 years. On the other hand, delivering higher data rate per area requires more transmission power which is constrained not only by the safety limits but also by the importance of global warming issues and the need for greener communications. Therefore, high speed transmission would mean diminishing coverage range, as otherwise, an enormous increase of transmission power is required by both mobile terminals and base stations to maintain the current cell size and achieve the ambitious targets of the beyond IMT-advanced technologies.

[1]Source: Vodafone Group R&D, 2009.

Cell splitting, i.e., dividing large cells into a number of smaller cells, is a promising method that can significantly increase both capacity and coverage of the future cellular networks. Due to the scarcity of bandwidth resources, the divided cells would have to operate with full spectrum reuse across all base stations. As a result, cochannel interference becomes one of the major issues in cell splitting.

Cochannel interference has been identified as one of the major impairments that degrades the performance of wireless systems [3–5]. Cochannel interference is caused by simultaneous transmission of data to proximal users assigned the same frequency-time resources. The presence of interference forces BSs to increase their transmit power if certain quality of service for their user terminals is to be maintained. Therefore, mitigating cochannel interference is a key factor leading to the reduction of BSs' transmit power. Interference management techniques used in practice may be classified by the interference strength as follows [6]:

- **Consider as noise:** when interference is weak, the interfering signal is treated as noise and single user encoding/decoding is adequate.
- **Decode:** when the interference is strong, the interfering signal can be decoded along with the desired signal. This approach is less common in practice due to the complexity of multi-user detection.
- **Orthogonalise**: Interference is mitigated by orthogonalising the channel access if the strength of interference is comparable to the desired signal. This concept, also known as cake-cutting fashion, is used in time and frequency division medium access methods.

Scarcity of resources and increasing demands in user data rates compel the next generation wireless networks to use the same channels, i.e., the same time and frequency resources, in all cells for supporting users. Thus, interference in the future system are expected to be stronger than that in the current cellular system. The first interference management technique is not applicable for such systems while the second technique may not be affordable due to its complexity drawback. The third technique is not suitable for such aggressive-resource-reused system neither. Hence finding new interference management techniques is an open problem to be researched.

In wireless communications, transmit beamforming can be used to improve the system performance and to manage interference. Transmit beamforming is a technique using at least two antennas to transmit a radio frequency signal. The phases of the transmissions across these antennas are controlled such that useful signals are constructively added up at a given desired receiver while interfering signals are eliminated

at unintended user terminals. Given a fixed transmit power at each antenna element, an ideal transmit beamforming with M antenna elements yields a M^2-fold gain in received power compared to a single-antenna transmission [7]. Therefore in a power-limited regime, transmit beamforming with M antenna elements results in a M-fold increase in rate, a M-fold increase in free space propagation range or a M-fold decrease in the net transmitted power.

Given the channel state information of a set of active user terminals, the task of a beamforming designer is to calculate beamforming vectors, known as beamformers, for the user terminals under a certain system requirement. It must be noted that channel state information is assumed to be available to the beamforming designer. Channel estimation techniques can be found in [8–14] and references therein. The system requirement in transmit beamforming usually defines an optimisation problem. The following complementary optimisation problems are commonly considered in literature. The first of these subject to a power constraint aims to maximise the minimal signal-to-interference-plus-noise ratio (SINR), e.g., [15–17]. The second problem minimises the total average transmit power subject to SINR constraint as described in [3, 18–21]. It is impossible to minimise the power while maximising the SINRs or vice versa due to average power metric and SINR metric conflict [22].

Recently, the idea of multi-cell processing (MCP) in cellular networks has been recognised as an effective technique to overcome inter-cell interference and substantially improve the capacity [23–29]. In MCP, a coordinated virtual architecture is mapped over a cellular infrastructure such that the individual mobile user is collaboratively served by its surrounding base stations rather than only by its designated base station. In this architecture, base stations are equipped with multiple antennas but user terminals can have either single or multiple antennas. Using coordinated scheduling alone or incorporation with beamforming amongst a number of local base stations enables the network to constructively overlay the desired signals at an intended user and eliminate or sufficiently mitigate them at the other unintended users. Ideally, in this way, each user within a cell feels free of inter-cell interference and, hence, can potentially achieve the highest capacity with the lowest energy consumption under the reuse one regime, i.e., while all the available spectrum is fully reused within the adjacent cells. Theoretically, MCP can overcome inter-cell interference and, hence, provides the ground for achieving a high throughput at a low energy cost. However, there are still many problems transferring the theory to practical implementation.

This thesis focuses on reduction in energy consumption of the cellular network by proposing interference management techniques based on beamforming. The objective

is to minimise the total transmit power of coordinating BSs while assuring required quality of service, i.e. signal-to-interference-plus-noise ratio, for all user terminals in the network. Additionally, the following problems are investigated and addressed:

- Backhaul and extra signal processing load are inevitable due to the nature of MCP. Hence there is a need for research on flexible system designs that allow the use of signal processing algorithms with various levels of complexity according to defined circumstances. For instance, users within a cluster of coordinating BSs can be served by full or partial coordination amongst BSs or even with no coordination in relation to their locations. Information sharing via backhaul links among the BSs can either be limited to the channel state information or include users' data. In the former, as a result of coordinating beamforming and scheduling, each BS sends data to its local users, while in the latter, data transmission jointly takes place by the coordinating BSs towards a single user.

- With an ideal backhaul assumption, i.e., unlimited capacity, low latency, error-free and no power consumption, MCP is superior over single-cell processing in terms of throughput and spectral efficiency, e.g., [30]. However, in practical scenarios the assumption of ideal backhaul is not realistic and the effects of the backhaul on the performance of a MCP network should be taken into consideration. Establishing and maintaining a fast wireless backhaul, inter-connecting the coordinating BSs in MCP, is a challenging issue.

- A possible implementation of MCP, which requires minor changes in the current system, is conditional upon a centralised manner where all coordinating BSs are connected to a central processing unit, i.e. a base station controller, and all signal processing tasks are carried out by the central processing unit. The drawback with this implementation lies in the fact that a single point of failure can severely affect the system performance. Therefore, distributed MPC algorithms, where individual BS can independently perform signal processing tasks using locally attained information or with limited exchange of information between BSs, are currently of interest to researchers.

1.2 Thesis overview

This thesis comprises 7 chapters. A brief account of each chapter is given below.

Chapter 1 includes the motivation, overview and states the contributions of the thesis.

Chapter 2 describes an overview of two standard conic programs, i.e. second order cone programming (SOCP) and semidefinite programming (SDP). A linear array antenna used in beamforming is presented followed by the introduction of an optimisation problem of single-cell multiuser beamforming. Algorithms that solve the optimisation problem using SOCP and SDP are recalled. Furthermore, the uplink-downlink duality and the Lagrangian duality are unified using the duality theory in convex optimisation. The presented concepts are used to develop beamforming schemes for a multi-cell scenario discussed in Chapters 3, 4 and 6.

In Chapter 3, a cluster-based multi-cell processing strategy is developed to both tackle inter-cell interference problem and improve energy efficiency in cellular wireless networks. In the proposed strategy, which herein after is referred to as multi-cell beamforming (MBF), user data is globally shared by all coordinating BSs for joint transmission to every user, while the designing unit possesses full global channel state information of all users. The objective of the MBF scheme is to design a set of beamformers for a number of simultaneously active users such that the total transmit power across the cluster of coordinating BSs is minimised, while the required SINR is maintained for each user. Using the duality theory, an iterative MBF algorithm is proposed to solve the optimisation problem. In order to reduce backhaul burnden imposed by the MBF strategy, a user-position-aware algorithm is introduced to circulate the data of each user amongst the most beneficial BSs based on information of the user location.

In Chapter 4, user data is not shared amongst the coordinating BSs. However, full global channel state information of all users is still required at the designing unit. In this case, each user terminal is only served by its local BS and a number of BSs coordinate at beamforming level to minimise their mutual inter-cell interferences. The strategy is known as coordinated beamforming (CBF). The objective of the CBF scheme is also to minimise the total transmit power across coordinating BSs subject to user SINR constraints. The CBF algorithms for finding beamforming vectors are developed based on standard semidefinite programming formulation using instantaneous and second-order-statistical channel state information. A robust CBF algorithm is also introduced for imperfect channel information.

Chapter 5 discusses backhaul issue. Using network coding concept, Ring and Star protocols are proposed, respectively, for a cluster of inter-connected three BSs and a cluster of a controlling BS and three fixed relay stations. These protocols can be used either individually or in an overlaid fashion in a coordinated multi-cell system or in a cellular-distributed-antenna system to exchange information in the backhaul. Upper bounds on the achievable throughput of the proposed protocols are derived. Based

on the proposed Ring protocol for the wireless backhaul, a framework is introduced to evaluate the overall performance of the proposed MBF and CBF schemes, i.e., including the effects of backhaul on latency and power consumption.

In Chapter 6, inter-cell interferences are tackled under a limited cooperation amongst BSs. A decentralised beamforming (DBF) is introduced where individual BSs independently design their own beamforming vectors using locally attainable channel state information at each BS. In this scheme, while each BS minimises a combination of its total transmit power and the resulting total interference on the other vulnerable users of the adjacent cells, it also ensures that certain targeted SINR levels are achieved at its local users. In order to extend the SINR range in a power-efficient way, two pricing strategies are developed to assign the interference pricing factors for the objective function of the proposed optimisation problem. A fast-converging iterative algorithm is developed using second-order-statistical channel state information.

The closing Chapter 7 deals with conclusions and future work.

1.3 Contributions

By addressing the problems mentioned in Section 1.1, following contributions are made in this thesis:

1. Chapter 3 considers a network of coordinating BSs where each BS is equipped with multiple antennas. The antenna arrays of those BSs form a distributed-array antenna (DAA). A new multi-cell beamforming (MBF) technique for the DAA is developed by introducing a channel model between the DAA and a user that includes an angular spread due to the existence of local scatterers surrounding that user. A spatial covariance matrix for the resulting DAA channel model is derived. The channel model developed in this chapter is a generalised version of the channel model given in [31]. The model is able to capture the effects of local scatterers and shadow fading. A user position aware algorithm that only allocates users to nearby BSs, thus reduces data circulation on backhaul, is also developed. Additionally, an iterative algorithm that solves the optimisation problem of minimising the total transmit power subject to users' SINR constraints is proposed. Despite using uplink-downlink duality via Lagrangian theory like papers [22] and [32], the algorithm developed in this chapter differs in the following facts: (a) The iterative algorithm is based on second-order statistical CSI. (b) The uplink-beamforming vectors are calculated using the dominant eigenvector method. These contributions are published in [31], [33], [34] and [35].

2. The iterative-Lagrangian-based algorithm proposed in [32] solves the optimisation problem for CBF with instantaneous CSI. This is referred to as iCBF in this thesis. The downlink beamforming vectors of the iCBF are found as the multiplication of some scalars by the corresponding virtual uplink beamforming vectors which, in turn, are found by the MMSE solution, i.e., [32]. Limitation of the dual uplink solution to MMSE can be interpreted as an additional constraint to the original optimisation problem. The added constraint degrades the system performance as the feasibility region of the equivalent problem is smaller than the feasibility region of the original problem. In Chapter 4, the optimisation problem for CBF is formulated in the SDP form to avoid the problem of narrowing down the original feasibility region imposed by iCBF. Moreover, casting the problem in the SDP form is independent of the uplink and downlink duality. The proposed scheme uses instantaneous CSI which requires frequent signaling between users and their serving BSs. According to [36], the variation of CSI due to the motion of a user can be confined to a certain subspace. Therefore, a CBF scheme using channel covariance matrix is developed. The scheme is designed to tolerate a certain level of error in the estimation of the covariance matrix. Although the robustness is achieved at the expense of increased transmit power, a significant reduction in signaling overhead can be achieved with minor increase in total transmit power at moderately low SINRs. These particular contributions are published in [37], [34] and [35].

3. In Chapter 5, a theoretical bound of power-saving gain obtained by splitting a cell into tiers of smaller cells is derived. In an infrastructure arisen from cell splitting, unoccupied UHF frequency bands with very good propagation characteristics can be used to establish robust wireless links amongst the neighbouring BSs. Chapter 5 contributes to the wireless backhaul by introducing a Ring protocol to exchange information amongst 3 BSs and a Star protocol to exchange information amongst 3 fixed relay stations (RSs) and one BS as a controlling unit using network coding concept. Time sharing principles for maximisation of throughput in the Star and Ring protocols are derived proceeded with the throughput maximising expressions for the protocols. Using derivation, it is concluded that the imbalance in the number of bits received by the controlling unit from any two source nodes, i.e., BSs or RSs, has to be minimised in the MAC phase of both protocols in order to achieve the highest backhaul throughput. Backhaul transmission strategies for the models are also proposed using the signal to noise ratios of the wireless links amongst the BSs. The above contributions are published in [34, 38, 39] and [35].

4. A significant utilisation of backhaul is required to overcome inter-cell interference in multi-cell processing networks where multiple BSs simultaneously transmit to their intended local users with aggressive frequency reuse. In order to reduce backhaul burden, Chapter 6 proposes a downlink transmission strategy together with an iterative algorithm that enables each BS to design locally its own beamforming vectors without relying on data or downlink CSI of links from other BSs to the users. This algorithm is the solution to an inter-cell interference balancing optimisation problem that minimises a linear combination of data transmission power and the resulting inter-cell interference power at each BS, and maintains the required SINRs by the users. Two pricing strategies are introduced to calculate the interference pricing factors. The convergence of the proposed algorithm in cellular systems is proven and the impact of the pricing factors in saving power at BSs is characterised. A feasibility condition for the existence of such an iterative algorithm is derived. This condition can be used as a scheduling algorithm to choose a set of active users within each cell. Simulation results show that the proposed algorithm quickly converges to a network-wide equilibrium point by both balancing and stabilising the mutual inter-cell interference levels together with assigning power optimal beamforming vectors to the BSs. The results also confirm the effectiveness of the proposed algorithm in closely following the performance limits of its centralised coordinated beamforming counterpart. These contributions are accepted for publication in [40] and are currently under review in [41].

1.3.1 Publications

A collection of contributions for this thesis has been complied from the following list of publications:

1. T. A. Le and M. R. Nakhai, "Possible power-saving gains by dividing a cell into tiers of smaller cells," *IET Electronics Letters*, vol. 46, no. 16, pp. 1163–1165, Aug. 2010.

2. T. A. Le and M. R. Nakhai, "Throughput analysis of network coding enabled wireless backhauls," *IET Communications*, vol. 5, no. 10, pp. 1318–1327, Jul. 2011.

3. T. A. Le and M. R. Nakhai, "User position aware multi-cell beamforming for a distributed antenna system," in *Proc. IEEE 22nd International Symposium on PIMRC*, Sep. 2011, pp. 1398–1342.

4. C. Han, T. Harrold, S. Armour, I. Krikidis, S. Videv, P. M. Grant, H. Haas, J. S. Thompson, I. Ku, C.-X. Wang, T. A. Le, M. R. Nakhai, J. Zhang, and L. Hanzo, "Green radio: Radio techniques to enable energy-efficient wireless networks," *IEEE Wireless Communications Magazine*, vol. 49, no. 6, pp. 46–54, Jun. 2011.

5. T. A. Le, S. Nasseri, A. Zarrebin-Esfahani, A. Mills, and M. R. Nakhai, "Power-efficient downlink transmission in multicell networks with limited wireless backhaul," *IEEE Wireless Communications Magazine, Special Issue on Technologies for Green Radio Communication Networks*, vol. 18, no. 5, pp. 82–88, Oct. 2011.

6. T. A. Le and M. R. Nakhai, "An iterative algorithm for downlink multi-cell beamforming," in *Proc. IEEE Global Telecommun. Conf. (GLOBECOM 2011)*, Dec. 2011, pp. 1–6.

7. T. A. Le and M. R. Nakhai, "Coordinated beamforming using semidefinite programming," in *Proc. IEEE Int. Conf. Commun. (ICC 2012)*, Jun. 2012, pp. 1–5.

8. M. R. Nakhai, T. A. Le, A. M. Akhtar, and O. Holland, "Chapter: Cooperative multi-cell processing techniques for energy-efficient cellular wireless networks," in *E. Hossain, V. K. Bhargava and G. P. Fettweis, Green Radio Communication Networks*, Cambridge University Press, 2012.

9. T. A. Le and M. R. Nakhai, "A decentralized downlink beamforming algorithm for multi-cell processing," in *Proc. IEEE Global Telecommun. Conf. (GLOBECOM 2012)*, to appear.

10. T. A. Le and M. R. Nakhai, "Downlink optimization with interference pricing and statistical CSI," *IEEE Trans. Commun.*, under review.

Chapter 2

Background study

2.1 Introduction

Having the ability of solving very large, practical engineering problems reliably and efficiently, convex optimisation has become the most widely researched area in optimisation. Since a local minimum in a convex optimisation problem is also the global minimum, the global minimum can be attained by any "Gradient Descent" or "Hill Climbing" algorithm [42]. Linear programming, i.e., a program with linear objective function and linear/affine constraints, is a well researched topic in convex programming. Recent developments in convex programming extend the results and algorithms of linear programming to more complicated convex programs, e.g., conic programming. A conic programming is a linear programming with generalised inequalities.

This chapter concisely reviews two standard conic programs, i.e. second order cone programming (SOCP) and semidefinite programming (SDP). Concepts of a linear antenna array used for beamforming are described. Applications of SOCP and SDP for solving the problem of multiuser beamforming in a single-cell scenario are discussed. Using the duality theory in convex optimisation, the connection between uplink-downlink duality and Lagrangian duality is presented. The concepts presented in this chapter are beneficial to the developments of beamforming schemes introduced in Chapters 3, 4 and 6. Readers interested in convex optimisation and applications of convex optimisation in communications are referred to [42], [43] and [44] for more details.

2.2 Second order cone programming and semidefinite programming

This section recalls two standard conic programs which are SOCP and SDP. The standard form of a SOCP is defined as [42], [22]:

$$\begin{aligned} \min_{\mathbf{x}} \quad & \Re\left\{\mathbf{f}^H\mathbf{x}\right\} \\ \text{subject to} \quad & \|\mathbf{A}_i^H\mathbf{x}+\mathbf{b}_i\| \leq \mathbf{c}_i^H\mathbf{x}+d_i, \quad \forall 1 \leq i \leq N, \end{aligned} \tag{2.1}$$

where the vector $\mathbf{x}$ is the optimisation variable with the length of n; $\mathbf{f}$, $\mathbf{A}_i$, $\mathbf{b}_i$, $\mathbf{c}_i$ and d_i are deterministic parameters with appropriate sizes.

The standard form of a SDP is defined as [42], [22]:

$$\begin{aligned} \min_{\mathbf{x}} \quad & \Re\left\{\mathbf{f}^H\mathbf{x}\right\} \\ \text{subject to} \quad & \mathbf{A}(\mathbf{x}) \succeq 0 \end{aligned} \tag{2.2}$$

where

$$\mathbf{A} = \mathbf{A}_0 + \sum_{i=1}^{n} x_i\mathbf{A}_i \tag{2.3}$$

is a Hermitian matrix that depends affinely on $\mathbf{x}$ and the $m \times m$ Hermitian matrix $\mathbf{A}_i$, $\forall 1 \leq i \leq n$, is deterministic data.

The dual problem associated with the SDP (2.2) is [45]

$$\begin{aligned} \max_{\mathbf{Z}} \quad & -\operatorname{Tr}\left(\mathbf{A}_0\mathbf{Z}\right) \\ \text{subject to} \quad & \operatorname{Tr}\left(\mathbf{A}_i\mathbf{Z}\right) = f_i, i = 1, 2, \cdots, n \\ & \mathbf{Z} = \mathbf{Z}^H \succeq 0. \end{aligned} \tag{2.4}$$

The dual problem (2.4) is also a SDP like the primal problem, i.e., it can be cast in the same form as the primal problem (2.2). The proof [45] is sketched in the following. For simplicity, assuming that the matrices $\mathbf{A}_1, \mathbf{A}_2, \cdots, \mathbf{A}_n$ are linearly independent. Then the affine set $\operatorname{Tr}(\mathbf{A}_i\mathbf{Z}) = f_i, \forall i$ can be expressed in the form:

$$\mathbf{G}(\mathbf{y}) = \mathbf{G}_0 + y_1\mathbf{G}_1 + \cdots + y_p\mathbf{G}_p \tag{2.5}$$

where $p = m(m+1)/2 - n$ and $\mathbf{G}_i$ are appropriate matrices. Defining

$$\mathbf{d} = \begin{bmatrix} \operatorname{Tr}(\mathbf{F}_0\mathbf{G}_1) & \operatorname{Tr}(\mathbf{F}_0\mathbf{G}_2) & \cdots & \operatorname{Tr}(\mathbf{F}_0\mathbf{G}_p) \end{bmatrix}^T.$$

Hence,

$$\mathbf{d}^T\mathbf{y} = \mathrm{Tr}\left(\mathbf{F}_0[\mathbf{G}(\mathbf{y}) - \mathbf{G}_0]\right).$$

Therefore, the dual problem (2.4) becomes

$$\begin{aligned} \min_{\mathbf{y}} \quad & \Re\left\{\mathbf{d}^T\mathbf{y}\right\} \\ \text{subject to} \quad & \mathbf{G}(\mathbf{y}) \succeq 0 \end{aligned} \tag{2.6}$$

which is a standard SDP form defined in (2.2). This concludes that the problem (2.4) is also a SDP.

In the following, a transformation from a second-order-cone constraint to a semidefinite constraint, also known as a linear matrix inequality (LMI) constraint, is presented. Defining a matrix $\mathbf{M} \in \mathcal{C}^{(q+t)\times(q+t)}$:

$$\mathbf{M} = \begin{bmatrix} \mathbf{A}_{q\times q} & \mathbf{B}_{q\times t} \\ \mathbf{C}_{t\times q} & \mathbf{D}_{t\times t} \end{bmatrix} \tag{2.7}$$

where the dimensions of $\mathbf{A}$, $\mathbf{B}$, $\mathbf{C}$ and $\mathbf{D}$ as shown in the block display, $\mathbf{A}$ and $\mathbf{D}$ are square matrices but $\mathbf{B}$ and $\mathbf{C}$ are not square unless $t = q$. Recall the Schur complement definition:

Definition 2.1. *If* $\mathbf{D}$ *is nonsingular, the Schur complement of* $\mathbf{M}$ *with respect to* $\mathbf{D}$ *is defined as*

$$\mathbf{S} = \mathbf{A} - \mathbf{B}\mathbf{D}^{-1}\mathbf{C}. \tag{2.8}$$

Matrix $\mathbf{S}$ has the following main properties [43]:

- $\mathbf{M} \succ 0$ if and only if $\mathbf{D} \succ 0$ and $\mathbf{S} \succ 0$.
- If $\mathbf{D} \succ 0$, then $\mathbf{M} \succeq 0$ if and only if $\mathbf{S} \succeq 0$.

Since $\mathbf{c}_i^H\mathbf{x} + d_i > 0$, $\left(\mathbf{c}_i^H\mathbf{x} + d_i\right)\mathbf{I} \succ 0$. Using the second property of $\mathbf{S}$, one can show that the ith SOC constraint in (2.1), i.e.,

$$\|\mathbf{A}_i^H\mathbf{x} + \mathbf{b}_i\| \leq \mathbf{c}_i^H\mathbf{x} + d_i, \tag{2.9}$$

is equivalent to the following LMI constraint:

$$\begin{bmatrix} \mathbf{c}_i^H\mathbf{x} + d_i & \mathbf{x}^H\mathbf{A}_i + \mathbf{b}_i^H \\ \mathbf{A}_i^H\mathbf{x} + \mathbf{b}_i & \left(\mathbf{c}_i^H\mathbf{x} + d_i\right)\mathbf{I} \end{bmatrix} \succeq 0. \tag{2.10}$$

Hence (2.1) can be written in a standard SDP form as:

$$\begin{aligned} \min_{\mathbf{x}} \quad & \Re\left\{\mathbf{f}^H\mathbf{x}\right\} \\ \text{subject to} \quad & \begin{bmatrix} \mathbf{c}_i^H\mathbf{x}+d_i & \mathbf{x}^H\mathbf{A}_i+\mathbf{b}_i^H \\ \mathbf{A}_i^H\mathbf{x}+\mathbf{b}_i & \left(\mathbf{c}_i^H\mathbf{x}+d_i\right)\mathbf{I} \end{bmatrix} \succeq 0, \quad \forall 1 \leq i \leq N. \end{aligned} \tag{2.11}$$

The SeDuMi solver [46] is a common optimisation packet that can be used to solve SOCP and SDP. An elegant Matlab-based modeling system for convex optimisation, i.e., CVX which supports the SeDuMi solver, has been developed by Michael Grant and Stephen Boyd [47].

2.3 Linear antenna array

Smart antennas are composed of two or more antennas working in harmony to create a unique radiation pattern for the electromagnetic environment at hand. The antenna elements are allowed to work in harmony by means of the array element phasing, which is performed with hardware or is carried out digitally [48]. Arrays of antennas can be in any geometry form such as linear arrays, circular arrays, planar arrays and conformal arrays. In this section, a concept of a linear antenna array in [49] is reviewed. Thorough treatments for all arrays of antennas can be found in [50] and [51].

Consider a signal wavefront, $z(t)$, impinging on an antenna array comprising M antennas spaced d apart each other at angle θ, shown in Fig. 2.1. It is assumed that the wavefront has a bandwidth B and is expressed as:

$$z(t) = \beta(t)e^{j2\pi\nu_c t} \tag{2.12}$$

where $\beta(t)$ is the complex envelope representation of the signal and ν_c is the carrier frequency. Let T_z be the traveling time of the wavefront across any two adjacent antennas. It is clear that

$$T_z = \frac{dsin(\theta)}{c} \tag{2.13}$$

where c is the speed of light.

The maximum time of the wavefront traveling along one array is assumed to be much smaller than the reciprocal of the bandwidth of all transmitted signals, i.e.,

$$B \ll \frac{1}{(M-1)T_z}. \tag{2.14}$$

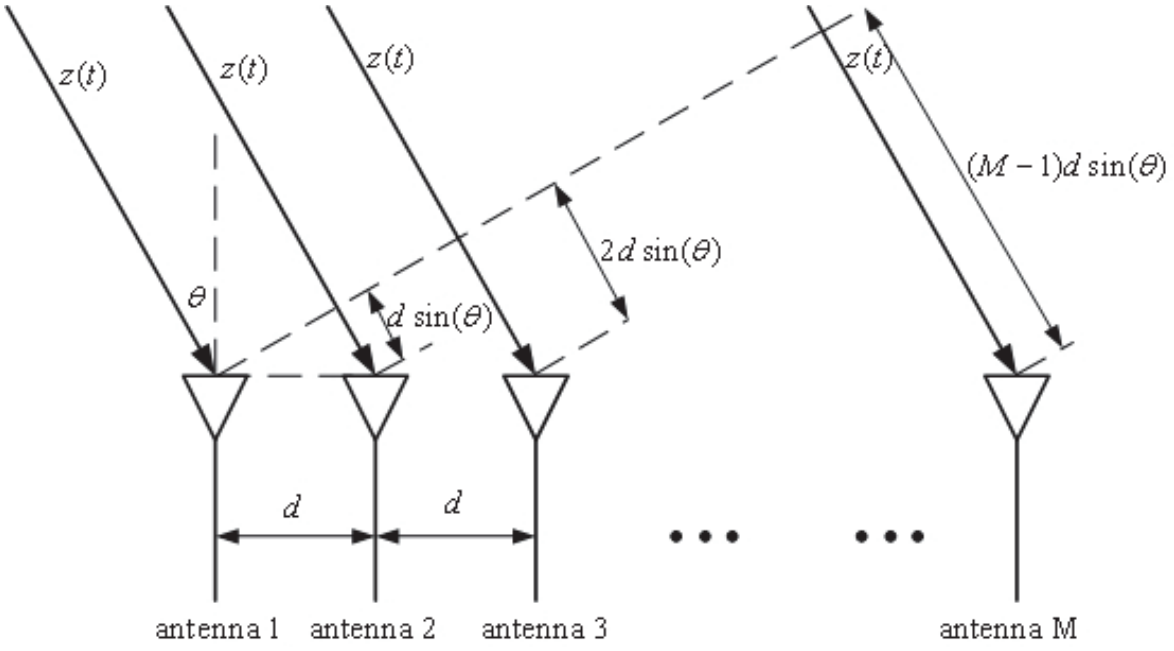

Figure 2.1: Schematic of a wavefront impinging across an antenna array. Under the narrowband assumption the antenna outputs are identical except for a complex scalar.

Assuming that antenna element patterns are identical. Provided the received signal at the first antenna is

$$y_1(t) = z(t) = \beta(t)e^{j2\pi\nu_c t}, \tag{2.15}$$

then the received signal at the second antenna is

$$y_2(t) = z(t - T_z) = \beta(t - T_z)e^{j2\pi\nu_c(t-T_z)}. \tag{2.16}$$

Under the narrowband assumption in (2.14), $B \ll 1/T_z$. It can be stated that

$$\beta(t - T_z) \approx \beta(t). \tag{2.17}$$

Let λ_c be the wavelength of the signal wavefront. Using $\nu_c/c = 1/\lambda_c$, (2.13), (2.15) and (2.17) in (2.18), one can arrive at

$$y_2(t) = y_1(t)e^{-j2\pi sin(\theta)\frac{d}{\lambda_c}}. \tag{2.18}$$

Similarly, the received signal at the kth antenna, i.e., $k = 1, 2, \cdots, M$, is given as

$$y_k(t) = y_1(t)e^{-j2\pi(k-1)sin(\theta)\frac{d}{\lambda_c}}. \tag{2.19}$$

From (2.15), (2.18) and (2.19), it can be seen that the signals received at any two array elements are identical except for a phase shift which depends on the angle of arrival and the array geometry.

Consider a free field environment, i.e., neither scatterers and nor multipath. A planar continuous-wave wavefront of frequency ν_c arriving from an angle θ will introduce a spatial signature across the antenna array. This spatial signature is a function of angle of arrival, antenna element patterns and antenna array geometry. The complex $M \times 1$ vector, $\mathbf{a}(\theta) = \begin{bmatrix} a_1(\theta) & a_2(\theta) & \cdots & a_M(\theta) \end{bmatrix}^T$, is called the array response vector. For the linear antenna array with identical element patterns, the array response vector is given as

$$\mathbf{a}(\theta) = \begin{bmatrix} 1 \\ e^{-j2\pi sin(\theta)\frac{d}{\lambda_c}} \\ \vdots \\ e^{-j2\pi(M-1)sin(\theta)\frac{d}{\lambda_c}} \end{bmatrix}. \tag{2.20}$$

Similarly, it is possible write the array response vector for a transmit linear antenna array with identical element patterns as

$$\mathbf{a}(\theta) = \begin{bmatrix} 1 & e^{-j2\pi sin(\theta)\frac{d}{\lambda_c}} & \cdots & e^{-j2\pi(M-1)sin(\theta)\frac{d}{\lambda_c}} \end{bmatrix}. \tag{2.21}$$

Hence, the MISO channel between the antenna array and a user i can be written as

$$\mathbf{h}_i = \xi_i \mathbf{a}(\theta_i) \tag{2.22}$$

where ξ_i captures both effects of channel fading, i.e. fast and slow fading, and pathloss, θ_i is the angle of departure, with respect to the broadside of the antenna array, of the user i.

Using antenna arrays opens up a spatial dimension to improve capacities of wireless communication systems. This improvement is due to the fact that smart beam patterns can be shaped by controlling the phases of individual antennas of the array. Hence power-efficient beams can be steered towards intended users while minimum/non interference are imposed on unintended users. Smart beam patterns are performed via algorithms based on certain criteria. These algorithms can be implemented using hardware. However, it is more easily performed using software, i.e., using digital signal processing [48]. These criteria could be either minimising transmit power with constraints on users' SINRs or maximising users' sum rate with constraints on transmit power to name a few. In the following section, the first strategy, i.e., minimising transmit power under constraint of users' SINR, is reviewed.

2.4 Multiuser downlink beamforming

Consider a base station (BS) equipped with an array of M antenna elements transmitting to U single-antenna users. The signal received by an user i, i.e., $y_i, i \in \{1, \cdots, U\}$, is given by

$$y_i = \mathbf{h}_i \mathbf{w}_i s_i + \sum_{j=1, j\neq i}^{U} \mathbf{h}_i \mathbf{w}_j s_j + n_i \tag{2.23}$$

where $\mathbf{h}_i \in \mathcal{C}^{1\times M}$ is the MISO vector channel between user i and the BS, $\mathbf{w}_i \in \mathcal{C}^{M\times 1}$ represents the beamforming vector for user i, s_i is the intended symbol for user i and finally n_i is the zero mean circularly symmetric complex Gaussian (ZMCSCG) random variable, i.e., $n_i \sim \mathcal{N}(0, \sigma^2)$, modeling the additive white Gaussian noise at the receiving point of user i. Without loss of generality, assuming that $\mathbb{E}\left(|s_i|^2\right) = 1, \forall i$. The signal-to-interference-plus-noise ratio for any user i is expressed as

$$\text{SINR}_i = \frac{|\mathbf{h}_i \mathbf{w}_i|^2}{\sum_{j=1, j\neq i}^{U} |\mathbf{h}_i \mathbf{w}_j|^2 + \sigma^2}. \tag{2.24}$$

A common class of optimal transmit downlink beamforming for multiple users is to find a set of $\mathbf{w}_i$ that minimises the total transmit power while guaranteing all users' SINR requirements $\gamma_i, \forall i$:

$$\begin{aligned} \min_{\mathbf{w}_i} \quad & \sum_{i=1}^{U} \mathbf{w}_i^H \mathbf{w}_i \\ \text{subject to} \quad & \frac{|\mathbf{h}_i \mathbf{w}_i|^2}{\sum_{j=1, j\neq i}^{U} |\mathbf{h}_i \mathbf{w}_j|^2 + \sigma^2} \geq \gamma_i, \forall 1 \leq i \leq U. \end{aligned} \tag{2.25}$$

For simplicity, it is assumed that the set of γ_i in (2.25) is feasible. It can be verified that the SINR constraints in (2.25) are non-convex. In the next section, a technique to reformulate (2.25) in SOCP and SDP forms is presented.

2.5 SOCP and SDP algorithms

In this section, the method developed in [22] to cast (2.25) in a convex form using SOCP and SDP is reviewed. Let

$$\mathbf{H} = \begin{bmatrix} \mathbf{h}_1 \\ \mathbf{h}_2 \\ \vdots \\ \mathbf{h}_U \end{bmatrix} \quad \text{and} \quad \mathbf{W} = \begin{bmatrix} \mathbf{w}_1 & \mathbf{w}_2 & \cdots & \mathbf{w}_U \end{bmatrix}. \tag{2.26}$$

In introducing a real slack variable P_o, (2.25) can be written as [22]:

$$\begin{aligned} \min_{\mathbf{W}, P_o} \quad & P_o \\ \text{subject to} \quad & \frac{\left|[\mathbf{HW}]_{i,i}\right|^2}{\sum_{j=1, j\neq i}^{U} \left|[\mathbf{HW}]_{i,j}\right|^2 + \sigma^2} \geq \gamma_i, \forall 1 \leq i \leq U \\ & \mathrm{Tr}\left(\mathbf{W}\mathbf{W}^H\right) \leq P_o \end{aligned} \tag{2.27}$$

where $[\mathbf{X}]_{i,j}$ represents the (i,j)-th entry of matrix $\mathbf{X}$. The i-th SINR constraint in (2.27) can be rearrange as:

$$\frac{1}{\gamma_i} \left|[\mathbf{HW}]_{i,i}\right|^2 \geq \sum_{j=1, j\neq i}^{U} \left|[\mathbf{HW}]_{i,j}\right|^2 + \sigma^2. \tag{2.28}$$

Adding $\left|[\mathbf{HW}]_{i,i}\right|^2$ to both sides results in

$$\left(1 + \frac{1}{\gamma_i}\right) \left|[\mathbf{HW}]_{i,i}\right|^2 \geq \sum_{j=1}^{U} \left|[\mathbf{HW}]_{i,j}\right|^2 + \sigma^2. \tag{2.29}$$

Equivalently,

$$\left(1 + \frac{1}{\gamma_i}\right) \left|[\mathbf{HW}]_{i,i}\right|^2 \geq \left\| \begin{bmatrix} \mathbf{W}^H \mathbf{H}^H \mathbf{e}_i \\ \sigma^2 \end{bmatrix} \right\|^2. \tag{2.30}$$

One can verify the fact that an arbitrary phase rotation can be added to the beamformers without affecting the SINR constraints and objective of (2.27). In other words, if $\mathbf{W}$ is optimal solution to (2.27) then $\mathbf{W}\mathrm{diag}\{e^{j\phi_i}\}$, where ϕ_i for $i = 1, 2, \cdots, U$ are arbitrary phases, is also an optimal solution. Therefore $\mathbf{W}$ can be selected in such a manner that $[\mathbf{HW}]_{i,i} > 0$, i.e., $[\mathbf{HW}]_{i,i}$ can be chosen to be real, for all i without the loss of generality. Since $[\mathbf{HW}]_{i,i} > 0, \forall i$, taking the square root of the equation (2.30)

leads to

$$\left(1+\frac{1}{\gamma_i}\right)[\mathbf{HW}]_{i,i} \geq \left\| \begin{bmatrix} \mathbf{W}^H\mathbf{H}^H\mathbf{e}_i \\ \sigma^2 \end{bmatrix} \right\|. \tag{2.31}$$

Using vec(.) operator, one can cast the power constraint of (2.27) as

$$p \geq \|\text{vec}(\,\mathbf{W}\,)\| \tag{2.32}$$

where $p = \sqrt{P_o}$. Therefore, problem (2.27) can be reformulated in a SOCP form as

$$\begin{aligned} \min_{\mathbf{W},p} \quad & p \\ \text{subject to} \quad & \left\| \begin{bmatrix} \mathbf{W}^H\mathbf{H}^H\mathbf{e}_i \\ \sigma^2 \end{bmatrix} \right\| \leq \left(1+\frac{1}{\gamma_i}\right)[\mathbf{HW}]_{i,i}, \forall 1 \leq i \leq U \\ & \|\text{vec}(\,\mathbf{W}\,)\| \leq p. \end{aligned} \tag{2.33}$$

Using (2.10), the SOCP in (2.33) can be written in a SDP form as

$$\begin{aligned} \min_{\mathbf{W},p} \quad & p \\ \text{subject to} \quad & \begin{bmatrix} \left(1+\frac{1}{\gamma_i}\right)[\mathbf{HW}]_{i,i} & \begin{bmatrix} \mathbf{e}_i^T\mathbf{HW} & \sigma^2 \end{bmatrix} \\ \begin{bmatrix} \mathbf{W}^H\mathbf{H}^H\mathbf{e}_i \\ \sigma^2 \end{bmatrix} & \left(1+\frac{1}{\gamma_i}\right)[\mathbf{HW}]_{i,i}\mathbf{I} \end{bmatrix} \succeq 0, \forall 1 \leq i \leq U \\ & \begin{bmatrix} p & \text{vec}^H(\mathbf{W}) \\ \text{vec}(\mathbf{W}) & p\mathbf{I} \end{bmatrix} \succeq 0. \end{aligned} \tag{2.34}$$

Solving (2.33) or (2.34) provides the optimal beamforming matrix $\mathbf{W}$ and the optimal downlink power as p^2. Beamformer for user i can be obtained as the ith column of $\mathbf{W}$.

2.6 Semidefinite relaxation algorithm

The introduction of the semidefinite relaxation (SDR) technique in early 2000s has provided a capability of obtaining accurate, and sometime near optimal, approximation convex forms from non-convex problems, see [52], [53] and references therein. This section illustrates a method to cast (2.25) in a convex form using the SDR technique.

Let $\mathbf{R}_i = \mathbf{h}_i^H\mathbf{h}_i$ and $\mathbf{F}_i = \mathbf{w}_i\mathbf{w}_i^H$. It is clear that $\mathbf{F}_i$, $\forall 1 \leq i \leq U$, is a positive semidefinite and Hermitian matrix. Further more the rank of the matrix is one. The

multiuser downlink beamforming problem in (2.25) can be expressed as

$$\begin{aligned} \min_{\mathbf{w}_i} \quad & \sum_{i=1}^{U} \mathbf{w}_i^H \mathbf{w}_i \\ \text{subject to} \quad & \frac{\mathbf{w}_i^H \mathbf{R}_i \mathbf{w}_i}{\sum_{j=1, j\neq i}^{U} \mathbf{w}_j^H \mathbf{R}_i \mathbf{w}_j + \sigma^2} \geq \gamma_i, \forall 1 \leq i \leq U. \end{aligned} \tag{2.35}$$

Recall the following equality:

$$\mathbf{x}^H \mathbf{A} \mathbf{x} = \mathrm{Tr}\left(\mathbf{A} \mathbf{x} \mathbf{x}^H\right). \tag{2.36}$$

If $\mathbf{A} = \mathbf{I}$ then

$$\mathbf{x}^H \mathbf{x} = \mathrm{Tr}\left(\mathbf{x} \mathbf{x}^H\right). \tag{2.37}$$

Rearrange the ith SINR constraints of (2.35), one can arrive at

$$\left(1 + \frac{1}{\gamma_i}\right) \mathrm{Tr}\left(\mathbf{R}_i \mathbf{F}_i\right) - \sum_{j=1, j\neq i} \mathrm{Tr}\left(\mathbf{R}_i \mathbf{F}_j\right) - \sigma^2 \geq 0. \tag{2.38}$$

The problem (2.35) can be posed as

$$\begin{aligned} \min_{\mathbf{F}_i} \quad & \sum_{i=1}^{U} \mathrm{Tr}\left(\mathbf{F}_i\right) \\ \text{subject to} \quad & \frac{1}{\gamma_i} \mathrm{Tr}\left(\mathbf{R}_i \mathbf{F}_i\right) - \sum_{j=1, j\neq i} \mathrm{Tr}\left(\mathbf{R}_i \mathbf{F}_j\right) - \sigma^2 \geq 0, \\ & \mathbf{F}_i = \mathbf{F}_i^H \succeq 0, \\ & \mathrm{rank}\left(\mathbf{F}_i\right) = 1, \forall 1 \leq i \leq U. \end{aligned} \tag{2.39}$$

The second constraints in (2.39) is to guarantee that $\mathbf{F}_i$, $\forall 1 \leq i \leq U$, is a positive semidefinite and Hermitian matrix. Dropping the last constraints in (2.39), i.e., $\mathrm{rank}\left(\mathbf{F}_i\right) = 1$, results in a SDP form, i.e.,

$$\begin{aligned} \min_{\mathbf{F}_i} \quad & \sum_{i=1}^{U} \mathrm{Tr}\left(\mathbf{F}_i\right) \\ \text{subject to} \quad & \frac{1}{\gamma_i} \mathrm{Tr}\left(\mathbf{R}_i \mathbf{F}_i\right) - \sum_{j=1, j\neq i} \mathrm{Tr}\left(\mathbf{R}_i \mathbf{F}_j\right) - \sigma^2 \geq 0, \\ & \mathbf{F}_i = \mathbf{F}_i^H \succeq 0, \forall 1 \leq i \leq U. \end{aligned} \tag{2.40}$$

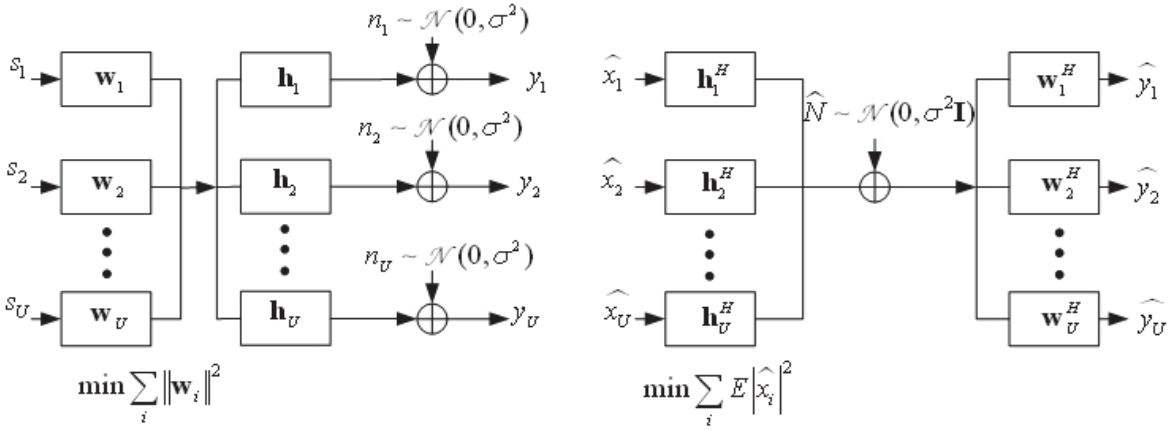

Figure 2.2: Uplink-downlink duality can be interpreted as a Lagrangian duality in convex optimisation [44].

Dropping these rank one constraints not only enlarges the feasible set of the problem (2.39) but also leads to a relaxed SDP problem. This relaxation is referred to as semidefinite relaxation technique. For general nonconvex quadratic problems, solving a SDR problem usually gives an optimal solution with rank of larger than one. In such cases, SDR can only provide a lower bound on the optimal objective function and possibly attain an approximate solution to the original problem [53]. When using SDR results in $\mathbf{F}_i$ solutions with ranks higher than one, a randomization procedure, e.g., see [52], [54] and [55], can be used to find approximate rank-one solutions.

Since (2.25) has a specific structure that it can be turned into a convex form, i.e., as shown in the previous section, strong duality holds for (2.25). Furthermore, it can be shown that the SDR of (2.39), i.e., (2.40), is the Lagrangian dual of the Lagrangian dual of (2.25) [53]. Therefore, (2.40) is exactly equivalent to the original problem (2.25). This fact has been confirmed in [56]. The authors of [56] noticed that the solution to (2.40) always admits rank-one matrices $\mathbf{F}_i, \forall i$, which directly yields the solution to (2.25) using $\mathbf{F}_i = \mathbf{w}_i \mathbf{w}_i^H$.

2.7 Lagrangian duality and Uplink-downlink duality

It has been well documented in literature that the minimum power required to provide a set of SINR targets in a downlink multiple-input-multiple-output channel is identical to the minimum power required to attain the same set of SINR targets in the uplink,

where the uplink channel is obtained by reversing the input and output of the downlink [3, 16–18, 20]. This fact is referred to as uplink-downlink duality. The authors of [57] show that the uplink-downlink duality can also be realised via Lagrangian duality in convex optimisation. This result has been recently extended from a single-cell-multiuser scenario to a multiple-cell-multiuser scenario in [32]. This section reviews main steps for the single-cell-multiuser beamforming.

The Lagrangian of the problem (2.25) is formed as

$$\begin{aligned} L(\mathbf{w}_i, \lambda_i) &= \sum_{i=1}^{U} \mathbf{w}_i^H \mathbf{w}_i + \sum_{i=1}^{U} \lambda_i \left[\sum_{j=1, j\neq i}^{U} |\mathbf{h}_i \mathbf{w}_j|^2 + \sigma^2 - \frac{1}{\gamma_i} |\mathbf{h}_i \mathbf{w}_i|^2 \right] \\ &= \sum_{i=1}^{U} \mathbf{w}_i^H \mathbf{w}_i + \sum_{i=1}^{U} \lambda_i \left[\sum_{j=1, j\neq i}^{U} \mathbf{w}_j^H \mathbf{h}_i^H \mathbf{h}_i \mathbf{w}_j + \sigma^2 - \frac{1}{\gamma_i} \mathbf{w}_i^H \mathbf{h}_i^H \mathbf{h}_i \mathbf{w}_i \right] \end{aligned}$$

where λ_i is the ith Lagrange multiplier associated with the ith constraint. Equivalently,

$$L(\mathbf{w}_i, \lambda_i) = \sum_{i=1}^{U} \lambda_i \sigma^2 + \sum_{i=1}^{U} \mathbf{w}_i^H \left[\mathbf{I} + \sum_{j=1, j\neq i}^{U} \lambda_j \mathbf{h}_i^H \mathbf{h}_i - \frac{\lambda_i}{\gamma_i} \mathbf{h}_i^H \mathbf{h}_i \right] \mathbf{w}_i. \tag{2.41}$$

The dual objective is

$$g(\lambda_i) = \inf_{\mathbf{w}_i} L(\mathbf{w}_i, \lambda_i). \tag{2.42}$$

It is clear that

$$g(\lambda_i) = \begin{cases} \sum_{i=1}^{U} \lambda_i \sigma^2, & \text{if } \left(\mathbf{I} + \sum_{j=1, j\neq i}^{U} \lambda_j \mathbf{h}_i^H \mathbf{h}_i - \frac{\lambda_i}{\gamma_i} \mathbf{h}_i^H \mathbf{h}_i \right) \succeq 0 \\ -\infty, & \text{otherwise .} \end{cases} \tag{2.43}$$

Therefore, the Lagrangian dual problem can be stated as

$$\begin{aligned} \max_{\lambda_i} \quad & \sum_{i=1}^{U} \lambda_i \sigma^2 \\ \text{subject to} \quad & \left(\mathbf{I} + \sum_{j=1, j\neq i}^{U} \lambda_j \mathbf{h}_i^H \mathbf{h}_i - \frac{\lambda_i}{\gamma_i} \mathbf{h}_i^H \mathbf{h}_i \right) \succeq 0, \forall 1 \leq i \leq U. \end{aligned} \tag{2.44}$$

It is shown in [57] that the solution to the dual problem and the solution to the following

dual uplink problem are identical:

$$\begin{aligned} \min_{p_i} \quad & \sum_{i=1}^{U} p_i \\ \text{subject to} \quad & \max_{\|\hat{\mathbf{w}}_i\|=1} \frac{p_i \left|\hat{\mathbf{w}}_i^H \mathbf{h}_i^H\right|^2}{\sum_{j=1,j\neq i} p_j \left|\hat{\mathbf{w}}_i^H \mathbf{h}_j^H\right|^2 + \sigma^2 \hat{\mathbf{w}}_i^H \hat{\mathbf{w}}_i} \geq \gamma_i, \forall i \in \mathcal{S}_l, \end{aligned} \tag{2.45}$$

where $p_i = \lambda_i \sigma^2$ is the uplink power associated with user i, $\hat{\mathbf{w}}_i$ is the uplink beamforming vector for user i which can be found as the MMSE filter

$$\hat{\mathbf{w}}_i = \left(\sum_{j=1}^{U} p_j \mathbf{h}_j^H \mathbf{h}_j + \sigma^2 \mathbf{I} \right)^{-1} \mathbf{h}_i^H. \tag{2.46}$$

The values for the set of $\hat{\mathbf{w}}_i$ in (2.46) is a function of p_i or precisely λ_i, i.e., $p_i = \lambda_i \sigma^2$. The values for the set of λ_i are attained by an iterative algorithm derived from (2.45). Finally, optimal downlink beamforming vectors to the original problem (2.25) are calculated by scaling $\hat{\mathbf{w}}_i$. Details of the iterative algorithms can be found in [32, 57].

Fig. 2.2 illustrates the uplink-downlink duality which can be interpreted as a Lagrangian duality in convex optimisation. The dual uplink problem is obtained from the downlink problem by swapping the input and output vectors and by transposing the channel vectors. In the dual uplink, each remote transmitter has single antenna and transmits with a power of

$$p_i = \mathbb{E}|\widehat{x}_i|^2. \tag{2.47}$$

The task of a receive beamforming designer is to jointly optimise the power allocation p_i and the receiver beamforming vector $\hat{\mathbf{w}}^H$ such that a set of SINR constraints γ_i is satisfied.

2.8 Conclusion

This chapter reviews principles of beamforming via linear antenna array along with concepts of second order cone programming and semidefinite programming. An optimisation problem to calculate transmit beamformers for multiple active users in a single-cell scenario is sketched. The problem is non-convex due to its non-convex constraints. Three methods are presented to transform the problem into second order cone programming and semidefinite programming forms, which can be effectively solved by available optimisation packets. Additionally, a dual uplink problem associated with

the original problem is reviewed using Lagrangian duality.

Chapter 3

Multi-cell beamforming

In this chapter, BSs are allowed to cooperate at signal level where user data are circulated amongst them for joint transmissions to every user within the network. Beamforming vectors for all users are calculated as if coordinating BSs were a single BS. A user-position-aware algorithm for multi-cell processing is introduced so that a user is only assigned to nearby BSs, thus the amount of data circulation is reduced. Using uplink-downlink duality, an iterative multi-cell beamforming algorithm that minimises the total transmit power of the network is proposed.

3.1 Introduction

The implementation of transmit beamforming in cellular networks has been well studied since over a decade, e.g., [18] and [56]. Beamforming is a space-division-multiple-access technique where multiple antennas and advanced spatial signal processing are used to serve multiple co-channel users. In linear beamforming, for example, the data stream for each user is modulated by a precoding vector, i.e., a spatial signature, prior to passing through the transmit antennas. Careful selection of precoding vectors results in mutual interference amongst different streams to be mitigated or even removed [30]. Therefore, using beamforming yields improvements in transmission range, rate and power efficiency [7]. However, as the user moves towards the severe inter-cell-interference areas of cell-edges, the technique cannot assure and maintain a consistent level of data rate to the user. Recently, the idea of multi-cell processing (MCP) has promised a solution to the cell-edge problem by allowing inter-cell cooperation, e.g., [23–29]. The coordinated design of precoding vectors for multiple coordinated-cells significantly improves the throughput with respect to uncoordinated design, e.g., [30], [25]. Full cooperation amongst BSs within a cluster offers significant sum throughput

and cell-edge user rate gains [58], [59]. Under the context of a distributed antenna system, the authors of [60] showed that jointly designed transmit preprocessing matrix of all the cooperative remote antennas combined with fractional frequency reuse is capable of achieving an increased throughput for the entire cell-edge area.

In the forward link of MCP, i.e., base station (BS) to mobile, the Wyner model and the hexagonal model are two types of channel model that are widely used. In the former model, BSs are assumed to be placed in either a linear array, i.e., [23], [26] and [27], or in a circular array, e.g., [24], [25]. Thus, [26] and users may receive energy from two adjacent BSs. In the latter model, each BS is placed in the centre of a hexagon and users may receive energy from more than two BSs, i.e., [61–69]. The highest energy for a user in a cell border are mainly from three mutually interfering sectors of three neigbouring cells, e.g. [64, 68, 69].

Regarding the level of coordination amongst BSs, the following two strategies can be recognised. The first strategy is at signal level where users' data are made available to either all BSs, e.g. [59], or proper subgroups of BSs, e.g. [70]. The second strategy is at beamforming level where users' data are kept locally by each BS, i.e., [18], [71]. In both strategies, when precoding vectors are jointly designed, users' CSI need to be available at either all BSs or the central unit for the decentralised or centralised method, respectively. A broadcast channel can be realised when entire users' data are available to all BSs.

With an ideal backhaul assumption, i.e., unlimited capacity, low latency, error-free and no power consumption, MCP is superior over single-cell processing in terms of throughput and spectral efficiency, i.e., [30], [64] and [65]. However, in practical scenarios this assumption is not realistic and the performance of a MCP network strongly depends on the required backhaul overhead. In [66] and [67], authors propose a framework to improve the downlink capacity and fairness in multi-cell networks with limited backhaul infrastructure. In order to reduce the overhead of CSI feedback from users to BSs, subsets of users are selected for joint transmissions. The partition of the cellular network into individual subsystems that can be optimised in a decetralised manner. In [68], a framework to mitigate the overhead of CSI feedback is introduced and the effect of feedback error on the performance of the proposed framework is investigated. Taking a further step in [69], the authors propose a scheme that can jointly reduce CSI feedback and users' data circulation overhead in the backhaul. Using distributed signal-to-interference-leakage-plus-noise-ratio techniques [72], a range of reduced-complexity MCP structures are proposed in [62] to decrease the amount data exchange.

The problem of designing transmit-beamforming vectors for MCP that minimises

the transmit power of the system, while maintaining a certain signal-to-interference-plus-noise ratio (SINR) for each user, has also been a major concern in the literature. The solution to the problem using iterative methods is desirable for practical implementations. Employing uplink-downlink duality property, uplink-beamforming vectors are attained and used for the iterative achievement of the optimal solution to the downlink [18, 22, 32]. The uplink-beamforming vector for each user is chosen such that the associated SINR is maximised via either a minimum mean squared error technique, i.e., [22], [32], or a minimum variance distortionless response method, i.e., [18]. These iterative schemes use instantaneous channel state information (CSI) which requires frequent-signaling overhead amongst BSs and users. The fluctuation of CSI due to the motion of user can be confined to a certain subspace [36]. Therefore second-order statistical CSI is desirable as it reduces signaling overhead. In [31], the optimisation problem for multi-cell is presented in a semidefinite programming form [45] which can be solved by optimisation packages, e.g., the SeDuMi solver [46]. According to the in depth literature survey conducted in this research, it can be stated that there is no iterative algorithm for the multi-cell optimisation problem using second-order statistical CSI.

This chapter considers a network of coordinating BSs where each BS is equipped with multiple antennas. The antenna arrays of the BSs form a distributed-array antenna (DAA). A new multi-cell beamforming (MBF) technique for the DAA is introduced using a channel model between the DAA and a user. The model includes an angular spread due to the existence of local scatterers surrounding the user. A spatial covariance matrix for the resulting DAA channel model is derived. The channel model developed in this chapter is a generalised version of the channel model given in [31] to capture the effects of local scatterers and shadow fading. A user-position-aware algorithm that only allocates users to nearby BSs and reduces data circulation on backhaul is developed. An iterative algorithm to solve the optimisation problem of total transmit power minimisation subject to users' SINR constraints is proposed. Despite using uplink-downlink duality via Lagrangian theory like papers [22] and [32], the algorithm introduced in this chapter is different due to the followings. Firstly, the iterative algorithm is based on second-order statistical CSI. Secondly, uplink-beamforming vectors are calculated using the dominant eigenvector method.

The rest of this chapter is organised as follows. In section 3.2, a system model is presented. A user position aware algorithm is introduced in section 3.3. An iterative algorithm is proposed in section 3.4. Simulation results are presented in section 3.5. Finally, section 3.6 concludes the chapter.

3.2 System model

Consider a network of N coordinating cells in which the BS of each cell is equipped with an array of M antenna elements. Thus, up to N geographically distributed antenna arrays (DAA) can coordinate to serve U simultaneous single-antenna user terminals anywhere within the coverage of N cells. The available spectrum is globally reused within the coordinating area. It is assumed that each user belonging to a cell receives dominant interference only from $N-1$ base stations. Hence, the model described in this section and used throughout this chapter considers interference from the non-coordinating base stations surrounding the coordinating area on a user as noise.

It is assumed that each user is surrounded by Q randomly positioned local-scatterers, that are at the far-field distances from the BSs, and there is no line-of-sight (LoS) transmission from the BSs to the user. Thus, wavefronts originated from each one of the serving BSs hit all of the Q local scatterers of each user. The spacing between the antenna elements of a BS is negligible with respect to the distance of the BS from the scatterers. Hence, rays departing from M antenna elements of a BS towards a scatterer can be assumed to have the same fading coefficients. Let $s_i, i = 1, \cdots, U$, be the intended symbol for the ith user and $\mathbf{x}_p = \begin{bmatrix} x_p(1) & x_p(2) & \cdots & x_p(M) \end{bmatrix}^T$, where $x_p(k)$ is the transmitted signal by the kth antenna element of the pth BS, $p = 1, 2, \cdots, N$. The transmitted signal by N BSs can be written as

$$\begin{bmatrix} \mathbf{x}_1 \\ \mathbf{x}_2 \\ \vdots \\ \mathbf{x}_N \end{bmatrix} = \begin{bmatrix} \mathbf{w}_1(1) & \mathbf{w}_2(1) & \cdots & \mathbf{w}_U(1) \\ \mathbf{w}_1(2) & \mathbf{w}_2(2) & \cdots & \mathbf{w}_U(2) \\ \vdots & \vdots & \vdots & \vdots \\ \mathbf{w}_1(N) & \mathbf{w}_2(N) & \cdots & \mathbf{w}_U(N) \end{bmatrix} \begin{bmatrix} s_1 \\ s_2 \\ \vdots \\ s_U \end{bmatrix}, \tag{3.1}$$

where $\mathbf{w}_i(p) = \begin{bmatrix} w_i(p,1) & w_i(p,2) & \cdots & w_i(p,M) \end{bmatrix}^T$ is the beamforming vector of the ith user at the pth BS and $w_i(p,k)$ is the corresponding beamforming coefficient of the kth antenna element. The received signal at user i is given by

$$y_i = \mathbf{h}_i \mathbf{x} + z_i, \tag{3.2}$$

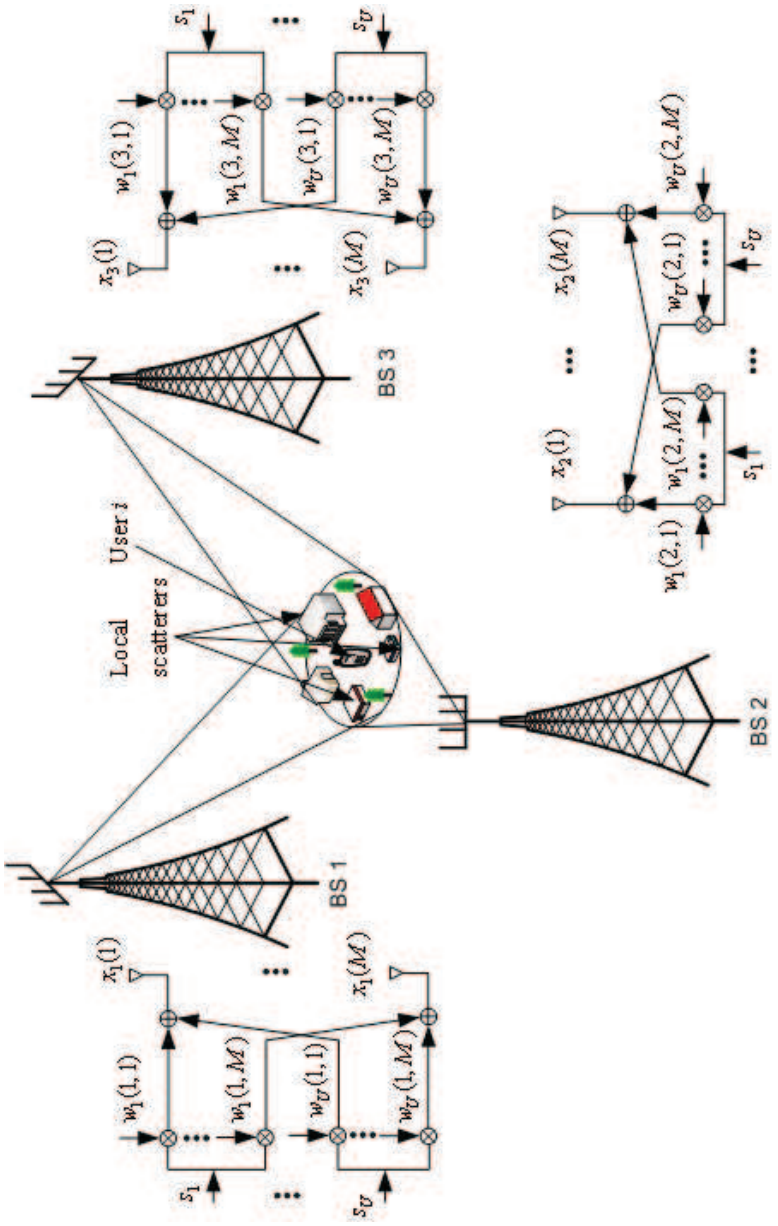

Figure 3.1: Illustration for system model with $N = 3$ [35].

where $\mathbf{x} = \begin{bmatrix}\mathbf{x}_1^T & \mathbf{x}_2^T & \cdots & \mathbf{x}_N^T\end{bmatrix}^T$,

$$\mathbf{h}_i = \begin{bmatrix}\varrho_{i,1} & \varrho_{i,2} & \cdots & \varrho_{i,Q}\end{bmatrix} \begin{bmatrix} \xi_{i,1}(1)\mathbf{h}_{i,1}(1) & \xi_{i,1}(2)\mathbf{h}_{i,1}(2) & \cdots & \xi_{i,1}(N)\mathbf{h}_{i,1}(N) \\ \xi_{i,2}(1)\mathbf{h}_{i,2}(1) & \xi_{i,2}(2)\mathbf{h}_{i,2}(2) & \cdots & \xi_{i,2}(N)\mathbf{h}_{i,2}(N) \\ \vdots & \vdots & \vdots & \vdots \\ \xi_{i,Q}(1)\mathbf{h}_{i,Q}(1) & \xi_{i,Q}(2)\mathbf{h}_{i,Q}(2) & \cdots & \xi_{i,Q}(N)\mathbf{h}_{i,Q}(N) \end{bmatrix}, \tag{3.3}$$

$\varrho_{i,t} = e^{-j\frac{2\pi c}{\lambda}\tau_{i,t}}$ is the phase shift due to the time delay $\tau_{i,t}$ between the tth scatterer and the ith user, $\xi_{i,t}(p) = a_i(p)\sqrt{S_{i,t}(p)L_{i,t}(p)}$ models the path loss and the large scale fading coefficients with $S_{i,t}(p) = 10^{-\frac{x}{10}}$ and $L_{i,t}(p)$ being the log-normal shadow fading coefficient, i.e., $x \sim \mathcal{N}(0, \sigma_S^2)$, and the path loss coefficient, respectively, between the pth BS and the tth scatterer of user i. The coefficients $\xi_{i,t}(p)$ include the effect of user distribution in cellular network in the MCP channel model. The controlling coefficient $a_i(p)$ is either 1, if the ith user is allocated to be served by the pth BS, or zero, otherwise. Furthermore in (3.3), the row vector $\mathbf{h}_{i,t}(p) = \begin{bmatrix}h_{i,t}(p,1) & h_{i,t}(p,2) \cdots h_{i,t}(p,M)\end{bmatrix}$, where $h_{i,t}(p,k)$ is the channel between the tth scatterer of the ith user and the kth antenna element of the pth BS and finally z_i is the zero mean circularly symmetric complex Gaussian (ZMCSCG) random variable, i.e., $z_i \sim \mathcal{N}(0, \sigma_N^2)$, modeling the additive white Gaussian noise at the ith user's receiving point. Let $d_i(p)$ be the distance from BS p to user i, and $d_{i,\min} = \min_p d_i(p)$. One can write

$$h_{i,t}(p,k) = F_{i,t}(p)e^{j\frac{2\pi}{\lambda}\left[d_i(p)-d_{i,\min}\right]}e^{j\frac{2\pi\Delta}{\lambda}(k-1)\sin[\theta_i(p)+\phi_{it}(p)]}, \tag{3.4}$$

where $F_{i,t}(p)$ is the complex Gaussian fading coefficient between BS p and scatterer t of user i with variance σ_F^2, λ is the carrier wavelength, Δ is the spacing between the BS antenna elements within a sector, $\theta_i(p)$ is the angle of departure with respect to the broadside of BS p for user i and $\phi_{it}(p)$ is the angular offset of the scatterer t with respect to $\theta_i(p)$. It is assumed that the local scatterers are distributed randomly around each user i and the resulting angle spread has a normal distribution with standard deviation of σ, i.e., $\phi_{it}(p) \sim \mathcal{N}(0, \sigma^2)$. The channel coefficient of the kth ray of the DAA in (3.4) differs from the channel coefficient of the kth ray of a conventional linear antenna array in factor $e^{j\frac{2\pi}{\lambda}[d_i(p)-d_{i,\min}]}$ which represents the phase difference between the geographically separated BSs. Note that (3.4) reduces to the kth ray channel of the conventional antenna array by substituting $d_{i,\min} = d_i(p)$.

Let $\mathbf{R}_i = \mathbb{E}\left(\mathbf{h}_i^H\mathbf{h}_i\right)$ denote the spatial channel covariance matrix between the DAA, i.e, the distributed antenna array formed by the coordinating BSs, and the ith user.

In the following, we find an expression for entries of $\mathbf{R}_i$. Assume that each scatterer sees the antenna arrays of different BSs under independent fading coefficients, i.e.,

$$\mathbb{E}\left(\xi_{i,t}^*(p)\xi_{i,t}(q)\right) = 0, \quad \text{if} \quad p \neq q, \tag{3.5}$$

and the channels between any two different scatterers and the same multi-antenna base station fade independently, i.e.,

$$\mathbb{E}\left(\xi_{i,t}^*(p)\xi_{i,g}(p)\right) = 0, \quad \text{if} \quad t \neq g. \tag{3.6}$$

From (3.3), (3.5) and (3.6) one can write

$$\mathbf{R}_i = \text{diag}\left[\mathbf{R}_i(1), \mathbf{R}_i(2), \cdots, \mathbf{R}_i(N)\right] \tag{3.7}$$

where the pth block is given as

$$\mathbf{R}_i(p) = \mathbb{E}\left(\sum_{t=1}^{Q} \varrho_{i,t}^* \xi_{i,t}^*(p)\mathbf{h}_{i,t}^H(p) \sum_{q=1}^{Q} \varrho_{i,q}\xi_{i,q}(p)\mathbf{h}_{i,q}(p)\right). \tag{3.8}$$

Using (3.6) again yields

$$\begin{aligned}\mathbf{R}_i(p) &= \mathbb{E}\left(\sum_{t=1}^{Q} \varrho_{i,t}^*\xi_{i,t}^*(p)\mathbf{h}_{i,t}^H(p)\varrho_{i,t}\xi_{i,t}(p)\mathbf{h}_{i,t}(p)\right) \\ &= \mathbb{E}\left(\sum_{t=1}^{Q} \xi_{i,t}^*(p)\mathbf{h}_{i,t}^H(p)\xi_{i,t}(p)\mathbf{h}_{i,t}(p)\right).\end{aligned} \tag{3.9}$$

Using (3.4), one can write the (m,n)th entry, i.e., $m, n \in [1, M]$, of $\mathbf{R}_i(p)$ as

$$\begin{aligned}\mathbf{R}_i^{[m,n]}(p) &= \mathbb{E}\left(\sum_{t=1}^{Q} \xi_{i,t}^*(p)\xi_{i,t}(p)\right)\mathbb{E}\left(h_{i,t}^*(p,m)\, h_{i,t}(p,n)\right) \\ &= a_i^2(p)\sum_{t=1}^{Q}\mathbb{E}\left(S_{i,t}(p)\right)\mathbb{E}\left(L_{i,t}(p)\right)\mathbb{E}\left(F_{i,t}(p)\right) \\ &\quad \times \mathbb{E}_{\phi_{it}}\left(e^{j\frac{2\pi\Delta}{\lambda}(n-m)\sin[\theta_i(p)+\phi_{it}(p)]}\right).\end{aligned} \tag{3.10}$$

Using the fact that $\mathbb{E}\left(10^{\frac{-x}{10}}\right) = e^{-0.5\frac{(\ln 10\sigma_s)^2}{100}}$ with $x \sim \mathcal{N}(0, \sigma_S^2)$ [1], (3.10) can be rewritten

[1] See Appendix A for the proof.

as

$$\mathbf{R}_i^{[m,n]}(p) = a_i^2(p) \sum_{t=1}^{Q} e^{-0.5\frac{(\ln 10\sigma_s)^2}{100}} L_{i,t}(p)\sigma_F^2 \mathbb{E}_{\phi_{it}} \left(e^{j\frac{2\pi\Delta}{\lambda}(n-m)\sin[\theta_i(p)+\phi_{it}(p)]} \right). \quad (3.11)$$

Then using $\phi_{it}(p) \sim \mathcal{N}(0, \sigma^2)$, the expectation in (3.11) is rewritten as follows

$$\mathbb{E}_{\phi_{it}} \left(e^{j\frac{2\pi\Delta}{\lambda}(n-m)\sin[\theta_i(p)+\phi_{it}(p)]} \right) = \frac{1}{\sqrt{2\pi}\sigma} \int_{-\infty}^{\infty} e^{\frac{-\phi_{it}(p)^2}{2\sigma^2}} e^{j\frac{2\pi\Delta}{\lambda}(n-m)\sin[\theta_i(p)+\phi_{it}(p)]} \mathrm{d}\phi_{it}(p) \quad (3.12)$$

Employing the fact that $\sin(\theta+\phi) = \sin\theta\cos\phi + \cos\theta\sin\phi$ and for a small ϕ (in radians), $\cos\phi \approx 1$ and $\sin\phi \approx \phi$, one can arrive at

$$\mathbb{E}_{\phi_{it}} \left(e^{j\frac{2\pi\Delta}{\lambda}(n-m)\sin[\theta_i(p)+\phi_{it}(p)]} \right) = \frac{1}{\sqrt{2\pi}\sigma} \int_{-\infty}^{\infty} e^{\frac{-\phi_{it}(p)^2}{2\sigma^2}} e^{j\frac{2\pi\Delta}{\lambda}(n-m)[\sin\theta_i(p)+\cos\theta_i(p)\phi_{it}(p)]} \mathrm{d}\phi_{it}(p). \quad (3.13)$$

Applying the following formula [73]

$$\int_{-\infty}^{\infty} x^{\rho} e^{-\eta x^2+2\omega x} \mathrm{d}x = \rho! e^{\frac{\omega^2}{\eta}} \sqrt{\frac{\pi}{\eta}} \left(\frac{\omega}{\eta}\right)^{\rho} \sum_{k=0}^{\lfloor \rho/2 \rfloor} \frac{1}{(\rho-2k)!\,(k)!} \left(\frac{\eta}{4\omega^2}\right)^k$$

with $x = \phi_{it}(p)$, $\rho = 0$, $\eta = \frac{1}{2\sigma^2}$ and $\omega = \frac{j\pi\Delta}{\lambda}\left[(n-m)\cos\theta_i(p)\right]$ in (3.13) results in

$$\mathbb{E}_{\phi_{it}} \left(e^{j\frac{2\pi\Delta}{\lambda}(n-m)\sin[\theta_i(p)+\phi_{it}(p)]} \right) = e^{\frac{j2\pi\Delta}{\lambda}[(n-m)\sin\theta_i(p)]} e^{-2\left[\frac{\pi\Delta\sigma}{\lambda}\{(n-m)\cos\theta_i(p)\}\right]^2}. \quad (3.14)$$

Finally, substituting from (3.14) in (3.11) yields

$$\mathbf{R}_i^{[m,n]}(p) = \sum_{t=1}^{Q} L_{i,t}(p) a_i^2(p) \sigma_F^2 e^{\frac{-0.5(\ln 10\sigma_s)^2}{100}} e^{\frac{j2\pi\Delta}{\lambda}(n-m)\sin\theta_i(p)} e^{-2\left[\frac{\pi\Delta\sigma}{\lambda}(n-m)\cos\theta_i(p)\right]^2}. \quad (3.15)$$

The $M \times M$ matrix $\mathbf{R}_i(p)$ indicates the spatial covariance matrix between the base station p and the user i and is substituted by a zero matrix when the pth BS is not allocated to transmit to user i, i.e., $a_i(p) = 0$ in (3.3). In the following section, an algorithm is introduced to select the controlling coefficient $a_i(p)$ based on information of user ith position.

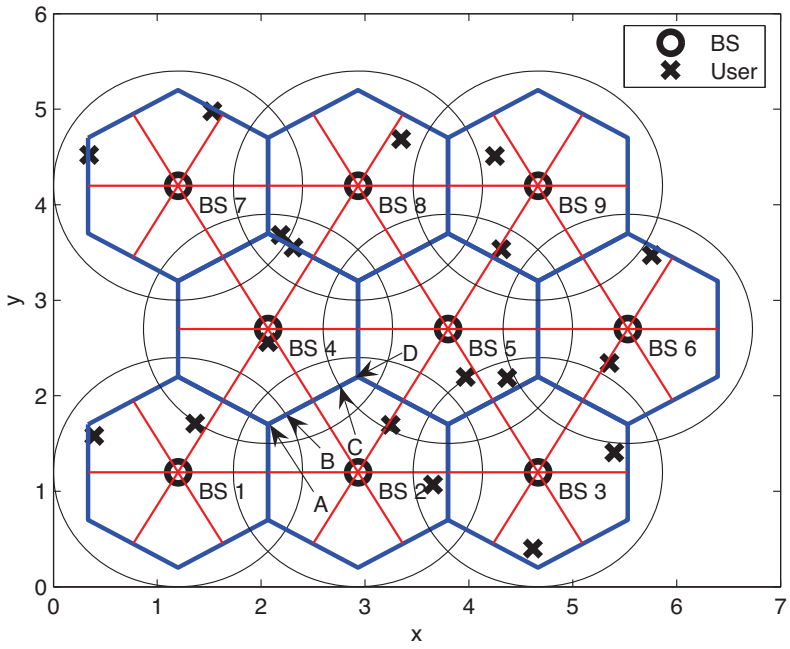

Figure 3.2: Illustration of a network of 9 cells with 18 users.

3.3 User-position-aware multi-cell processing

A cellular network is divided into several triangular zones where 3 adjacent BSs are located at vertices of a triangular zone as shown in Fig. 3.2. Despite of the number of coordinating BSs, a triangular zone is the smallest area unit where a user can be allocated, i.e., based on its location, to be served by up to 3 adjacent BSs. Next, a user position aware algorithm is introduced for a triangular zone to further reduce backhaul overhead.

The radius of the QoS guarantee circle of a cell is determined by the path-loss exponent, the user's targeted SINR and the transmit power limit at the BS. The QoS circles are assumed equal and shown as the outer-cell circles in Fig. 3.2. Let us consider a triangular zone created by BSs p, q and v, as shown in Fig 3.3. The radii of the corresponding outer-cell circles of BSs p, q and v are defined by D_p, D_q and D_v, respectively, and assumed to be equal in Fig. 3.3. Within the triangular zone, we distinguish 3 areas as follows. Area 3 is the overlapping part of 3 outer-cell circles, i.e., A_{pqv}, where users are supported by 3 BSs. Area 2 refers to the mutually overlapping parts of any 2 outer-cell circles, i.e., A_{pq}, A_{pv} and A_{qv}, where users are served by 2 nearby BSs. Area 1 refers to the remaining parts of the triangular zone, i.e., A_p,

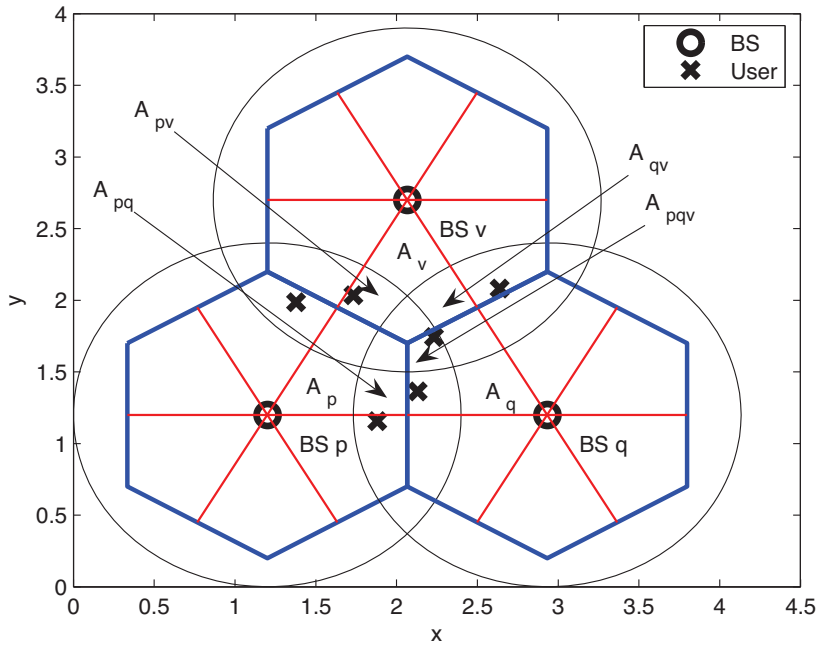

Figure 3.3: Classification of areas within a triangular zone covered by BSs p, q and v at 3 vertices.

A_q and A_v, where users are supported by the nearest local BS only. Algorithm 3.1 summarises the proposed UPA algorithm allocating users within the triangular zone of 3 BSs p, q, and v.

The UPA algorithm described in Algorithm 3.1 can be also implemented for sectoral cells. Fig. 3.4 shows a distributed antenna system of 7 cells, each cell consists of 3 sectors. The modification of the UPA algorithm for that distributed antenna system is described in the Appendix B.

3.4 An iterative algorithm for Multi-cell beamforming

In this section, an iterative algorithm is developed to find a set of U beamforming vectors that minimises the total transmit power of the coordinating BSs while a targeted

Algorithm 3.1 User position aware algorithm

for i=1 **to** U **do**
  if $(d_i(p) > D_p)$ **and** $(d_i(q) > D_q)$ **and** $(d_i(v) \leq D_v)$ **then**
    User $i \in A_v$ hence assign to BS v, i.e., $a_i(v) = 1$.
  else if $(d_i(p) > D_p)$ **and** $(d_i(v) > D_v)$**and** $(d_i(q) \leq D_q)$ **then**
    User $i \in A_q$ hence assign to BS q, i.e., $a_i(q) = 1$.
  else if $(d_i(q) > D_q)$ **and** $(d_i(v) > D_v)$ **and** $(d_i(p) \leq D_p)$ **then**
    User $i \in A_p$ hence assign to BS p, i.e., $a_i(p) = 1$.
  else if $(d_i(p) \leq D_p)$ **and** $(d_i(q) \leq D_q)$ **and** $(d_i(v) > D_v)$ **then**
    User $i \in A_{pq}$ hence assign to BSs p and q, i.e., $a_i(p) = a_i(q) = 1$.
  else if $(d_i(q) \leq D_q)$ **and** $(d_i(v) \leq D_v)$ **and** $(d_i(p) > D_p)$ **then**
    User $i \in A_{qv}$ hence assign to BSs q and v, i.e., $a_i(q) = a_i(v) = 1$.
  else if $(d_i(v) \leq D_v)$ **and** $(d_i(p) \leq D_p)$ **and** $(d_i(q) > D_p)$ **then**
    User $i \in A_{vp}$ hence assign to BSs v and p, i.e., $a_i(v) = a_i(p) = 1$.
  else if $(d_i(p) \leq D_p)$ **and** $(d_i(q) \leq D_q)$ **and** $(d_i(v) \leq D_v)$ **then**
    User $i \in A_{pqv}$ hence assign to BSs p, q and v, i.e., $a_i(p) = a_i(q) = a_i(v) = 1$.
  end if
end for

SINR is maintained at each user. First, the optimisation problem for MBF is stated as

$$\begin{aligned} \min_{\mathbf{w}_i} \quad & \sum_{i=1}^{U} \mathbf{w}_i^H \mathbf{w}_i \\ \text{subject to} \quad & \frac{\mathbf{w}_i^H \mathbf{R}_i \mathbf{w}_i}{\sum_{t=1,t\neq i}^{U} \mathbf{w}_t^H \mathbf{R}_i \mathbf{w}_t + \sigma^2} \geq \gamma_i, 1 \leq i \leq U, \end{aligned} \tag{3.16}$$

where γ_i is the required SINR at user i and $\mathbf{w}_i = \begin{bmatrix} \mathbf{x}_i^T(1) & \mathbf{x}_i^T(2) & \cdots & \mathbf{x}_i^T(N) \end{bmatrix}^T$.

Following the same technique in the proof of the theorem 1 in [32], one can show that the solution to the Lagrange dual problem of (3.16) is identical with the solution to the following dual-uplink problem

$$\begin{aligned} \min_{p_i} \quad & \sum_{i=1}^{U} p_i \\ \text{subject to} \quad & \max_{\hat{\mathbf{w}}_i} \frac{p_i \hat{\mathbf{w}}_i^H \mathbf{R}_i \hat{\mathbf{w}}_i}{\sum_{t=1,t\neq i}^{U} p_t \hat{\mathbf{w}}_i^H \mathbf{R}_t \hat{\mathbf{w}}_i + \sigma^2 \hat{\mathbf{w}}_i^H \hat{\mathbf{w}}_i} \geq \gamma_i, \\ & 1 \leq i \leq U, \end{aligned} \tag{3.17}$$

where $p_i = \lambda_i \sigma^2$ and $\hat{\mathbf{w}}_i$, i.e., $\hat{\mathbf{w}}_i^H \hat{\mathbf{w}}_i = 1$, are the dual-uplink power and a dual-uplink beamforming vector for user i, respectively, and λ_i is the i^{th} Lagrange multiplier associated with the i^{th} constraint in (3.16).

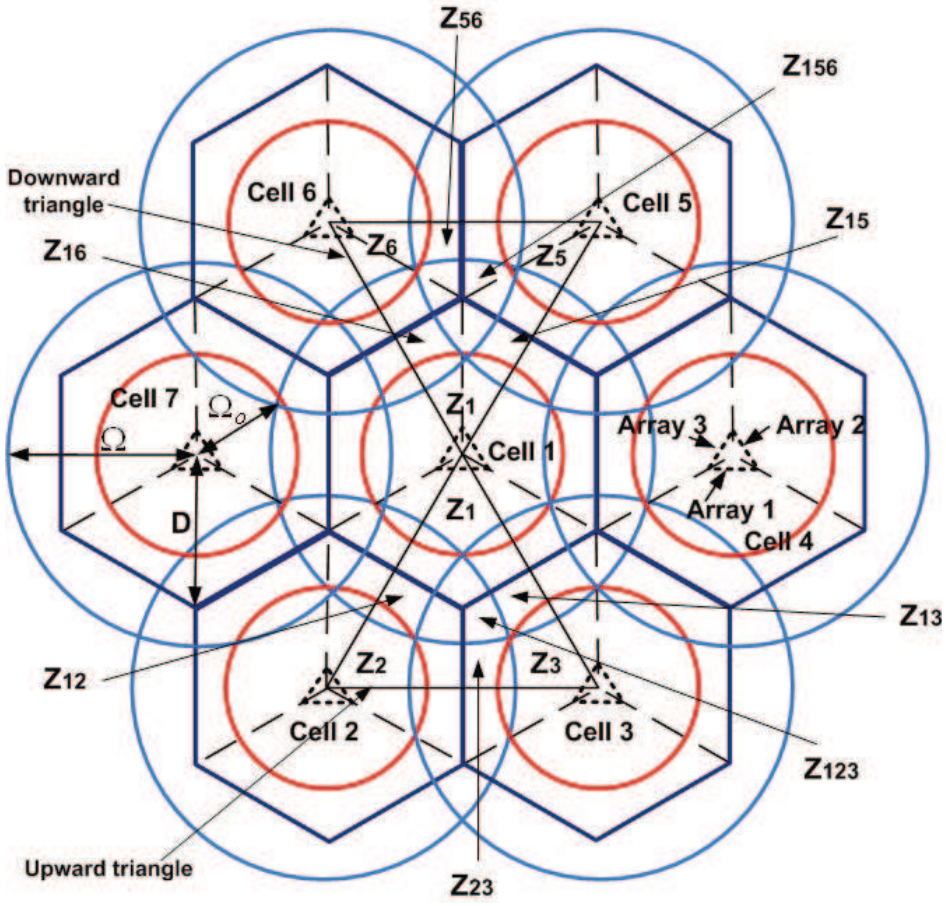

Figure 3.4: A distributed antenna system with zone classifications for the UPA algorithm [31].

To find an iterative solution to the problem (3.17), the set of constraints is rewritten in the following equivalent form:

$$\mathbf{p} \succeq \mathbf{\Gamma t}(\mathbf{p}) \tag{3.18}$$

where

$$\mathbf{p} = \left[p_1 \quad p_2 \quad \cdots \quad p_U\right]^T, \tag{3.19}$$

$$\mathbf{\Gamma} = \mathrm{diag}\left[\gamma_1, \gamma_2, \cdots, \gamma_U\right], \tag{3.20}$$

$$\mathbf{Q}_i\left(\mathbf{p}\right) = \left(\sum_{t=1, t\neq i}^{U} p_t \mathbf{R}_t + \sigma^2 \mathbf{I}\right), \tag{3.21}$$

$$\mathbf{t}(\mathbf{p}) = \left[t_1\left(\mathbf{p}\right) \quad t_2\left(\mathbf{p}\right) \quad \cdots \quad t_U\left(\mathbf{p}\right)\right]^T \tag{3.22}$$

and finally

$$t_i(\mathbf{p}) = \min_{\hat{\mathbf{w}}_i} \frac{\hat{\mathbf{w}}_i^H \mathbf{Q}_i(\mathbf{p}) \hat{\mathbf{w}}_i}{\hat{\mathbf{w}}_i^H \mathbf{R}_i \hat{\mathbf{w}}_i}, \tag{3.23}$$

which is the effective interference function of user i. The dual-uplink problem (3.17) can be recast as follows

$$\begin{aligned} \min_{p_i} \quad & \sum_{i=1}^{U} p_i \\ \text{subject to} \quad & \mathbf{p} \succeq \mathbf{\Gamma t}(\mathbf{p}). \end{aligned} \tag{3.24}$$

One can verify the fact that the uplink vector $\hat{\mathbf{w}}_i^\star$ maximising the left hand side of the i^{th} constraint in (3.17) is identical with the vector minimising the right hand side of (3.23). Vector $\hat{\mathbf{w}}_i^\star$ is determined as the eigenvector associated with the maximum eigenvalue, i.e., the dominant eigenvector, of the following matrix

$$\mathbf{G}_i = p_i \mathbf{Q}_i^{-1}(\mathbf{p}) \mathbf{R}_i. \tag{3.25}$$

In order to solve the dual-uplink problem (3.24), let us introduce the following lemma:

Lemma 3.1. *The interference function* $\mathbf{t}(\mathbf{p})$ *is standard as it satisfies the following criteria for all* $\mathbf{p} \succeq 0$*:*

- *Positivity:* $\mathbf{t}(\mathbf{p}) \succ 0$.
- *Monotonicity: If* $\mathbf{p} \succ \mathbf{p}'$ *then* $\mathbf{t}(\mathbf{p}) \succ \mathbf{t}(\mathbf{p}')$.
- *Scalability: For all* $\mu > 1$ *then* $\mu\mathbf{t}(\mathbf{p}) \succ \mathbf{t}(\mu\mathbf{p})$.

Proof.

- *Positivity:* As $\mathbf{R}_i$ is positive-semidefinite for all i, it is easy to verify from (3.23) that $\mathbf{t}(\mathbf{p}) \succ 0$ for all $\mathbf{p} \succeq 0$.
- *Monotonicity:* If $\mathbf{p} \succeq \mathbf{p}'$, using (3.23) we calculate $t_i(\mathbf{p}) - t_i(\mathbf{p}')$ as follows:

$$t_i(\mathbf{p}) - t_i(\mathbf{p}') = \frac{\sum_{t=1, t\neq i}^{U} (p_t - p_t') \hat{\mathbf{w}}_i^{\star H} \mathbf{R}_t \hat{\mathbf{w}}_i^\star}{\hat{\mathbf{w}}_i^{\star H} \mathbf{R}_i \hat{\mathbf{w}}_i^\star} \geq 0,$$

  for all $1 \leq i \leq U$. Therefore $\mathbf{t}(\mathbf{p}) \succeq \mathbf{t}(\mathbf{p}')$.

- *Scalability:* For all $\mu > 1$, $\mu t_i(\mathbf{p})$ is calculated as

$$\mu t_i(\mathbf{p}) = \frac{\sum_{t=1, t\neq i}^{U} \mu p_t \hat{\mathbf{w}}_i^{\star H} \mathbf{R}_t \hat{\mathbf{w}}_i^\star + \mu\sigma^2 \hat{\mathbf{w}}_i^{\star H} \hat{\mathbf{w}}_i^\star}{\hat{\mathbf{w}}_i^{\star H} \mathbf{R}_i \hat{\mathbf{w}}_i^\star}. \tag{3.26}$$

  From (3.26), one can verify that

$$\mu t_i(\mathbf{p}) > \frac{\sum_{t=1, t\neq i}^{U} \mu p_t \hat{\mathbf{w}}_i^{\star H} \mathbf{R}_t \hat{\mathbf{w}}_i^\star + \sigma^2 \hat{\mathbf{w}}_i^{\star H} \hat{\mathbf{w}}_i^\star}{\hat{\mathbf{w}}_i^{\star H} \mathbf{R}_i \hat{\mathbf{w}}_i^\star}$$

or $\mu t_i(\mathbf{p}) > t_i(\mu\mathbf{p})$ for all $1 \leq i \leq U$. Therefore $\mu\mathbf{t}(\mathbf{p}) \succ \mathbf{t}(\mu\mathbf{p})$.

□

According to [74], if $\mathbf{t}(\mathbf{p})$ is standard and $\mathbf{\Gamma}$ is a diagonal matrix of positive elements, the solution to the dual-uplink problem (3.24) can be found via the following iterative algorithm:

$$\mathbf{p}\,(n+1) = \mathbf{\Gamma}\mathbf{t}\,(\mathbf{p}\,(n))\,. \tag{3.27}$$

When the optimal values of user i for the problem (3.17) are determined, i.e., $p_i^\star$ and $\hat{\mathbf{w}}_i^\star$, its downlink beamforming vector is calculated using the optimal uplink beamforming vector. In the following we find the expression for the downlink beamforming vector.

Rearranging the primal constraint in (3.16) yields

$$\sum_{t=1}^{U} \mathbf{w}_t^H \mathbf{R}_i \mathbf{w}_t + \sigma^2 - \mathbf{w}_i^H \mathbf{R}_i \mathbf{w}_i \left(1 + \frac{1}{\gamma_i}\right) \leq 0, \forall 1 \leq i \leq U. \tag{3.28}$$

Using algebra, the Lagrangian of the problem (3.16), can be written as

$$L(\mathbf{w}_i, \lambda_i) = \sum_{i=1}^{U} \lambda_i \sigma^2 + \sum_{i=1}^{U} \mathbf{w}_i^H \left(\mathbf{I} + \sum_{t=1}^{U} \lambda_t \mathbf{R}_t - \lambda_i \left(1 + \frac{1}{\gamma_i}\right) \mathbf{R}_i \right) \mathbf{w}_i. \tag{3.29}$$

At the optimal point, i.e., $\lambda_i^\star$ and $\mathbf{w}_i^\star$, the gradient of Lagrangian (3.29) with respect to $\mathbf{w}_i$ vanishes. Using algebra and the fact that $p_i^\star = \lambda_i^\star \sigma^2$, one can arrive at

$$\left(\mathbf{I}\sigma^2 + \sum_{t=1}^{U} p_t^\star \mathbf{R}_t - p_i^\star \left(1 + \frac{1}{\gamma_i}\right) \mathbf{R}_i \right) \mathbf{w}_i^\star = \mathbf{0}. \tag{3.30}$$

Hence,

$$\left(\mathbf{I}\sigma^2 + \sum_{t=1, t\neq i}^{U} p_t^\star \mathbf{R}_t \right) \mathbf{w}_i^\star - \frac{p_i^\star}{\gamma_i} \mathbf{R}_i \mathbf{w}_i^\star = \mathbf{0}. \tag{3.31}$$

Therefore,

$$\gamma_i \mathbf{w}_i^\star = p_i^\star \left(\mathbf{I}\sigma^2 + \sum_{t=1, t\neq i}^{U} p_t^\star \mathbf{R}_t \right)^{-1} \mathbf{R}_i \mathbf{w}_i^\star. \tag{3.32}$$

The optimal uplink-beamforming vector $\hat{\mathbf{w}}_i^\star$ is the dominant eigenvector of the matrix

$\mathbf{G}_i$ in (3.25). Denoting the maximum eigenvalue of the matrix $\mathbf{G}_i$ as β_i, one can write

$$p_i^\star \left(\mathbf{I}\sigma^2 + \sum_{t=1,t\neq i}^{U} p_t^\star \mathbf{R}_t \right)^{-1} \mathbf{R}_i \hat{\mathbf{w}}_i^\star = \beta_i \hat{\mathbf{w}}_i^\star. \tag{3.33}$$

Comparing (3.32) and (3.33), one can conclude that downlink-beamforming vector is a scaled version of the uplink-beamforming vector which can be expressed as

$$\mathbf{w}_i^\star = \sqrt{\alpha_i}\hat{\mathbf{w}}_i^\star. \tag{3.34}$$

Since the constraint in the original problem (3.16) can be reformulated in a relaxed semi-definite-programming form [31], which is convex, then strong duality holds. Therefore $\sum_{i=1}^{U} \mathbf{w}_i^{\star H}\mathbf{w}_i^\star = \sum_{i=1}^{U} p_i^\star$. Using complementary slackness from KKT conditions of the downlink problem with $\lambda_i > 0$, one can arrive at

$$\sum_{t=1,t\neq i}^{U} \gamma_i \mathbf{w}_t^{\star H}\mathbf{R}_i\mathbf{w}_t^\star + \gamma_i\sigma^2 - \mathbf{w}_i^{\star H}\mathbf{R}_i\mathbf{w}_i^\star = 0, \quad \forall 1 \leq i \leq U. \tag{3.35}$$

Substituting for $\mathbf{w}_i^\star$ from (3.34) yields

$$\alpha_i \hat{\mathbf{w}}_i^{\star H}\mathbf{R}_i\hat{\mathbf{w}}_i^\star - \sum_{t=1,t\neq i}^{U} \gamma_i\alpha_t \hat{\mathbf{w}}_t^{\star H}\mathbf{R}_i\hat{\mathbf{w}}_t^\star = \gamma_i\sigma^2, \quad \forall 1 \leq i \leq U. \tag{3.36}$$

Denoting $\mathbf{a} = \begin{bmatrix} \alpha_1 & \alpha_2 & \cdots & \alpha_U \end{bmatrix}^T$, $\mathbf{c} = \begin{bmatrix} \gamma_1\sigma^2 & \gamma_2\sigma^2 & \cdots & \gamma_U\sigma^2 \end{bmatrix}^T$ and $U \times U$ matrix $\mathbf{B}$ where the $(i,j)^{\text{th}}$ entry is

$$\mathbf{B}_{i,j} = \begin{cases} \hat{\mathbf{w}}_i^{\star H}\mathbf{R}_i\hat{\mathbf{w}}_i^\star, & \text{if} \quad i = j \\ -\gamma_i \hat{\mathbf{w}}_j^{\star H}\mathbf{R}_i\hat{\mathbf{w}}_j^\star, & \text{if} \quad i \neq j \end{cases} \tag{3.37}$$

for all $i, j \in \{1, 2, \cdots, U\}$, (3.36) can be rewritten as

$$\mathbf{B}\mathbf{a} = \mathbf{c}. \tag{3.38}$$

Hence

$$\mathbf{a} = \mathbf{B}^{-1}\mathbf{c}. \tag{3.39}$$

The proposed iterative downlink algorithm for MBF is summarised in algorithm 3.2.

Algorithm 3.2 Iterative downlink algorithm for MBF

1: Define a stopping point ϵ.
2: $n = 1$.
3: Initialise $\mathbf{p}(n) \succeq 0$.
4: For $1 \leq i \leq U$, find $\hat{\mathbf{w}}_i(n)$ as the dominant eigenvector of the matrix $\mathbf{G}_i(n) = p_i(n)\,\mathbf{Q}_i^{-1}(\mathbf{p}(n))\,\mathbf{R}_i$ and calculate $t_i(\mathbf{p}(n)) = \frac{\hat{\mathbf{w}}_i^H(n)\mathbf{Q}_i(\mathbf{p}(n))\hat{\mathbf{w}}_i(n)}{\hat{\mathbf{w}}_i^H(n)\mathbf{R}_i\hat{\mathbf{w}}_i(n)}$.
5: Update $\mathbf{p}(n+1) = \boldsymbol{\Gamma}\mathbf{t}(\mathbf{p}(n))$.
6: $n = n + 1$.
7: Repeat steps 4 to 6 until $\| \mathbf{p}(n+1) - \mathbf{p}(n) \| \leq \epsilon$.
8: $\mathbf{p}^\star = \mathbf{p}(n+1)$ and $\hat{\mathbf{w}}_i^\star = \hat{\mathbf{w}}_i(n+1)$.
9: The optimal downlink beamforming vector for user i is given as $\mathbf{w}_i^\star = \sqrt{\alpha_i}\hat{\mathbf{w}}_i^\star$.

3.5 Simulation results

3.5.1 Simulation setup

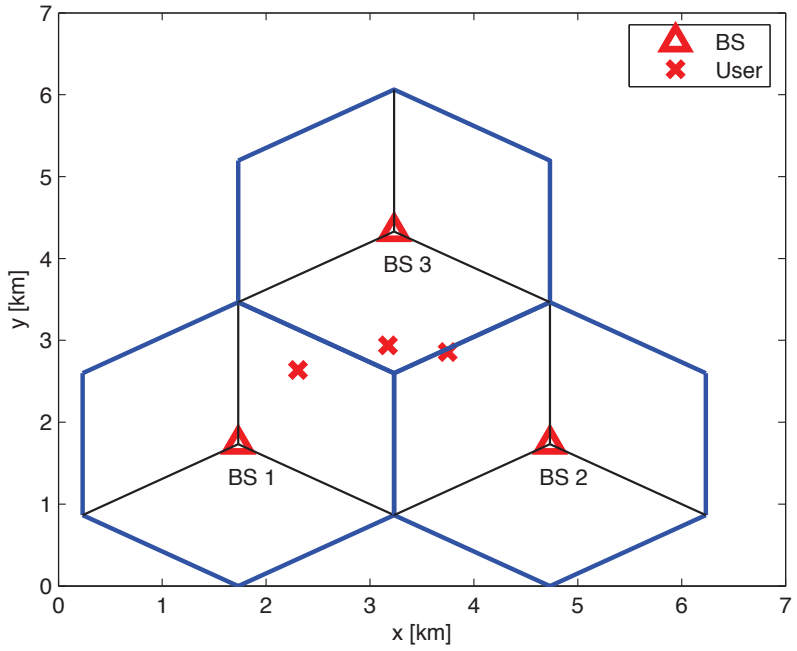

Figure 3.5: An example of random user distributions used in Monte-Carlo simulations.

In this section, an isolated 3-cell scenario which is used by several previous works, e.g., [69, 75], is used to evaluate the performance of the proposed beamforming scheme. In particular, one or two users were randomly distributed per cell such that they are located within the 3 adjacent sectors of 3 neighbouring cells. With this setup, a critical scenario in terms of severeness of inter-cell interference is considered. A set of locations

of 3 or 6 randomly users are referred to as one user distribution. Fig. 3.5 illustrates an example of one user distribution with 3 users. Monte Carlo simulations are carried out over 100 independent user distributions.

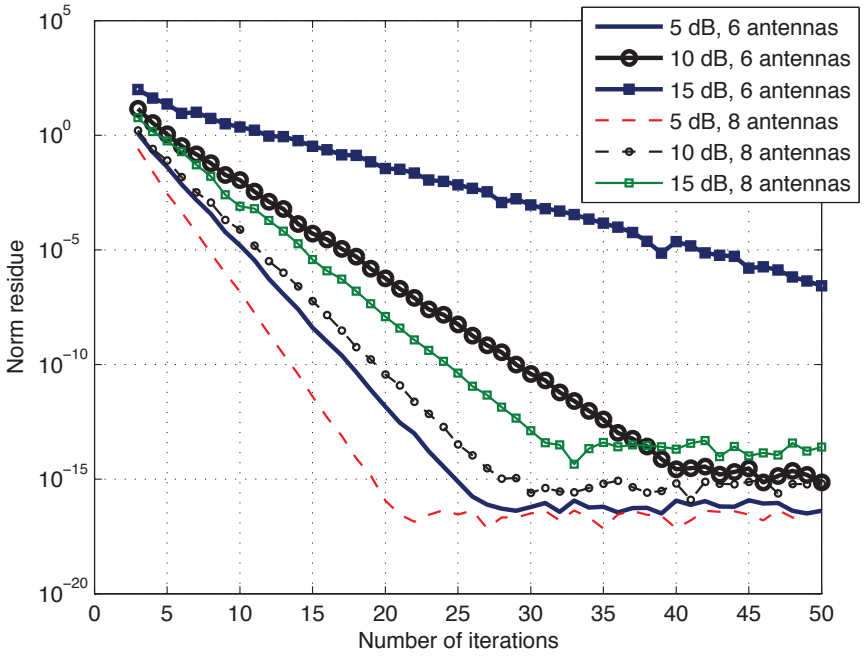

Figure 3.6: Norm residue versus number of iterations with 6 users, different required SINRs and number of antenna elements.

The antenna array element spacing in each sector is $\lambda/2$. The downlink carrier frequency is assumed at 2 GHz. The simulation setup assumes 5 scatterers per user and a standard deviation of 2° for the angular spread. It is assumed that the noise power spectral density for all users is -174 dBm/Hz, the noise figure at each user's receiver is 5 dB and the subcarrier bandwidth is 15 kHz wide. The array antenna gain for all BSs is set at 15dBi. The simulation setup uses $128.1 + 37.6\log_{10}(l)$, where l is in kilometers, as the path loss model and assume log-normal shadowing with a standard deviation of 8 dB. A Complex Gaussian distribution with a variance of $1/2$ on each of its real and imaginary components is set for the downlink channel fading coefficients. Also, any two neighbouring BSs are located 3 km apart from one another.

3.5.2 Performance evaluation

The proposed scheme's convergence is observed and its performance is compared with a baseline scheme in [31]. In the baseline scheme, the original problem (3.16) is recast

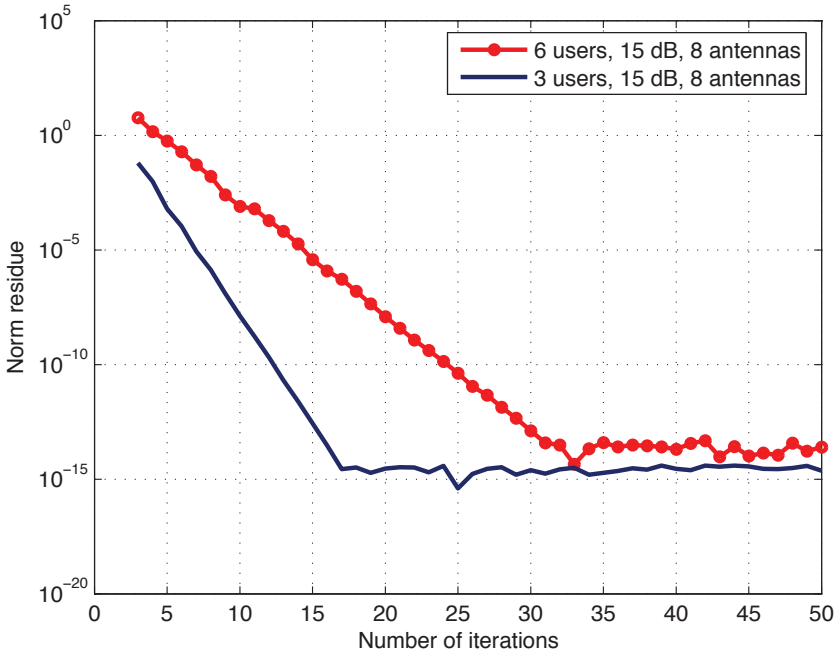

Figure 3.7: Norm residue versus number of iterations with 3 and 6 users, 8 antenna elements and required SINR of 15 dB.

in a semi-definite-programming form [45]. Then, the SeDuMi solver [46] is used to attain the optimal global solution.

Figs. 3.6 and 3.7 represent the convergence of the proposed algorithm. In these figures, norm residue is plotted versus a number of iterations, where the norm residue of n^{th} iteration is defined as $\| \mathbf{p}(n) - \mathbf{p}^{\star} \|$ in which $\mathbf{p}^{\star}$ is the optimal value.

The convergence of the proposed algorithm depends on the number of antenna elements and targeted SINRs. It is clear from Fig. 3.6 that with the same number of active users, the more number of antenna elements, the faster the convergence is. Moreover, it is also shown in the figure that with a given number of antenna elements, the algorithm converges faster with a lower required SINR.

The convergence of the algorithm is also affected by the number of active users. It can be observed from Fig. 3.7 that with a given number antenna elements and the same required SINR, the proposed algorithm converges faster with a smaller number of active users.

Results show that the proposed algorithm converges quickly. For example, after 16 iterations, the trend of the norm residue with 3 users levels off at around 10^{-15} while the one with 6 users requires 31 iterations to level off, i.e., Fig. 3.7. With the 6 users scenario in Fig. 3.6, after 50 iterations, the residue norms are all around 10^{-14} and

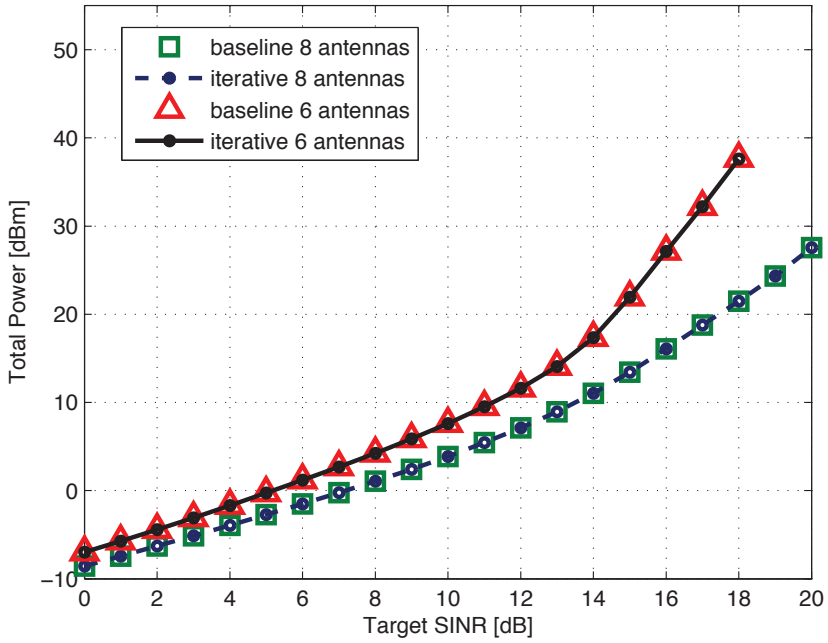

Figure 3.8: Total power comparisons between the iterative algorithm and baseline with 6 users.

10^{-17} except one at 10^{-7}.

Fig. 3.8 shows total power comparisons between the iterative algorithm and the baseline using the SeDuMi solver. The curves for iterative algorithm were attained over 50 iterations. Fig. 3.8 confirms that the proposed iterative algorithm achieves the same performance as the baseline.

3.6 Conclusion

In this chapter, a multi-cell beamforming scheme has been proposed to minimise the total transmit power across the network while maintaining required SINR level for each user. Downlink beamforming vectors for all users of the network are jointly designed as if all coordinating BSs were a single BS. A channel model of distributed-array antenna has been introduced. The model captures angular spreads due to the existence of local scatterers surrounding each user. A spatial covariance matrix for the DAA channel model has been derived. In order to reduce backhaul burden, the network is divided into several triangular zones where 3 adjacent BSs are located at vertices of a triangular zone. As a user is always confined to a triangular zone, data for that user will only be circulated within 3 BSs of that triangular zone. Then, a user position aware algorithm

has been introduced for a triangular zone such that any user is only allocated to the nearby BSs. An iterative algorithm has been proposed to find optimal solution to the optimisation problem of multi-cell beamforming using uplink-downlink duality. The convergence of the algorithm depends on the number of antenna elements, the targeted SINRs and the number of active users. Monte-Carlo simulation results confirm that the proposed algorithm can attain the optimal solution with the accuracy of 10^{-7} for the worst case, after just 50 iterations. In this chapter, BSs are coordinated at signal level where user data are shared amongst BSs. In order to reduce backhaul burden, a beamforming scheme that does not require users' data circulation is developed in the next chapter.

Chapter 4

Coordinated beamforming

In order to avoid data circulation, BSs are allowed to cooperate at beamforming level. This chapter covers a coordinated beamforming (CBF) scheme for a multi-cell scenario where precoding/beamforming vectors for all coordinating BSs are jointly designed in a manner that each BS only transmits to local users. Total transmit power across coordinating BSs is minimised while keeping the signal-to-interference-plus-noise ratio (SINR) at each user above the required level. The optimisation problem for CBF is formulated in a standard semidefinite programming form using both instantaneous and second-order-statistical channel state information. Taking into consideration the uncertainty in the estimation of channel covariance matrix, the CBF algorithm based on the second-order-statistical properties of channel is developed so that the robustness of the designed system parameters is guaranteed within a tolerable channel estimation error. It is shown that, although this robustness comes at the expense of increased overall power, a significant reduction in signalling overhead can be attained with a minor increase in total transmit power at moderately low SINRs.

4.1 Introduction

The problem of finding beamforming vectors that minimise the transmit power at a base station (BS) while maintaining certain levels of signal-to-interference-plus-noise ratios (SINRs) for its users is known as a non-convex optimisation problem [56] which is NP-hard. Semidefinite programming (SDP) [45], otherwise known as linear matrix inequalities programming, is regarded as a convex optimisation technique [56]. Using SDP to implement beamforming schemes in practice has become easier thanks to recent advances in real-time convex optimisation [76]. Elegant frameworks have been proposed in [56] and [22] to formulate the aforementioned optimisation problem in a standard SDP form employing channel covariance matrix and instantaneous channel

state information (CSI), respectively, in a single-cell scenario. When neighbouring BSs use different carrier frequencies, these solutions work in a multi-cell network, otherwise, they face the ping-pong-effect problem with cell-edge users, i.e., each BS keeps increasing its transmit power to maintain its users' required SINRs, due to inter-cell interference. Recently, the work in [56] has been developed in [77] to independently design beamforming vectors in each BS while tolerating controlled levels of interference from users of other cells. The solution solves the ping-pong-effect problem, although, the total transmit power across all BSs is not always globally optimal.

In order to achieve the global optimal solution to the total transmit power, beamforming vectors for all coordinating BSs should be jointly designed in a manner that each BS only transmits to local users. This technique is referred to as coordinated beamforming (CBF). It is most likely that no work to formulate optimisation problem for CBF, i.e., multi-cell scenario, in a SDP form has ever been carried out. Based on Lagrangian theory, an iterative algorithm has been proposed in [71] to solve the optimisation problem for CBF with instantaneous CSI. This is referred to as iCBF scheme in this chapter. The downlink beamforming vectors of the iCBF are determined by multiplication of some scalars and the corresponding virtual uplink beamforming vectors which, in turn, are found by the MMSE solution, i.e., [71]. Limitation of the dual uplink solution to MMSE can be interpreted as an additional constraint to the original optimisation problem. This additional constraint degrades system performance as the feasibility region of the equivalent problem is smaller than the one of the original problem.

In this chapter, in order to avoid the problem of narrowing down the original feasibility region imposed by iCBF, the optimisation problem for CBF is formulated in the SDP form. Casting of the problem in the SDP form is independent of the uplink and downlink duality. The proposed scheme uses instantaneous CSI which requires frequent signaling amongst users and the serving BSs. According to [36], the variation of CSI due to the motion of a user can be confined to a certain subspace. Therefore, in this work, a CBF scheme using channel covariance matrix is developed. The scheme is designed to tolerate a certain level of error in the estimation of the covariance matrix. Despite the occurrence of the robustness at the expense of increased transmit power, a significant reduction in signaling overhead can be achieved with a minor increase in total transmit power at moderately low SINRs.

The chapter is organised as follows. Section 4.2 introduces the system model. Sections 4.3 and 4.4 formulate the optimisation problem for CBF using instantaneous CSI and channel covariance matrix, respectively. Simulation results are presented and

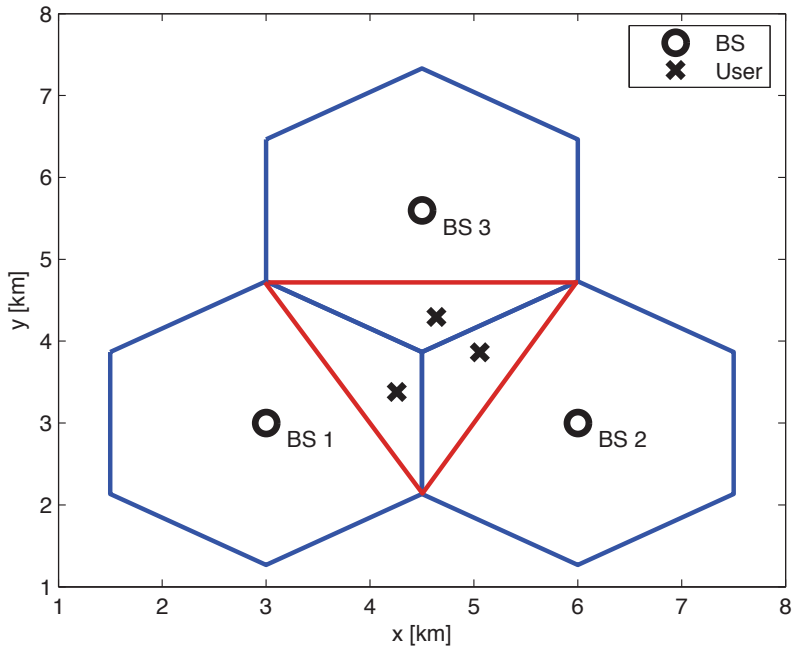

Figure 4.1: Illustration of a network of 3 cells with 3 users, i.e., 1 user per cell. Users are randomly dropped within the triangle.

discussed in Section 4.5. Finally, Section 4.6 concludes the chapter.

4.2 System model

Consider the downlink for a joint-processing network of N cells in which a BS of each cell is equipped with M antennas. Without any loss of generality, assuming that each cell has U users. Within that network, the same carrier frequency is used to support NU simultaneous single-antenna users. Fig. 4.1 illustrates an example of a network of 3 cells with 1 user per cell. Let $\mathbf{w}_i(p) \in \mathcal{C}^{M\times 1}$ represent the beamforming vector for the ith user of cell p, $s_{i(p)}$ denote the ith user's symbol at the pth cell, $\mathbf{x}_p = \sum_{i=1}^{U} \mathbf{w}_i(p) s_{i(p)}$ be the transmitted signal by the pth base station, i.e., $\mathbf{x}_p \in \mathcal{C}^{M\times 1}$, and $\mathbf{x} = \begin{bmatrix} \mathbf{x}_1^T & \mathbf{x}_2^T & \cdots & \mathbf{x}_N^T \end{bmatrix}^T$. It is assumed that $\mathbb{E}\left(s_{i(p)}^* s_{i(p)}\right) = 1$ for all users. Furthermore, let

$$\overline{\mathbf{H}}_{i(p)} = \begin{bmatrix} \mathbf{h}_{i(p)}(1) & \mathbf{0} & \cdots & \mathbf{0} \\ \mathbf{0} & \mathbf{h}_{i(p)}(2) & \cdots & \mathbf{0} \\ \vdots & \vdots & \vdots & \vdots \\ \mathbf{0} & \mathbf{0} & \cdots & \mathbf{h}_{i(p)}(N) \end{bmatrix}, \tag{4.1}$$

where the subscript $i(p)$ denotes user i in cell p, $\mathbf{h}_{i(p)}(q) \in \mathcal{C}^{1\times M}$ is the channel of user $i(p)$ as seen by cell q and $\mathbf{0}$ represents $1\times M$ vector with all zeros elements. Throughout the paper, $i, u, m \in \{1, 2\cdots, U\}$ while $p, q \in \{1, 2\cdots, N\}$. The received signal at user $i(p)$, i.e., $y_{i(p)} \in \mathcal{C}$, is

$$y_{i(p)} = \sum_{q=1}^{N} \mathbf{e}_q^T \overline{\mathbf{H}}_{i(p)} \mathbf{x} + z_{i(p)}, \tag{4.2}$$

where $z_{i(p)}$ is the zero mean circularly symmetric complex Gaussian (ZMCSCG) random variable, i.e., $z_{i(p)} \sim \mathcal{N}(0, \sigma_N^2)$, modeling the additive white Gaussian noise at the receiving point of user $i(p)$.

4.3 Coordinated beamforming using instantaneous channel state information

For a joint-designing purpose, N vectors $\mathbf{w}_i(p)$ of N different cells are collected in a vector $\mathbf{w}_i \in \mathcal{C}^{NM\times 1}$ as

$$\mathbf{w}_i = \begin{bmatrix} \mathbf{w}_i(1) \\ \mathbf{w}_i(2) \\ \vdots \\ \mathbf{w}_i(N) \end{bmatrix}. \tag{4.3}$$

Each vector $\mathbf{w}_i$ contains precoding vectors for the ith group of N users. In general, the number of active users in each cell may be different which results in less than N active users in certain groups. A non-zero vector $\mathbf{w}_i(p)$ in $\mathbf{w}_i$ indicates an active user within cell p of group i. The optimisation problem for the joint design of precoding vectors in CBF is formulated as

$$\begin{aligned} \min_{\mathbf{w}_i} \quad & \sum_{i=1}^{U} \mathbf{w}_i^H \mathbf{w}_i \\ \text{subject to} \quad & \text{SINR}_{i(p)} \geq \gamma_{i(p)}, \\ & \text{for all } 1 \leq p \leq N, 1 \leq i \leq U \end{aligned} \tag{4.4}$$

where $\gamma_{i(p)}$ is the targeted SINR of user $i(p)$ and the value of $\text{SINR}_{i(p)}$ is given as

$$\text{SINR}_{i(p)} = \frac{\left|\mathbf{e}_p^T \overline{\mathbf{H}}_{i(p)} \mathbf{w}_i\right|^2}{\sum_{u=1,u\neq i}^{U} \left|\mathbf{e}_p^T \overline{\mathbf{H}}_{i(p)} \mathbf{w}_u\right|^2 + \sum_{q=1,q\neq p}^{N} \sum_{m=1}^{U} \left|\mathbf{e}_q^T \overline{\mathbf{H}}_{i(p)} \mathbf{w}_m\right|^2 + \sigma_N^2}. \tag{4.5}$$

Denoting

$$\mathbf{W} = \begin{bmatrix} \mathbf{w}_1 & \mathbf{w}_2 & \cdots & \mathbf{w}_K \end{bmatrix}, \tag{4.6}$$

$\text{SINR}_{i(p)}$ is rewritten as

$$\text{SINR}_{i(p)} = \frac{\left|\mathbf{e}_p^T \overline{\mathbf{H}}_{i(p)} \mathbf{W} \mathbf{e}_i\right|^2}{\sum_{u=1,u\neq i}^{U} \left|\mathbf{e}_p^T \overline{\mathbf{H}}_{i(p)} \mathbf{W} \mathbf{e}_u\right|^2 + \sum_{q=1,q\neq p}^{N} \sum_{m=1}^{U} \left|\mathbf{e}_q^T \overline{\mathbf{H}}_{i(p)} \mathbf{W} \mathbf{e}_m\right|^2 + \sigma_N^2}. \quad (4.7)$$

Introducing a slack variable P_0, (4.4) is recast as follows

$$\begin{aligned} \min_{\mathbf{W}, P_0} \quad & P_0 \\ \text{subject to} \quad & \text{SINR}_{i(p)} \geq \gamma_{i(p)}, \\ & \text{Tr}\left[\mathbf{W}^H \mathbf{W}\right] \leq P_0 \\ & \text{for all } 1 \leq p \leq N, 1 \leq i \leq U. \end{aligned} \quad (4.8)$$

In the following, the optimisation problem (4.8) is transformed into standard SDP form. First, rearranging the SINR constraint in (4.8) yields

$$\frac{1}{\gamma_{i(p)}} \left|\mathbf{e}_p^T \overline{\mathbf{H}}_{i(p)} \mathbf{W} \mathbf{e}_i\right|^2 \geq \sum_{u=1,u\neq i}^{U} \left|\mathbf{e}_p^T \overline{\mathbf{H}}_{i(p)} \mathbf{W} \mathbf{e}_u\right|^2 + \sum_{q=1,q\neq p}^{N} \sum_{m=1}^{U} \left|\mathbf{e}_q^T \overline{\mathbf{H}}_{i(p)} \mathbf{W} \mathbf{e}_m\right|^2 + \sigma_N^2. \quad (4.9)$$

Adding $\left|\mathbf{e}_p^T \overline{\mathbf{H}}_{i(p)} \mathbf{W} \mathbf{e}_i\right|^2$ to both sides of (4.9) results in

$$\left(1 + \frac{1}{\gamma_{i(p)}}\right) \left|\mathbf{e}_p^T \overline{\mathbf{H}}_{i(p)} \mathbf{W} \mathbf{e}_i\right|^2 \geq \sum_{q=1}^{N} \sum_{m=1}^{U} \left|\mathbf{e}_q^T \overline{\mathbf{H}}_{i(p)} \mathbf{W} \mathbf{e}_m\right|^2 + \sigma_N^2. \quad (4.10)$$

It can be verified that

$$\sum_{q=1}^{N} \sum_{m=1}^{U} \left|\mathbf{e}_q^T \overline{\mathbf{H}}_{i(p)} \mathbf{W} \mathbf{e}_m\right|^2 = \left\|\text{vec}\left(\overline{\mathbf{H}}_{i(p)} \mathbf{W}\right)\right\|^2 = \left\|\text{vec}\left(\mathbf{P}_i \mathbf{H}_p \mathbf{W}\right)\right\|^2 \quad (4.11)$$

where

$$\mathbf{H}_p = \begin{bmatrix} \overline{\mathbf{H}}_{1(p)} \\ \overline{\mathbf{H}}_{2(p)} \\ \vdots \\ \overline{\mathbf{H}}_{U(p)} \end{bmatrix}$$

and

$$\mathbf{P}_i = \begin{bmatrix} \cdots & \vdots & \mathbf{0} & \vdots & \mathbf{I} & \vdots & \mathbf{0} & \vdots & \cdots \end{bmatrix}$$

is a $N \times NU$ permutation block matrix with $N \times N$ identity matrix $\mathbf{I}$ as the ith block and blocks of $N \times N$ all zero matrices $\mathbf{0}$ elsewhere.

Using (4.11), (4.10) is rewritten as follows

$$\left(1+\frac{1}{\gamma_{i(p)}}\right)\left|\mathbf{e}_p^T\overline{\mathbf{H}}_{i(p)}\mathbf{W}\mathbf{e}_i\right|^2 \geq \left\|\begin{bmatrix}\mathrm{vec}\left(\mathbf{P}_i\mathbf{H}_p\mathbf{W}\right)\\ \sigma_N\end{bmatrix}\right\|^2. \tag{4.12}$$

Let $\mathbf{W}^\star$ be an optimal solution to (4.8) and

$$\mathbf{D}=\begin{bmatrix} e^{j\psi_1} & 0 & \cdots & 0\\ 0 & e^{j\psi_2} & \cdots & 0\\ \vdots & \vdots & \vdots & \vdots\\ 0 & 0 & \cdots & e^{j\psi_U}\end{bmatrix}$$

where ψ_i is an arbitrary phase. Consider $\mathbf{A}=\left(\mathbf{W}^\star\mathbf{D}\right)^H\left(\mathbf{W}^\star\mathbf{D}\right)$. Using (4.6) one can write

$$\mathbf{A}=\begin{bmatrix} \mathbf{w}_1^H\mathbf{w}_1 & \mathbf{w}_1^H\mathbf{w}_2e^{j(\psi_2-\psi_1)} & \cdots & \mathbf{w}_1^H\mathbf{w}_Ue^{j(\psi_U-\psi_1)}\\ \mathbf{w}_2^H\mathbf{w}_1e^{j(\psi_1-\psi_2)} & \mathbf{w}_2^H\mathbf{w}_2 & \cdots & \mathbf{w}_2^H\mathbf{w}_Ue^{j(\psi_U-\psi_2)}\\ \vdots & \vdots & \vdots & \vdots\\ \mathbf{w}_U^H\mathbf{w}_1e^{j(\psi_1-\psi_U)} & \mathbf{w}_U^H\mathbf{w}_2e^{j(\psi_2-\psi_U)} & \cdots & \mathbf{w}_U^H\mathbf{w}_U\end{bmatrix}. \tag{4.13}$$

On the other hand, denoting $\mathbf{B}=\left(\mathbf{W}^\star\right)^H\mathbf{W}^\star$ then

$$\mathbf{B}=\begin{bmatrix} \mathbf{w}_1^H\mathbf{w}_1 & \mathbf{w}_1^H\mathbf{w}_2 & \cdots & \mathbf{w}_1^H\mathbf{w}_U\\ \mathbf{w}_2^H\mathbf{w}_1 & \mathbf{w}_2^H\mathbf{w}_2 & \cdots & \mathbf{w}_2^H\mathbf{w}_U\\ \vdots & \vdots & \vdots & \vdots\\ \mathbf{w}_U^H\mathbf{w}_1 & \mathbf{w}_U^H\mathbf{w}_2 & \cdots & \mathbf{w}_U^H\mathbf{w}_U\end{bmatrix}. \tag{4.14}$$

From (4.13) and (4.14), it is clear that $\mathrm{Tr}\left[\mathbf{A}\right]=\mathrm{Tr}\left[\mathbf{B}\right]$. Moreover, plugging $\mathbf{W}^\star\mathbf{D}$ and $\mathbf{W}^\star$ into (4.7) result in the same value. Therefore, if $\mathbf{W}^\star$ is an optimal solution to the problem (4.8), then $\mathbf{W}^\star\mathbf{D}$ is also an optimal solution. As a result, one can design the beamforming matrix $\mathbf{W}$ up to an arbitrary phase scaling so that the scalar $\mathbf{e}_p^T\overline{\mathbf{H}}_{i(p)}\mathbf{W}\mathbf{e}_i$ is always non-negative and real. Then, from (4.12), we can write the SINR constraint in a second-order-cone form as

$$\sqrt{1+\frac{1}{\gamma_{i(p)}}}\mathbf{e}_p^T\mathbf{P}_i\mathbf{H}_p\mathbf{W}\mathbf{e}_i \geq \left\|\begin{bmatrix}\mathrm{vec}\left(\mathbf{P}_i\mathbf{H}_p\mathbf{W}\right)\\ \sigma_N\end{bmatrix}\right\| \tag{4.15}$$

for all $1 \leq p \leq N, 1 \leq i \leq K$. Equivalently,

$$\begin{bmatrix} \sqrt{1+\frac{1}{\gamma_{i(p)}}}\mathbf{e}_p^T\mathbf{P}_i\mathbf{H}_p\mathbf{W}\mathbf{e}_i \\ \text{vec}\left(\mathbf{P}_i\mathbf{H}_p\mathbf{W}\right) \\ \sigma_N \end{bmatrix} \succeq_K 0,\ 1 \leq i \leq U,\ 1 \leq p \leq N. \tag{4.16}$$

Using the Schur complement (see Chapter 2), the second-order-cone constraint in (4.16) can be cast in a semi-definite (also known as linear matrix inequalities) form as

$$\mathbf{L}_{i(p)} = \begin{bmatrix} \sqrt{1+\frac{1}{\gamma_{i(p)}}}\mathbf{e}_p^T\mathbf{P}_i\mathbf{H}_p\mathbf{W}\mathbf{e}_i & \begin{bmatrix}\text{vec}^H\left(\mathbf{P}_i\mathbf{H}_p\mathbf{W}\right) & \sigma_N\end{bmatrix} \\ \begin{bmatrix}\text{vec}\left(\mathbf{P}_i\mathbf{H}_p\mathbf{W}\right) \\ \sigma_N\end{bmatrix} & \sqrt{1+\frac{1}{\gamma_{i(p)}}}\mathbf{e}_p^T\mathbf{P}_i\mathbf{H}_p\mathbf{W}\mathbf{e}_i\mathbf{I} \end{bmatrix} \succeq 0$$

for all $1 \leq p \leq N,\ 1 \leq i \leq U$.

Finally, the left hand side of the power constraint in (4.8) can be rewritten as

$$\text{Tr}\left[\mathbf{W}^H\mathbf{W}\right] = \left\|\text{vec}\left(\mathbf{W}\right)\right\|^2. \tag{4.17}$$

Then, the power constraint in (4.8) is cast in the second-order-cone form as

$$p_0 \geq \left\|\text{vec}\left(\mathbf{W}\right)\right\| \tag{4.18}$$

or

$$\begin{bmatrix} p_0 \\ \text{vec}\left(\mathbf{W}\right) \end{bmatrix} \succeq_K 0 \tag{4.19}$$

where $p_0 = \sqrt{P_0}$. Therefore, the power constraint is written in semi-definite form as

$$\mathbf{N} = \begin{bmatrix} p_0 & \text{vec}^H\left(\mathbf{W}\right) \\ \text{vec}\left(\mathbf{W}\right) & p_0\mathbf{I} \end{bmatrix} \succeq 0. \tag{4.20}$$

Now the CBF problem is recast in the SDP form as

$$\begin{aligned} \min_{\mathbf{W},p_0} \quad & p_0 \\ \text{subject to} \quad & \mathbf{L}_{i(p)} \succeq 0, \mathbf{N} \succeq 0, \\ & \text{for all } 1 \leq p \leq N,\ 1 \leq i \leq U. \end{aligned} \tag{4.21}$$

The problem stated in (4.21) can be solved by using an optimisation package, e.g., the SeDuMi solver [46], to attain the precoding matrix $\mathbf{W}$.

4.4 Robust coordinated beamforming using second-order-statistical channel state information

In the following, a robust CBF scheme that can tolerate a certain level of error in the estimation of channel covariance matrix is developed. Define a channel covariance matrix $\mathbf{R}_{i(p)}(q) = \mathbb{E}\left(\mathbf{h}_{i(p)}^H(q)\mathbf{h}_{i(p)}(q)\right)$. Let $\hat{\mathbf{R}}_{i(p)}(q)$ be the estimated value of the true channel covariance matrix $\mathbf{R}_{i(p)}(q)$ and $\mathbf{\Gamma}$ be the uncertainty matrix of the estimation, i.e., $\mathbf{R}_{i(p)}(q) = \hat{\mathbf{R}}_{i(p)}(q) + \mathbf{\Gamma}$. Moreover, it is assumed that the Frobenius norm of matrix $\mathbf{\Gamma}$ is upper bounded by δ, i.e., $\|\mathbf{\Gamma}\|_F \leq \delta$. The value of δ represents the tolerable error level of the proposed beamforming scheme. According to Section 2.4 of [78], the true channel covariance matrix can be bounded below and above by

$$\underline{\mathbf{R}_{i(p)}(q)} \preceq \mathbf{R}_{i(p)}(q) \preceq \overline{\mathbf{R}_{i(p)}(q)} \tag{4.22}$$

where

$$\underline{\mathbf{R}_{i(p)}(q)} = \hat{\mathbf{R}}_{i(p)}(q) - \delta\mathbf{I}, \tag{4.23}$$

$$\overline{\mathbf{R}_{i(p)}(q)} = \hat{\mathbf{R}}_{i(p)}(q) + \delta\mathbf{I} \tag{4.24}$$

and the notation $\mathbf{A} \preceq \mathbf{B}$ implies that the matrix $\mathbf{B} - \mathbf{A}$ is positive semidefinite.

Let $\mathbb{B}_n^t(\mathbf{R})$ be an operation which creates a diagonal block matrix of n blocks with $\mathbf{R}$ at the tth block and $(n-1)$ blocks of all zero matrices $\mathbf{0}$ with the same dimension as $\mathbf{R}$ elsewhere. For joint beamforming design, we denote $\hat{\mathbf{Q}}_{i(p)}(q) = \mathbb{B}_N^q\left(\hat{\mathbf{R}}_{i(p)}(q)\right)$ and $\mathbf{A}_q = \mathbb{B}_N^q(\mathbf{I})$, where $\hat{\mathbf{R}}_{i(p)}(q)$ and $\mathbf{I}$ are $M \times M$ matrices. The worst case of SINR of user i of cell p, i.e., $\widehat{\mathrm{SINR}}_{i(p)}$, is given as

$$\frac{\mathbf{w}_i^H\left[\hat{\mathbf{Q}}_{i(p)}(p) - \delta\mathbf{A}_p\right]\mathbf{w}_i}{\sum_{u=1,u\neq i}^{U}\mathbf{w}_u^H\left[\hat{\mathbf{Q}}_{i(p)}(p) + \delta\mathbf{A}_p\right]\mathbf{w}_u + \sum_{q=1,q\neq p}^{N}\sum_{m=1}^{U}\mathbf{w}_m^H\left[\hat{\mathbf{Q}}_{i(p)}(q) + \delta\mathbf{A}_q\right]\mathbf{w}_m + \sigma_N^2}. \tag{4.25}$$

The target is to find beamforming vectors that minimise the total transmit power while guaranteeing the worst case of SINR above the required level. The optimisation problem is stated as

$$\begin{aligned} \min_{\mathbf{w}_i} \quad & \sum_{i=1}^{U}\mathbf{w}_i^H\mathbf{w}_i \\ \text{subject to} \quad & \widehat{\mathrm{SINR}}_{i(p)} \geq \gamma_{i(p)}, \\ & \text{for all } 1 \leq p \leq N, 1 \leq i \leq U, \end{aligned} \tag{4.26}$$

where $\mathbf{w}_i$ and $\gamma_{i(p)}$ are defined in Section 4.3.

Defining a Hermitian-positive-semidefinite matrix $\mathbf{F}_i = \mathbf{w}_i\mathbf{w}_i^H$, using the equality $\mathbf{a}^H\mathbf{R}\mathbf{a} = \mathrm{Tr}\left[\mathbf{R}\mathbf{a}\mathbf{a}^H\right]$ and rearranging the constraint in (4.26), one can arrive at

$$\begin{aligned}&\frac{1}{\gamma_{i(p)}}\mathrm{Tr}\left[\left(\hat{\mathbf{Q}}_{i(p)}(p) - \delta\mathbf{A}_p\right)\mathbf{F}_i\right] - \sum_{u=1,u\neq i}^{U}\mathrm{Tr}\left[\left(\hat{\mathbf{Q}}_{i(p)}(p) + \delta\mathbf{A}_p\right)\mathbf{F}_u\right]\\ &- \sum_{q=1,q\neq p}^{N}\sum_{m=1}^{U}\mathrm{Tr}\left[\left(\hat{\mathbf{Q}}_{i(p)}(q) + \delta\mathbf{A}_q\right)\mathbf{F}_m\right] - \sigma_N^2 \geq 0.\end{aligned} \tag{4.27}$$

Subtracting and adding $\mathrm{Tr}\left[\left(\hat{\mathbf{Q}}_{i(p)}(p) + \delta\mathbf{A}_p\right)\mathbf{F}_i\right]$ to the left hand side of (4.27) yields

$$\begin{aligned}&\frac{1}{\gamma_{i(p)}}\mathrm{Tr}\left[\left(\hat{\mathbf{Q}}_{i(p)}(p) - \delta\mathbf{A}_p\right)\mathbf{F}_i\right] - \sum_{q=1}^{N}\sum_{m=1}^{U}\mathrm{Tr}\left[\left(\hat{\mathbf{Q}}_{i(p)}(q) + \delta\mathbf{A}_q\right)\mathbf{F}_m\right] - \sigma_N^2\\ &+\mathrm{Tr}\left[\left(\hat{\mathbf{Q}}_{i(p)}(p) + \delta\mathbf{A}_p\right)\mathbf{F}_i\right] \geq 0.\end{aligned} \tag{4.28}$$

Denoting the left hand side of (4.28) by $C_{i(p)}$ one can proceed as

$$\begin{aligned}C_{i(p)} &= \left(1 + \frac{1}{\gamma_{i(p)}}\right)\mathrm{Tr}\left[\hat{\mathbf{Q}}_{i(p)}(p)\mathbf{F}_i\right] - \sum_{q=1}^{N}\sum_{m=1}^{U}\mathrm{Tr}\left[\hat{\mathbf{Q}}_{i(p)}(q)\mathbf{F}_m\right] - \sigma_N^2\\ &\quad +\delta\left(1 - \frac{1}{\gamma_{i(p)}}\right)\mathrm{Tr}\left[\mathbf{A}_p\mathbf{F}_i\right] - \delta\sum_{q=1}^{N}\sum_{m=1}^{U}\mathrm{Tr}\left[\mathbf{A}_q\mathbf{F}_m\right] \qquad (4.29)\\ &= \left(1 + \frac{1}{\gamma_{i(p)}}\right)\mathrm{Tr}\left[\hat{\mathbf{Q}}_{i(p)}(p)\mathbf{F}_i\right] - \sum_{q=1}^{N}\sum_{m=1}^{U}\mathrm{Tr}\left[\hat{\mathbf{Q}}_{i(p)}(q)\mathbf{F}_m\right] - \sigma_N^2\\ &\quad +\delta\left(1 - \frac{1}{\gamma_{i(p)}}\right)\mathrm{Tr}\left[\mathbf{A}_p\mathbf{F}_i\right] - \delta\sum_{m=1}^{U}\mathrm{Tr}\left[\mathbf{F}_m\right]. \qquad (4.30)\end{aligned}$$

From (4.29) to (4.30), the following fact has been used:

$$\sum_{q=1}^{N}\sum_{m=1}^{U}\mathrm{Tr}\left[\mathbf{A}_q\mathbf{F}_m\right] = \sum_{m=1}^{U}\mathrm{Tr}\left[\sum_{q=1}^{N}\mathbf{A}_q\mathbf{F}_m\right] = \sum_{m=1}^{U}\mathrm{Tr}\left[\mathbf{I}\mathbf{F}_m\right] = \sum_{m=1}^{U}\mathrm{Tr}\left[\mathbf{F}_m\right]. \tag{4.31}$$

Introducing a slack variable T_o, (4.26) is recast in the SDP form as

$$\begin{aligned} \min_{\mathbf{F}_i, T_o} \quad & T_o \\ \text{subject to} \quad & C_{i(p)} \geq 0, \\ & T_o - \sum_{i=1}^{U} \text{Tr}\left[\mathbf{F}_i\right] \geq 0, \\ & \mathbf{F}_i = \mathbf{F}_i^H \succeq 0, \text{for all } 1 \leq p \leq N,\ 1 \leq i \leq U, \end{aligned} \tag{4.32}$$

where the third constraint ensures that $\mathbf{F}_i$ is a Hermitian and a positive semidefinite matrix. If the rank of $\mathbf{F}_i$ is one, then the problems in (4.32) and (4.26) are equivalent. Otherwise, the randomisation technique in [54] can be used to produce a set of rank-one solutions of $\mathbf{F}_i$ for (4.26). Given a rank one $\mathbf{F}_i$ solution, one can easily verify that the i^{th} beamforming vector $\mathbf{w}_i$ can be obtained by $\mathbf{w}_i = \sqrt{\epsilon_i}\mathbf{x}_i$, where ϵ_i and $\mathbf{x}_i$ are the eigenvalue and the eigenvector of $\mathbf{F}_i$, respectively.

4.5 Simulation results

In this section, the proposed beamforming strategies are compared against the iCBF scheme introduced in [71].

4.5.1 Simulation setup

This chapter considers an isolated 3-cell scenario which is used by several previous works, e.g., [69, 75], to evaluate the performance of those beamforming schemes. As shown in Fig. 4.1, users are randomly dropped in the critical area within the triangle. A set of 3 or 6 randomly dropped users within 3 adjacent sectors of 3 neighbouring cells is referred to as one user location. A correlated channel model, similar to [49] and [79], is obtained by factorising $\mathbf{h}_{i(p)}(q)$ in (4.1) as

$$\mathbf{h}_{i(p)}(q) \quad = \quad \mathbf{h}_w \mathbf{R}_{i(p)}^{1/2}(q), \tag{4.33}$$

where $\mathbf{h}_w \in \mathcal{C}^{1\times M}$ is randomly generated ZMCSCG variables with unit variance, $\mathbf{R}_{i(p)}(q) \in \mathcal{C}^{M\times M}$ is the spatial covariance matrix of user $i(p)$ as seen by BS q. As shown in (3.15), the (m,n)th element of the spatial covariance matrix $\mathbf{R}_{i(p)}(q)$ in (4.33) is given by

$$\sum_{t=1}^{Q} L_{i(p)}^{t}(q)\sigma_F^2 e^{-0.5\frac{(\sigma_s \ln 10)^2}{100}} e^{\frac{j2\pi\Delta}{\lambda}\left[(n-m)\sin\theta_{i(p)}(q)\right]} e^{-2\left[\frac{\pi\Delta\sigma}{\lambda}\left\{(n-m)\cos\theta_{i(p)}(q)\right\}\right]^2},$$

Table 4.1: Simulation parameters

Parameter	**Value**
Number of cells (N)	3
Number of users per sector (K)	1 or 2
Number of antennas per sector (M)	6
Antenna spacing	$\lambda/2$
Array antenna gain	15 dBi
Downlink carrier frequency	2 GHz
Noise power spectral density (all users)	-174 dBm/Hz
Noise figure at user receiver	5 dB
BS-to-BS's distance	3 km
Path loss model (l in km)	$128.1 + 37.6\log_{10}(l)$
Angular offset's standard deviation	2°
Log-normal shadowing's standard deviation	8 dB
Number of scatterers per user	5
Subchannel bandwidth's wide	15 kHz

where $m, n \in [1, M]$, Q is the number of randomly distributed scatterers in the vicinity of each user, $L^t_{i(p)}(q)$ is the path loss coefficient between BS q and the scatterer t of user $i(p)$, σ_F^2 is the variance of the complex Gaussian fading coefficient between BS q and scatterer t, σ_s is the standard deviation of the log-normal shadow fading coefficient between BS q and scatterer t, i.e., $10^{-\frac{x}{10}}$, $x \sim \mathcal{N}(0, \sigma_s^2)$, Δ is the distance between any two adjacent antenna elements at BSs, λ is the carrier wavelength and $\theta_{i(p)}(q)$ is the angle of departure for user $i(p)$ with respect to the broadside of the array of BS q. Furthermore, it is assumed that the resulting angle spread/offset due to the scatterers is distributed according to a zero mean normal distribution with standard deviation of σ. Simulation parameters are shown in table I. Each simulation cycle to find the average transmitted power per subchannel is averaged over 100 random user locations with 10,000 channel realisations per location for those schemes using instantaneous CSI. The SeDuMi solver [46] is used to attain the optimal solutions to the problems of proposed CBF schemes.

4.5.2 Performance evaluation

For different beamforming strategies, Figs. 4.2 and 4.3 show the variation of the sum-transmit power of 3 BSs against targeted SINR levels at user terminals with 3 users and 6 users, respectively. Results for CBF using channel covariance matrix have been attained with perfect estimation, i.e., $\delta = 0$.

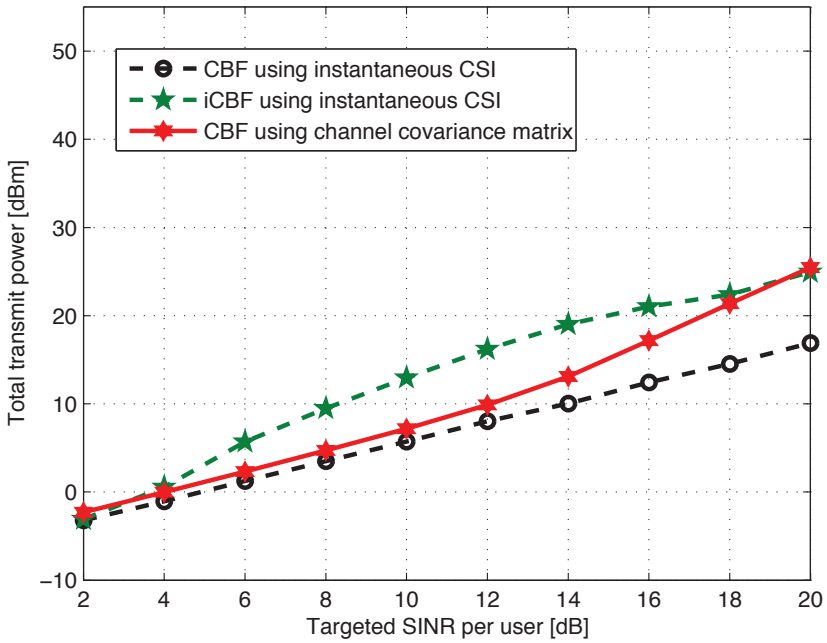

Figure 4.2: Total transmit power against targeted SINR at each user with 3 users.

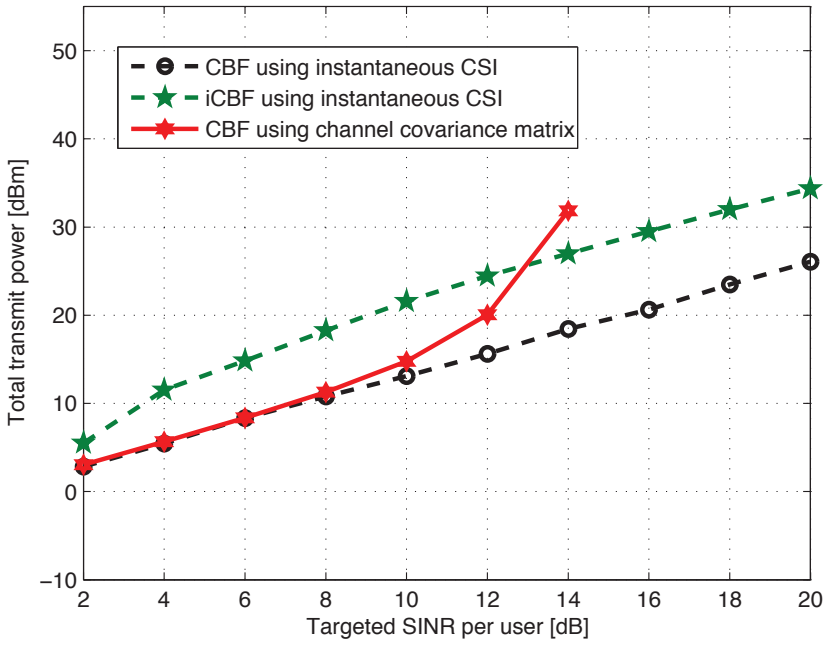

Figure 4.3: Total transmit power against targeted SINR at each user with 6 users.

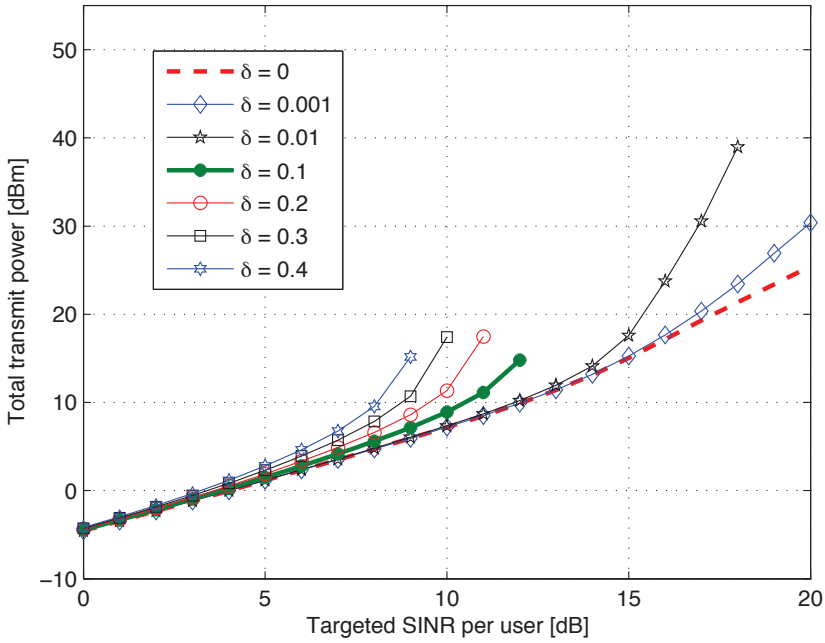

Figure 4.4: Total transmit power against targeted SINR at each user with 3 users and various values of δ.

It can be observed from Figs. 4.2 and 4.3 that despite using the same instantaneous CSI there is a gap between the CBF solution developed in this paper and the iCBF algorithm proposed in [71]. This performance gap can be explained as follows. The feasibility region of the iCBF optimisation problem in [71] is more restricted than the CBF optimisation problem in (4.4). In [71], the downlink beamforming vectors of the iCBF are found as the multiplication of some scalars by the corresponding virtual uplink beamforming vectors which are in turn found by the MMSE solution. Limitation of the dual uplink solution to MMSE can be interpreted as an additional constraint to the original optimisation problem (4.4). However this additional constraint is not imposed when formulating (4.4) in the SDP form. In other words, the iCBF algorithm only searches for the precoding vectors satisfying MMSE conditions within the original feasibility region of (4.4) while the CBF scheme introduced in this paper freely searches for every possible solution within the same original feasibility region.

From Figs. 4.2 and 4.3, one can conclude that CBF using channel covariance matrix is recommended instead of CBF using instantaneous CSI if the targeted SINR per user is less or equal 10 dB, since the former requires slightly higher transmit power but demands less signaling overhead than the latter. However, having instantaneous CSI

results in a high power saving in comparison with using channel covariance matrix when the targeted SINR per user is greater than 10 dB.

Fig. 4.4 illustrates the effect of estimation error on the performance of the proposed CBF using channel covariance matrix. At a given SINR, the total transmit power increases as the error level increases. For instance, at the targeted SINR of 10 dB the total transmit power is 7.3 dBm for $\delta = 0.01$ while it is 8.9 dBm for $\delta = 0.1$. For a given total transmit power, the lower level of error, the higher SINR can be attained. For example, at the total transmit power of 15 dBm, the scheme can attain 12 dB of SINR with $\delta = 0.1$ whereas it can provide more than 14 dB of SINR with $\delta = 0.01$. The fact can be explained as follows. Increasing the level of error in the estimation of channel covariance matrix is equivalent to the increase in the uncertainty of location of a user. Therefore, to ensure the required SINR for that user, the beam toward it needs to be wider. As a result, the transmit power increases.

It is worth noting that by using channel covariance matrix instead of instantaneous CSI, we accept more uncertainty/error in CSI estimation. Keeping that in mind to observe Figs. 4.2, 4.3 and 4.4, one can conclude that the performance of the proposed CBF schemes tend to converge at low region of SINR disregarding the level of uncertainty/error in CSI estimation. The observation points to the conclusion that signaling overhead between BSs and users can be significantly reduced with a minor sacrifice in terms of total transmit power when required SINRs are moderately low.

4.6 Conclusion

In this chapter, cooperation amongst BSs is performed at beamforming level to reduce backhaul burden. Beamforming vectors are jointly designed for coordinating BSs in a manner each BS only transmits to its own users. This chapter also aims to minimise the total transmit power across the network while maintaining required SINR level for every user. The optimisation problem for coordinated beamforming (CBF) using instantaneous CSI has been formulated in standard semidefinite programming (SDP) form. In order to reduce signalling overhead in attaining instantaneous CSI, the optimisation problem for CBF has also been cast in SDP form using second order statistical CSI, i.e., channel covariance matrix. The scheme is designed to tolerate a certain level of error in the estimation of the covariance matrix. Simulation results reveal that although the robustness comes at the cost of increased transmit power, a significant reduction in signaling overhead can be achieved with a minor increase in total transmit power at moderately low SINRs. The results also show that the perfor-

mance of two proposed CBF schemes tend to converge at the moderately low region of SINR disregarding the level of uncertainty/error in CSI estimation.

Since backhaul is essential to implement MBF and CBF, the next chapter proposes wireless backhaul protocols to enable links amongst coordinating BSs. Then a framework is introduced to evaluate the overall performance that includes backhaul affects of the proposed MBF and CBF schemes.

Chapter 5

Wireless backhaul for multi-cell processing

This chapter derives upper bounds on the throughput of the wireless backhaul link within a cluster of inter-connected three BSs or a cluster of a controlling BS and three fixed relay stations (RSs). Ring and Star protocols are proposed and analysed, respectively, for the former and the latter using network coding concept. The protocols can be used individually or in an overlaid fashion in a coordinated multi-cell system or in a cellular-distributed-antenna system to exchange information in the backhaul. In order to avoid the weakest link both acting as a bottleneck and determining the backhaul throughput, optimising time sharing factors that compensate for the resulting bit imbalances in the backhaul are derived. Based on the proposed Ring protocol for the wireless backhaul, a framework to evaluate the performance of the proposed MBF and CBF schemes is introduced.

5.1 Introduction

Recently, the idea of converting harmful inter-cell interferences into useful signals has motivated multi-cell processing (MCP) allowing inter-cell cooperation [23–26, 80, 81]. In MCP, multiple BSs are interconnected via a backhaul and their spatially distributed antennas are coordinated via joint decoding and encoding of messages, both in the uplink and in the downlink, e.g., [80–82]. Recent studies, i.e., [23–25], have confirmed the existence of high achievable gains of MCP in terms of coverage, performance and data rate. Furthermore, MCP in conjunction with a cellular-distributed-antenna system, i.e., [81], [83] and [84], can achieve a substantial energy saving at BSs through distributed antenna beamforming towards the intended users, forming nulls towards the unintended ones and avoiding long-range transmissions in the entire cellular network.

Distributed beamforming or multi-cell beamforming that is pivotal in coordinated multi-cell and distributed antenna systems relies on the exchange of information in an inter-connecting backhaul [26], [70] and [7]. Unlike conventional beamforming, where array antenna elements are co-located on one BS/RS, distributed beamforming is performed by a system of array antennas in several geographically separated BSs/RSs. In such scenarios, the transmitted data to the users need to be available to all BSs/RSs participating in the distributed beamforming process [7].

In this chapter, a theoretical bound of power-saving gain obtained by splitting a cell into tiers of smaller cells is derived. In an infrastructure arisen from cell splitting, unoccupied UHF frequency bands with very good propagation characteristics can be used to establish robust wireless links amongst the neighbouring BSs. This chapter contributes to the wireless backhaul by introducing a Ring protocol to exchange information amongst three BSs and a Star protocol to exchange information amongst three fixed RSs and one BS as the controlling unit. Throughout the chapter, a node refers to a BS or a RS, for simplicity. In literature, although network coding [85], [86] and, in particular, physical network coding [87] has been used for two-way communications between two source nodes [88–94]. Apparently, it has not yet been utilised for sharing information amongst more than two nodes in wireless backhaul. This work is inspired by [88], where physical network coding was used by a relay to establish a two-way communication between two nodes. In order to achieve the maximum throughput in the Star and Ring protocols, time sharing principles are derived. It is shown by derivation that the imbalance in the number of bits received by the controlling unit from any two source nodes has to be minimised in the MAC phase of both protocols. The throughput maximising expressions for the protocols are also found. Backhaul transmission strategies for these models based on the signal to noise ratios of the wireless links between the BSs are proposed.

The rest of this chapter is organised as follows. Targeted scenarios and system model are introduced in Section 5.3. Backhaul transmission protocols for Star and Ring models are proposed in Section 5.4. Section 5.5 covers throughput analysis for the proposed models. Comparisons of proposed beamforming schemes using the proposed Ring protocol are presented in Section 5.6. Finally, Section 5.7 concludes the chapter.

5.2 Cell splitting

The transmitting power level from both base stations and mobile terminals are constrained by not only the safety limits but also the so-called green communications. On

the other hand, huge increases in network capacity and coverage are envisaged due to the fast growing demand for mobile internet over the next decade. Hence, maintaining higher data rate per user terminal would mean diminishing coverage, as high speed transmission requires more power. Therefore, one needs to drop the coverage range, as the transmitted power by the base stations and the mobile terminals both are currently standing at the safety limits and well above the green communications targets. Cell splitting, i.e., dividing the existing macro cells into a number of smaller cells, can maintain the capacity and coverage while accounting for power safety limits at mobile terminals and avoiding high power macro cell base stations. Fig. 5.1 illustrates a divided macro cell into 4 tiers of smaller cells.

Consider the following definition:

Definition 5.1. *The power saving gain in cell splitting is defined as*

$$G = \frac{P_{eq}^{m}}{mP_0}, \tag{5.1}$$

where m is the number of small cells each having a central base station with power P_0 and P_{eq}^{m} is the required power by the macro cell base station to maintain the same received power at any given point on the macro cell edge as the power P_0 of a local small cell base station.

The structure of dividing one cell into seven smaller cells was studied in [81] and [83]. The power-saving again offered by splitting one cell into seven smaller cells was derived in [83]. Taking a further step, this chapter studies an architecture of an N-Tier system, where $N \geq 2$, and introduces *Lemma 5.1* as follows.

Lemma 5.1. *The possible power-saving gain when dividing a cell into N tiers of smaller cells is given as:*

$$G_N = \frac{[2.481N^2 - 2.135N + 0.654]^{\frac{\alpha}{2}}}{3N^2 - 3N + 1}, \tag{5.2}$$

where α is the path loss exponent which typically ranges from 2 to 6, i.e., [3] and [4].

Proof. See Appendix C. □

It is shown in Fig. 5.2 that G varies versus path loss exponents, with various number of tiers N as the parameter. It should be noted that Fig. 5.2 is plotted in the worst case where the base stations of all small cells are active with P_0 transmitting power. However, cell splitting offers the flexibility of shutting down a base station when no active user is present in the corresponding small cell area.

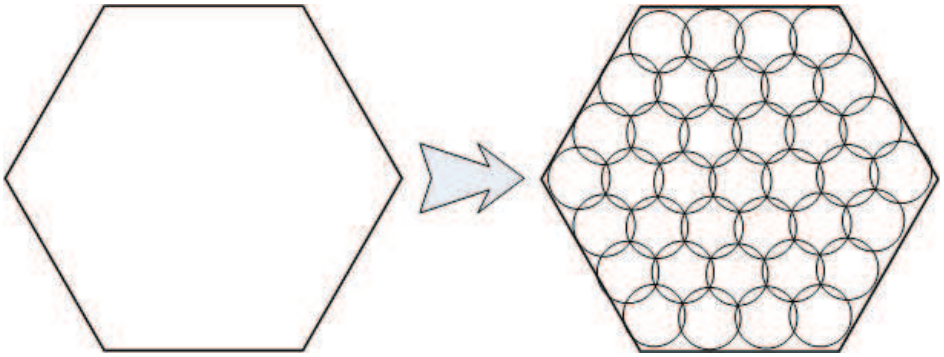

Figure 5.1: Dividing a cell into 4 tiers.

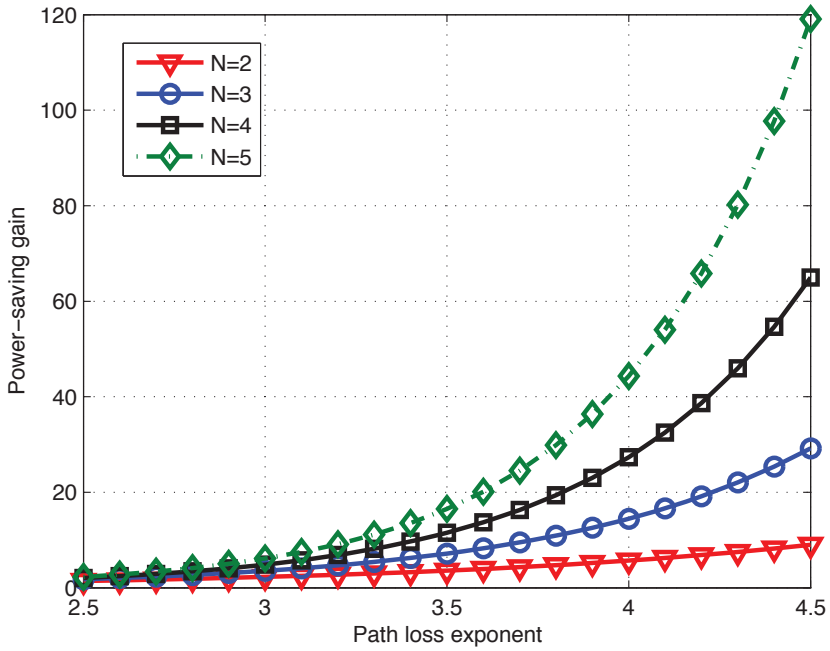

Figure 5.2: Power-saving gain against path loss exponent.

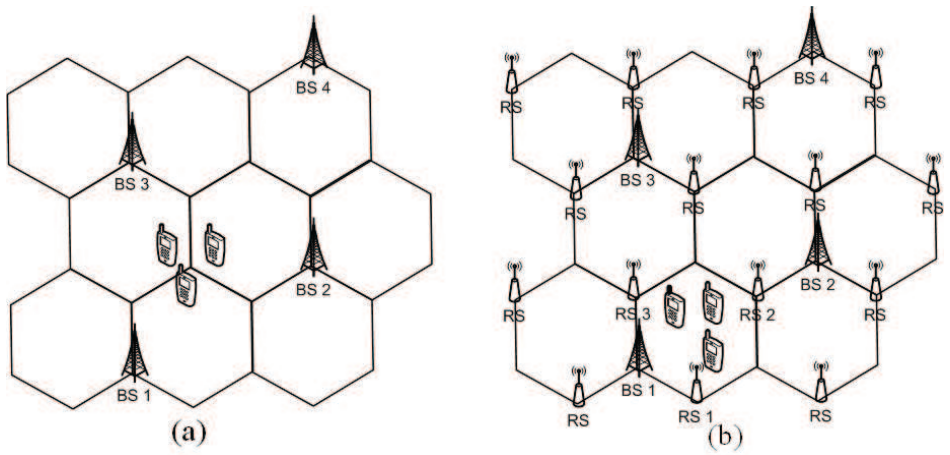

Figure 5.3: MCP scenarios: (a) Cooperative BSs. (b) Cellular distributed antenna system.

The scarcity of the available spectrum enforces an efficient reuse of bandwidth resources across small cells of a divided macro cell and, inevitably, the problem of inter-cell interference emerges as the major challenge in cell splitting. Inter-cell interference in cellular networks is influenced by two major factors, namely, path loss and cell size. According to the path-loss power model [4], the attenuation of the transmitted power over a distance d is proportional to $d^{-\alpha}$, where α is the path loss exponent. For a fixed cell size, inter-cell interference decreases exponentially with the increasing path loss exponent, as a result of a decreasing interference from an interfering transmitter. While, shrinking the cell size decreases the distance among the neighbouring BSs and, hence, increases inter-cell interference. In a MCP network, since the received signals at BSs are jointly decoded in the uplink and every user terminal receives useful signal from the cooperating BSs in the downlink, inter-cell interference is not only eliminated but it can also be beneficially used to provide diversity and multiplexing gains. However, achieving an energy efficient MCP network depends on whether the energy consumed on the backbone network and the joint processing can be balanced by the energy saved as a result of the eliminating inter-cell interference.

5.3 Scenarios and system model

5.3.1 Scenarios

The proposed wireless backhaul protocols and their respective throughput characterisations are motivated by the coordinated multi-cell scenarios and their associated clusters of cooperative BSs and/or fixed relay nodes, as depicted in Fig. 5.3. In Fig. 5.3a, a

cluster of three nearest neighbour BSs, i.e., BS1, BS2 and BS3 whose adjacent sector areas have common boundaries, jointly support the users in the vicinity of their inter-cell borders by distributed beamforming. As a result of this coordination, a consistent QoS, in terms of reception quality and data rate, can be guaranteed for the users within the cluster, irrespective of their distance from their respective BSs. This is because the inter-cell interference-free transmissions can be directed towards these users by forming a distributed antenna system with the geographically distributed antennas of their respective three BSs. In another scenario shown in Fig. 5.3b, a distributed antenna system composed of three fixed relay stations and a controlling BS, i.e., BS1, RS1, RS2, and RS3, is used to support the users within a sector. In this scenario, a substantial energy saving gain at BSs can be achieved by avoiding long-range transmissions [38] and exploiting the interference-free dimensions provided by coordinated distributed beamforming. Furthermore, a hybrid of these two scenarios can be used over the entire cellular network to achieve a substantial power saving gain at the BSs without compromising the consistency of the QoS at the user terminals, irrespective of their geographical locations. However, the distributed beamforming techniques in these scenarios require that the data available at each node within a cluster to be shared by the other nodes within the same cluster. In this chapter, fast network coding enabled wireless backhaul protocols are proposed for data exchange amongst the nodes within a cluster. Upper bounds on their respective overall throughputs are also derived.

5.3.2 System model

Let S_i, $i = 1, 2, 3$, and C be the i^{th} source node and a controlling unit, respectively. Star and Ring models are introduced according to Fig. 5.4 for the backhaul link. Consider the case that all nodes operate in half-duplex mode, i.e., they can only transmit or receive signal at a given time. Let x_{ij} be the symbol transmitted by node i and received by node j, where $i \neq j$ and $i, j \in \{1, 2, 3, C\}$, and m_{ij} denote the binary sequence mapped to x_{ij}. It is assumed that $\mathbb{E}(x_{ij}) = 0$ and $\mathbb{E}(|x_{ij}|^2) = 1$. Let n_j be a zero mean circularly symmetric complex Gaussian noise with variance N_0, i.e., $\mathcal{CN}(0, N_0)$, at node j and h_{ij} represent the complex channel coefficient between node i and node j. The received signal at node j is given by

$$y_j = h_{ij}x_{ij} + n_j. \tag{5.3}$$

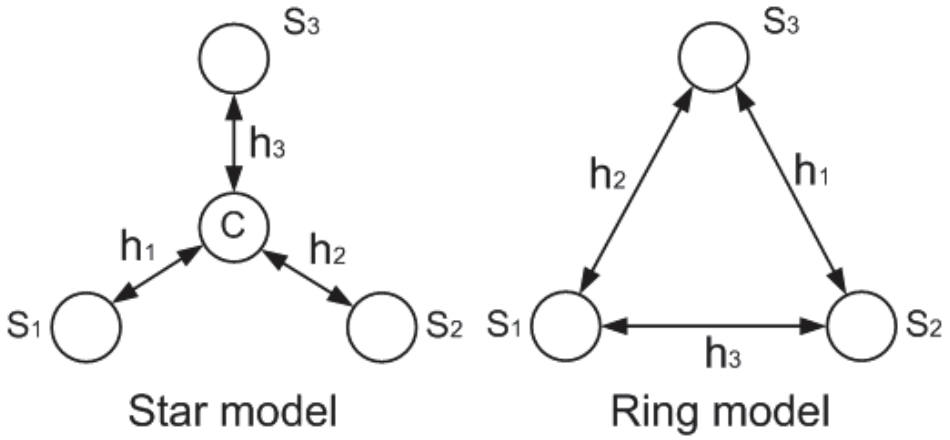

Figure 5.4: The Star and Ring models.

When node i and node j simultaneously transmit to node k, $k \neq i$, $k \neq j$ and $k \in \{1, 2, 3, C\}$, the received signal at node k can be written as

$$y_k = h_{ik}x_{ik} + h_{jk}x_{jk} + n_k. \tag{5.4}$$

Assuming that the forward and the reverse link coefficients from any node i to any node j are equal, remain unchanged, at least, during one cycle of information exchange in Star or Ring protocol and are known at all nodes. Hence, one can write $h_{1C} = h_{C1} = h_1$, $h_{2C} = h_{C2} = h_2$, $h_{3C} = h_{C3} = h_3$, for the Star model; and $h_{23} = h_{32} = h_1$, $h_{13} = h_{31} = h_2$, $h_{12} = h_{21} = h_3$, for the Ring model. Signal-to-noise ratio (SNR) values of γ_1, γ_2 and γ_3 are assigned, respectively, to the links with coefficients h_1, h_2 and h_3, where $\gamma_i = \frac{|h_i|^2}{N_0}$ for $i = 1, 2, 3$. Without loss of generality, it is assumed throughout this chapter that

$$\gamma_1 \leq \gamma_2 \leq \gamma_3. \tag{5.5}$$

Furthermore, assuming that the bandwidth is normalised to 1 [Hz], one can write the capacity of a link with SNR value of γ as $C(\gamma) = log_2(1 + \gamma)$ [bits/s/Hz].

Definition 5.2. *Let M be the total number of bits exchanged amongst all the nodes of the Star or Ring model over a time duration of T seconds and bandwidth of 1 Hz. Using the assumption that the coding and the decoding delays are small and can be ignored in comparison with T, the backhaul throughput is defined as*

$$R = \frac{M}{T} \qquad \textit{[bits/s/Hz]}. \tag{5.6}$$

In this chapter, $\oplus$, $|m_{ij}|$ and R_{ij} are used to represent bitwise XOR, number of bits in a packet m_{ij} and the data rate between node i and node j, respectively.

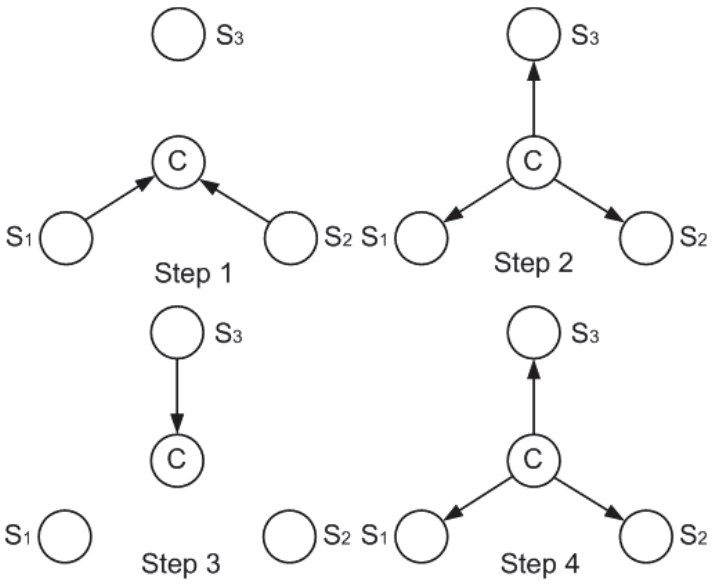

Figure 5.5: Steps of the transmission protocol for the Star model.

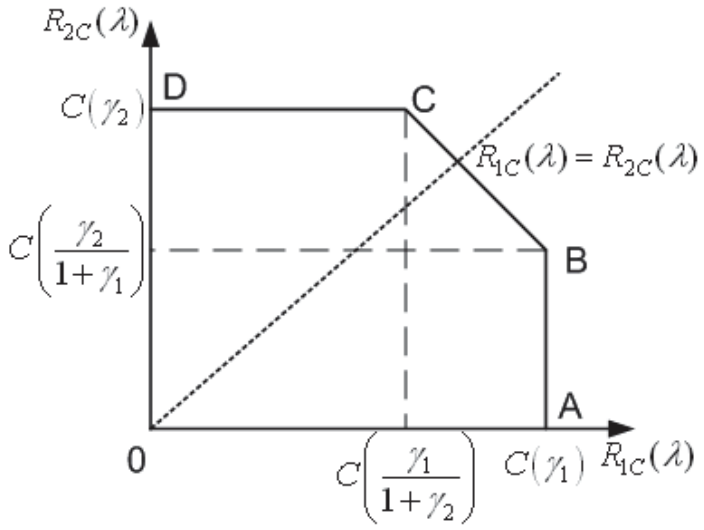

Figure 5.6: Capacity region for the Star model in step 1.

5.4 Backhaul transmission protocols

5.4.1 The Star model

Four steps are used to exchange information among three source nodes, as depicted in Fig. 5.5. In step 1, the controlling unit receives information from source node pairs (S_1, S_2), while in step 3 it only receives data from node S_3. Hence, data transmission in step 1 can be interpreted as a MAC phase. Whereas, in step 2 and step 4, controlling unit broadcasts information to all source nodes. Therefore, data transmission in step

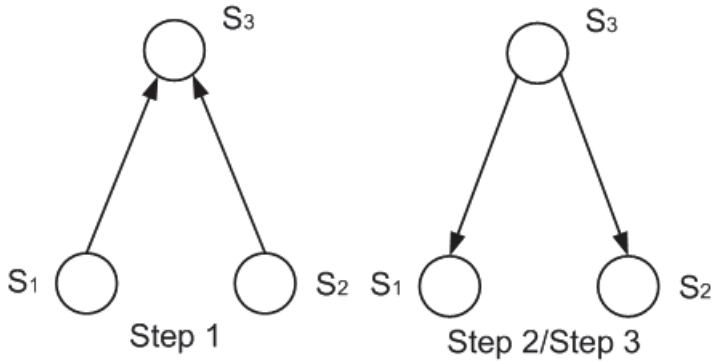

Figure 5.7: Steps of the transmission protocol for the Ring model.

2 or 4 can be interpreted as a BC phase.

In step 1, without loss of generality, let us consider the case where nodes S_1 and S_2 send their information with rates R_{1C} and R_{2C}, respectively, to the controlling unit C. If the rate pair (R_{1C}, R_{2C}) falls inside the capacity region of the MAC formed by S_1, S_2 and C, i.e., Fig. 5.6, C can decode the packets sent by S_1 and S_2. The sum-rate is maximised on the dominant face, i.e., on line CB, Fig. 5.6, and is given by [95]

$$R_{1C} + R_{2C} = C(\gamma_1 + \gamma_2). \tag{5.7}$$

The rate pairs on the dominant face of the MAC capacity region in Fig. 5.6 can be achieved by a time sharing factor $0 \leq \lambda \leq 1$, as follows [95]

$$R_{1C}(\lambda) = C\left(\frac{\gamma_1}{1+\gamma_2}\right) + \lambda\left(C(\gamma_1) - C\left(\frac{\gamma_1}{1+\gamma_2}\right)\right), \tag{5.8}$$

$$R_{2C}(\lambda) = C(\gamma_2) + \lambda\left(C\left(\frac{\gamma_2}{1+\gamma_1}\right) - C(\gamma_2)\right). \tag{5.9}$$

The time sharing factor $\lambda = \lambda_0$ that results in $R_{1C}(\lambda_0) = R_{2C}(\lambda_0) = \frac{C(\gamma_1+\gamma_2)}{2}$ is given by (see Appendix B),

$$\lambda_0 = \frac{2C(\gamma_2) - C(\gamma_1+\gamma_2)}{2C(\gamma_1) + 2C(\gamma_2) - 2C(\gamma_1+\gamma_2)}. \tag{5.10}$$

In the following, the details of the proposed Star protocol are described.

1. Step 1: Nodes S_1 and S_2 transmit packets m_{1C} with rate $R_{1C}(\lambda)$ and m_{2C} with rate $R_{2C}(\lambda)$, respectively, to controlling unit C. Since $R_{1C}(\lambda)$ and $R_{2C}(\lambda)$ are in the rate region of the corresponding MAC, the controlling unit C can decode m_{1C} and m_{2C}. Two cases, i.e., $R_{1C}(\lambda) > R_{2C}(\lambda)$ and $R_{1C}(\lambda) \leq R_{2C}(\lambda)$, are distinguished as follows:

- Case 1 [$R_{1C}(\lambda) > R_{2C}(\lambda)$]: In this case $|m_{1C}| > |m_{2C}|$ and controlling unit C splits m_{1C} into m_{1C}^1 with $|m_{1C}^1| = |m_{2C}|$ bits and m_{1C}^2 with $|m_{1C}^2| = |m_{1C}| - |m_{1C}^1|$ bits.
- Case 2 [$R_{1C}(\lambda) \leq R_{2C}(\lambda)$]: In this case $|m_{1C}| \leq |m_{2C}|$ and controlling unit C pads $|m_{2C}| - |m_{1C}|$ zero bits to the end of m_{1C} to form m_{1C}^p such that $|m_{1C}^p| = |m_{2C}|$ bits.

2. Step 2: Depending upon the occurrence of Case 1 or Case 2 in step 1, the process is continued as follows:

   - If $R_{1C}(\lambda) > R_{2C}(\lambda)$, first, controlling unit C combines m_{1C}^1 and m_{2C} as $m = m_{1C}^1 \oplus m_{2C}$ and broadcasts m with rate $C(\gamma_1)$, which is decodable at all nodes. Then, controlling unit C broadcasts m_{1C}^2 with a higher rate $C(\gamma_2)$ which is decodable only at nodes S_2 and S_3, because of assumption (5.5). Node S_1 extracts m_{2C} according $m_{2C} = m_{1C}^1 \oplus (m_{1C}^1 \oplus m_{2C})$ and node S_2 extracts m_{1C} as the concatenation of $m_{1C}^1 = m_{2C} \oplus (m_{2C} \oplus m_{1C}^1)$ and m_{1C}^2.
   - If $R_{1C}(\lambda) \leq R_{2C}(\lambda)$, the controlling unit combines m_{1C}^p and m_{2C} as $m = m_{1C}^p \oplus m_{2C}$ and broadcasts m with rate $C(\gamma_1)$, which is decodable at all nodes. Node S_1 extracts m_{2C} according $m_{2C} = m_{1C}^p \oplus (m_{1C}^p \oplus m_{2C})$ and node S_2 extracts m_{1C} as the first $|m_{1C}|$ bits of $m_{1C}^p = m_{2C} \oplus (m_{2C} \oplus m_{1C}^p)$.

   At the end of this step, although m_{1C} and m_{2C} are known to nodes S_1 and S_2, they are unknown to node S_3. In the following steps, i.e., 3 and 4, m_{1C} and m_{2C} are revealed to S_3, as well.

3. Step 3: Nodes S_3 transmits m_{3C} with rate R_{3C}, i.e., $0 < R_{3C} \leq C(\gamma_3)$, to the controlling unit C. As $R_{3C} \in (0, C(\gamma_3)]$, the controlling unit C can decode m_{3C}. Here, two cases, i.e., $R_{2C}(\lambda) \geq R_{3C}$ and $R_{2C}(\lambda) < R_{3C}$, can be distinguished as follows:

   - Case 3 [$R_{2C}(\lambda) \geq R_{3C}$]: In this case $|m_{2C}| \geq |m_{3C}|$, the controlling unit pads $|m_{2C}| - |m_{3C}|$ zero bits to the end of m_{3C} to form m_{3C}^p such that $|m_{3C}^p| = |m_{2C}|$ bits.
   - Case 4 [$R_{2C}(\lambda) < R_{3C}$]: In this case $|m_{2C}| < |m_{3C}|$, the controlling unit pads $|m_{3C}| - |m_{2C}|$ zero bits to the end of m_{2C} to form m_{2C}^p such that $|m_{2C}^p| = |m_{3C}|$ bits.

4. Step 4: Depending upon the occurrence of Case 3 or Case 4 in step 3, the process is continued as follows:

- If $R_{2C}(\lambda) \geq R_{3C}$, the controlling unit combines m_{3C}^p and m_{2C} as $m = m_{3C}^p \oplus m_{2C}$ and broadcasts m with rate $C(\gamma_1)$. Nodes S_1 and S_2 extract m_{3C} as the first $|m_{3C}|$ bits of $m_{3C}^p = m_{2C} \oplus (m_{3C}^p \oplus m_{2C})$. Then, S_3 extracts m_{2C} according $m_{2C} = m_{3C}^p \oplus (m_{3C}^p \oplus m_{2C})$. Finally, depending on whether Case 1 or Case 2 in step 1 is satisfied, S_3 decodes m_{1C} as the concatenation of $m_{1C}^1 = m_{2C} \oplus (m_{2C} \oplus m_{1C}^1)$ and m_{1C}^2 or as the first $|m_{1C}|$ bits of $m_{1C}^p = m_{2C} \oplus (m_{2C} \oplus m_{1C}^p)$, respectively.
- If $R_{2C}(\lambda) < R_{3C}$, the controlling unit combines m_{2C}^p and m_{3C} as $m = m_{2C}^p \oplus m_{3C}$ and broadcasts m with rate $C(\gamma_1)$. Nodes S_1 and S_2 extract m_{3C} according $m_{3C} = m_{2C}^p \oplus (m_{2C}^p \oplus m_{3C})$. Then, S_3 extracts m_{2C} according $m_{2C} = m_{3C}^p \oplus (m_{3C}^p \oplus m_{2C})$. Finally, depending on whether Case 1 or Case 2 in step 1 is satisfied, S_3 decodes m_{1C} as the concatenation of $m_{1C}^1 = m_{2C} \oplus (m_{2C} \oplus m_{1C}^1)$ and m_{1C}^2 or as the first $|m_{1C}|$ bits of $m_{1C}^p = m_{2C} \oplus (m_{2C} \oplus m_{1C}^p)$, respectively.

Therefore, in step 4, m_{1C}, m_{2C} and m_{3C} are fully decoded at every node S_1, S_2, S_3 and controlling unit C. Furthermore, if controlling unit C also acts as a source node, then in step 5, the controlling unit can share its own packet with nodes S_1, S_2 and S_3 by broadcasting it at the lowest rate $C(\gamma_1)$, so that it is decodable at all nodes.

5.4.2 The Ring model

This sub-section introduces a protocol based on a Ring model. In particular, the protocol is capable of handling at most one weak or broken link between any two nodes, i.e., due to a low SNR, shadowing or etc, efficiently in terms of backhaul throughput. Suppose without loss of generality that there is such a bad link between S_1 and S_2. In this case, as shown in Fig. 5.7, S_3 acts as a controlling unit and listens to the packets sent by S_1 and S_2 at rates R_{13} and R_{23}, respectively. It is assumed that R_{13} and R_{23} fall in the convex hull of the corresponding MAC capacity region and their sum is maximised on the dominant face as [95]

$$R_{13} + R_{23} = C(\gamma_1 + \gamma_2). \tag{5.11}$$

The rate pairs on the dominant face can be achieved by a time sharing factor

$0 \leq \lambda \leq 1$ as follows [95]

$$R_{23}(\lambda) = C\left(\frac{\gamma_1}{1+\gamma_2}\right) + \lambda\left(C(\gamma_1) - C\left(\frac{\gamma_1}{1+\gamma_2}\right)\right), \tag{5.12}$$

$$R_{13}(\lambda) = C(\gamma_2) + \lambda\left(C\left(\frac{\gamma_2}{1+\gamma_1}\right) - C(\gamma_2)\right). \tag{5.13}$$

The time sharing factor $\lambda = \lambda_0$ that results in $R_{13}(\lambda_0) = R_{23}(\lambda_0) = \frac{C(\gamma_1+\gamma_2)}{2}$ is given by (see Appendix B),

$$\lambda_0 = \frac{2C(\gamma_2) - C(\gamma_1+\gamma_2)}{2C(\gamma_1) + 2C(\gamma_2) - 2C(\gamma_1+\gamma_2)}. \tag{5.14}$$

In the following, the details of the proposed Ring protocol are described in three steps.

1. Step 1: Nodes S_1 and S_2 transmit m_{13} with rate $R_{13}(\lambda)$ and m_{23} with rate $R_{23}(\lambda)$, respectively, to the controlling unit S_3. Since $R_{13}(\lambda)$ and $R_{23}(\lambda)$ are in the rate region of the corresponding MAC, the controlling unit S_3 can decode m_{13} and m_{23}. Two cases are distinguished as follows:

   - Case 1 [$R_{23}(\lambda) > R_{13}(\lambda)$]: In this case $|m_{23}| > |m_{13}|$, and controlling unit S_3 splits m_{23} into m_{23}^1 with $|m_{23}^1| = |m_{13}|$ bits and m_{23}^2 with $|m_{23}^2| = |m_{23}| - |m_{13}|$ bits.
   - Case 2 [$R_{23}(\lambda) \leq R_{13}(\lambda)$]: In this case $|m_{23}| \leq |m_{13}|$, and controlling unit S_3 pads $|m_{13}| - |m_{23}|$ zero bits to the end of m_{23} to form m_{23}^p such that $|m_{23}^p| = |m_{13}|$ bits.

2. Step 2: Based on whether Case 1 or Case 2 occurs in step 1, the process is continued as follows:

   - If $R_{23}(\lambda) > R_{13}(\lambda)$, first controlling unit S_3 combines m_{23}^1 and m_{13} as $m = m_{23}^1 \oplus m_{13}$ and broadcasts m with rate $C(\gamma_1)$ which is decodable at S_1 and S_2. Then S_3 transmits m_{23}^2 with a higher rate $C(\gamma_2)$ to node S_1.
   - If $R_{23}(\lambda) \leq R_{13}(\lambda)$, then controlling unit S_3 combines m_{23}^p and m_{13} as $m = m_{23}^p \oplus m_{13}$ and broadcasts m with rate $C(\gamma_1)$ which is decodable at both S_1 and S_2.

3. Step 3: S_3 broadcasts its own packet m_3 to S_1 and S_2 with rate $C(\gamma_1)$.

The decoding processes at nodes S_1 and S_2 after the first two steps are similar to the Star model and are not repeated here for brevity. At the end of step 2, m_{13} and m_{23} are fully decoded at nodes S_1, S_2, S_3 and at the end of step 3, all packets are known to all nodes.

5.5 Throughput analysis

This section obtains expressions for the maximum backhaul throughput for our network coding enabled Star and Ring protocols.

5.5.1 The Star model

First, relations between various rate regions, obtained by time sharing between the nodes and their corresponding SNRs, are established by the introduction of *Lemma 5.2*. Then, *Theorem 5.1* states the achievable maximum backhaul throughput for the Star model.

Lemma 5.2. *The following statements hold for any time sharing factor* $\lambda \in [0, 1]$*:*
If $\gamma_2 > \gamma_1 + \gamma_1^2$*, then* $R_{2C}(\lambda) > R_{1C}(\lambda)$.
For $\gamma_1 \leq \gamma_2 < \gamma_1 + \gamma_1^2$*:*
if $\lambda < \lambda_0$*, then* $R_{2C}(\lambda) > R_{1C}(\lambda)$*;*
if $\lambda = \lambda_0$*, then* $R_{2C}(\lambda_0) = R_{1C}(\lambda_0)$*;*
if $\lambda > \lambda_0$*, then* $R_{2C}(\lambda) < R_{1C}(\lambda)$.

Proof. See Appendix D. □

As shown in section 5.4, after four steps, all packets are fully decoded at every source node and the controlling unit. If controlling unit also acts as a source node, then an additional fifth step is required to deliver its packet to the other three source nodes. In this section, we analyse the maximum throughput for both 4-step and 5-step Star protocols by introducing *Theorem 5.1*.

Theorem 5.1. *The achievable upper bounds for the backhaul throughputs in 4-step and 5-step Star models are given in two regions, as follows:*

1. *Region 1: If* $\gamma_1 \leq \gamma_2 < \gamma_1 + \gamma_1^2$*, then the maximum backhaul throughput is achieved when* $\lambda = \lambda_0$ *and* $R_{3C} = C(\gamma_3)$ *and is given by*

$$R_{1,max}^{s,4} = \frac{2C(\gamma_1)\left[C(\gamma_1 + \gamma_2) + C(\gamma_3)\right]}{4C(\gamma_1) + C(\gamma_1 + \gamma_2) + 2C(\gamma_3)}, \tag{5.15}$$

for the 4-step protocol, and

$$R_{1,max}^{s,5} = \frac{2C(\gamma_1)\left[C(\gamma_1 + \gamma_2) + C(\gamma_3) + C(\gamma_1)\right]}{6C(\gamma_1) + C(\gamma_1 + \gamma_2) + 2C(\gamma_3)}, \tag{5.16}$$

for the 5-step protocol.

2. *Region 2: If* $\gamma_2 > \gamma_1 + \gamma_1^2$*, then the maximum backhaul throughput is achieved when* $\lambda = 1$ *and* $R_{3C} = C(\gamma_3)$ *and is given by*

$$R_{2,max}^{s,4} = \frac{C(\gamma_1)\left[C(\gamma_1+\gamma_2)+C(\gamma_3)\right]}{C(\gamma_1)+C(\gamma_1+\gamma_2)+C(\gamma_3)}, \tag{5.17}$$

for the 4-step protocol, and

$$R_{2,max}^{s,5} = \frac{C(\gamma_1)\left[C(\gamma_1+\gamma_2)+C(\gamma_3)+C(\gamma_1)\right]}{2C(\gamma_1)+C(\gamma_1+\gamma_2)+C(\gamma_3)}, \tag{5.18}$$

for the 5-step protocol.

Proof. See Appendix E. □

5.5.2 The Ring model

Following the same analytical steps as the Star model, the achievable maximum backhaul throughput of the Ring model is characterised by the introductions of *Lemma 5.3* and *Theorem 5.2*.

Lemma 5.3. *The following statements hold for any time sharing factor* $\lambda \in [0,1]$*:*
If $\gamma_2 > \gamma_1 + \gamma_1^2$*, then* $R_{13}(\lambda) > R_{23}(\lambda)$*.*
For $\gamma_1 \leq \gamma_2 < \gamma_1 + \gamma_1^2$*:*
if $\lambda < \lambda_0$*, then* $R_{13}(\lambda) > R_{23}(\lambda)$*;*
if $\lambda = \lambda_0$*, then* $R_{13}(\lambda_0) = R_{23}(\lambda_0)$*;*
if $\lambda > \lambda_0$*, then* $R_{13}(\lambda) < R_{23}(\lambda)$*.*

Note that without loss of generality, node S_3 has been assumed to be the controlling unit.

Proof. Similar to the proof of *Lemma 5.2*. □

Theorem 5.2. *The achievable upper bounds for the backhaul throughput in the Ring model are given in two regions, as follows:*

1. *Region 1: If* $\gamma_1 \leq \gamma_2 < \gamma_1+\gamma_1^2$*, then the maximum backhaul throughput is achieved when* $\lambda = \lambda_0$ *and is given by*

$$R_{1,max}^{r} = \frac{2C(\gamma_1)[C(\gamma_1+\gamma_2)+C(\gamma_1)]}{4C(\gamma_1)+C(\gamma_1+\gamma_2)}. \tag{5.19}$$

2. *Region 2: If* $\gamma_2 > \gamma_1 + \gamma_1^2$*, then the maximum backhaul throughput is achieved when* $\lambda = 1$ *and is given by*

$$R_{2,max}^{r} = C(\gamma_1). \tag{5.20}$$

Proof. See Appendix F. □

5.5.3 Numerical results

Following the results described in theorems 5.1 and 5.2, the maximum backhaul throughput of the proposed protocols in comparison with the backhaul throughput of the equivalent models without using network coding have been shown in Fig. 5.8 for the Star model and in Fig. 5.9 for the Ring model. In these figures, the backhaul throughput are plotted against γ_1 and γ_2, both in the range of 15 to 150 with $\gamma_3 = 200$ in Fig. 5.8, in linear scale. Fig. 5.8 and Fig. 5.9 confirm that our network coding enabled protocols attain higher throughput than their corresponding equivalent protocols without network coding, as the backhaul throughput surface of the former is always above the backhaul throughput surface of the latter. The improvement of the backhaul throughput of the proposed protocols can be explained as follows. First, in network coding enabled protocols, the required number of time slots to exchange information amongst these source nodes is considerably reduced. Second, the time sharing opportunity offered by the MAC-nature of the proposed protocols allows us to fully exploit the combining feature of network coding, since bit flows to be combined at a controlling unit are maximised by adjusting time sharing factors.

It can also be observed from Fig. 5.8 and Fig. 5.9 that the network coding enabled wireless backhauls attain the best performance when link qualities of the controlling unit and two source nodes, in the MAC phase, are equal, i.e., $\gamma_1 = \gamma_2$. In the case of imbalanced link qualities, the backhaul throughput of the proposed protocols strongly depends on the SNR of the weakest link. When $\gamma_1 < \gamma_2$, for instance, the backhhaul throughput of the proposed schemes is determined by the surface on the left hand side of the plane $\gamma_1 = \gamma_2$. On this surface, a large increase in the value of γ_2 leads to a small improvement in the throughput as the backhaul throughput is dominated by the value of γ_1. Therefore, in order to increase the backhaul throughput in the Ring or the Star model, the weakest link needs to be improved. The results also suggest that, in the case that the weakest link can not be improved, the overall power consumption can be reduced, with a minor sacrifice in the backhaul throughput, by reducing the SNR of the stronger link in the MAC phase and making it to be equal to the SNR of the weakest one.

Fig. 5.10 compares the backhaul throughputs of the Star and the Ring protocols with and without network coding against γ_2 with $\gamma_1 = 10$ and $\gamma_3 = 100$, all in linear scale. It can be easily seen that the Ring model achieves higher backhaul throughput than the Star model. Although 5-step Star protocol requires one more step to exchange information, it outperforms 4-step Star protocol in terms of achievable backhaul throughput.

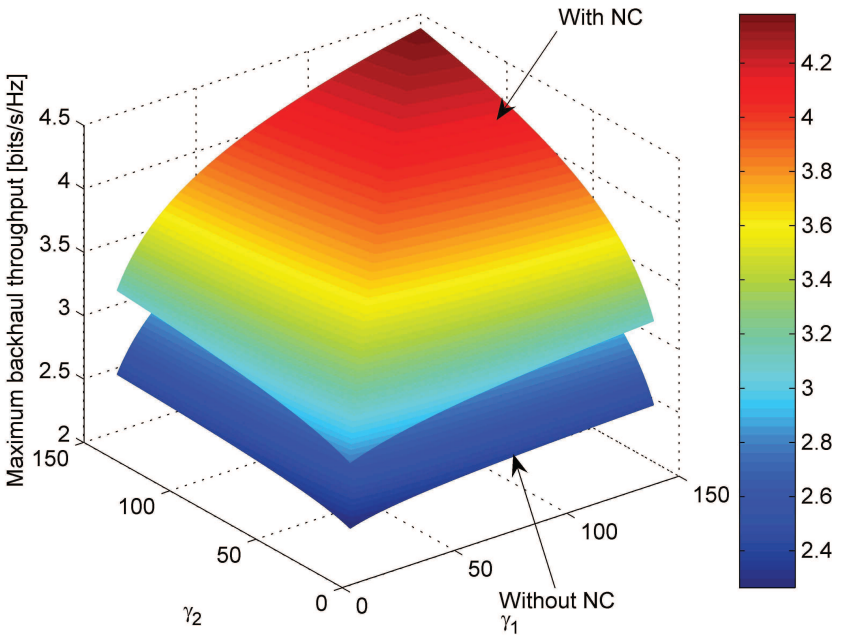

(a)

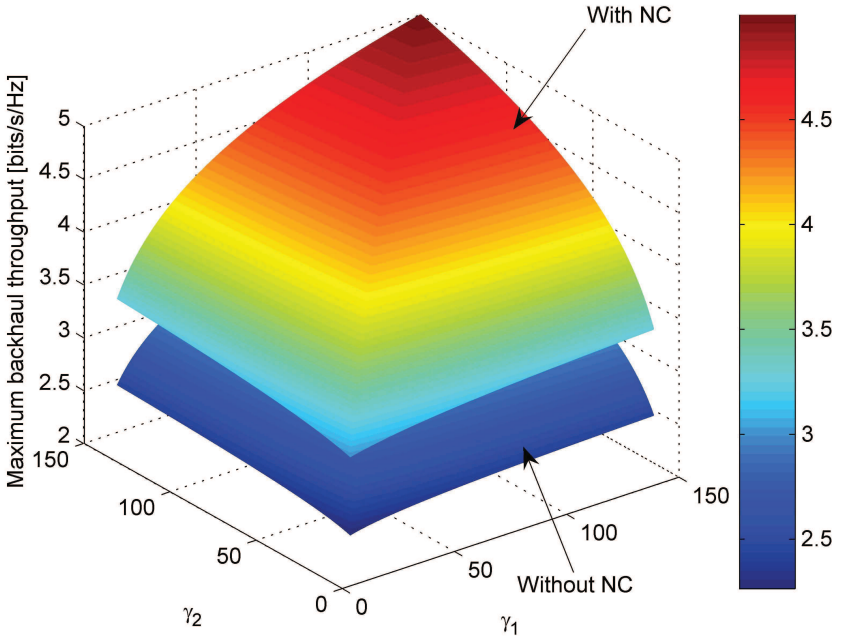

(b)

Figure 5.8: Maximum backhaul throughput for the Star model at $\gamma_3 = 200$ of the proposed protocol (With NC) in comparison with non-network coding protocol (Without NC) (a) 4-step protocol (b) 5-step protocol.

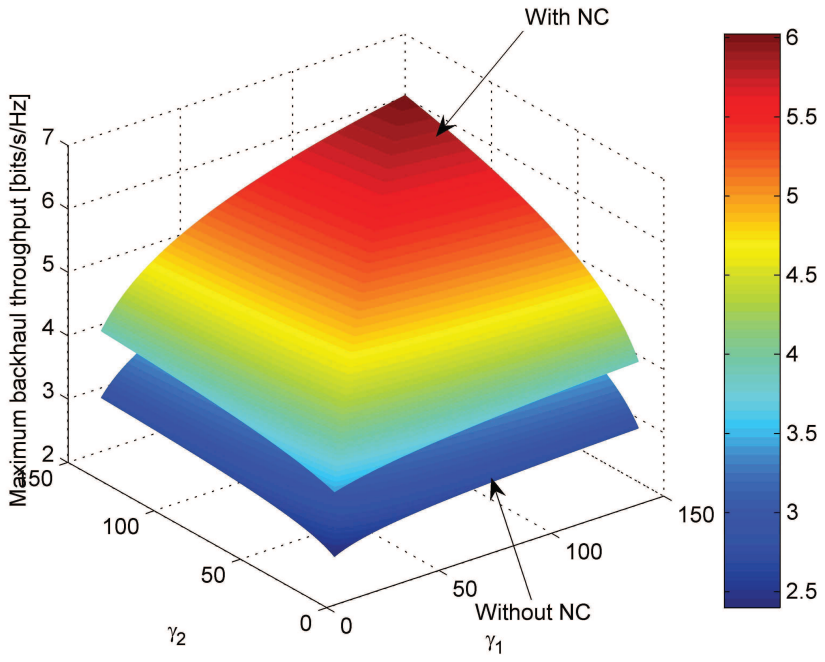

Figure 5.9: Maximum backhaul throughput for the Ring model of the proposed protocol (With NC) in comparison with non-network coding protocol (Without NC).

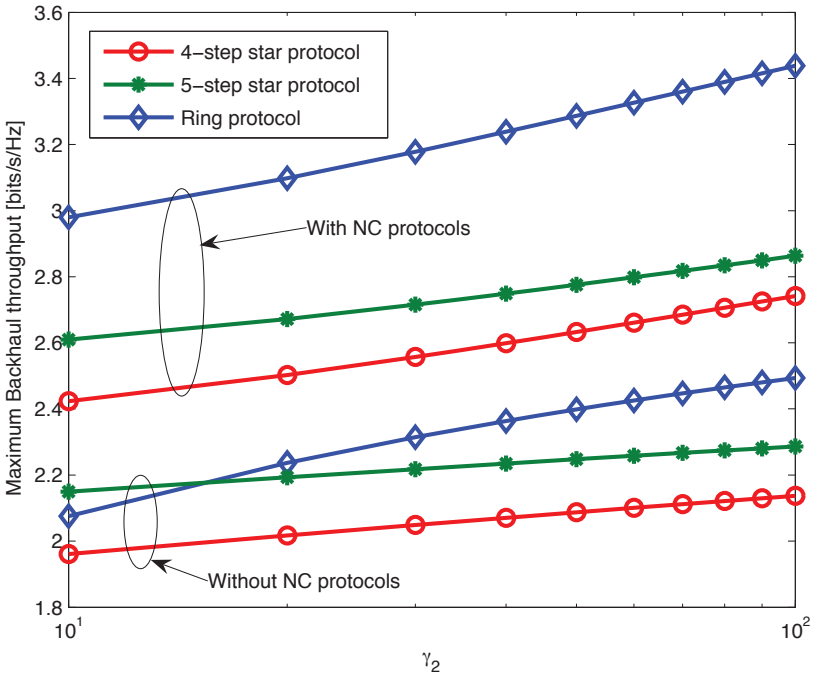

Figure 5.10: Maximum backhaul throughput comparisons between 4-step, 5-step protocols of the Star and Ring model at $\gamma_1 = 10$ and $\gamma_3 = 100$.

Assuming that power consumption is equal at every node, one can conclude that the Ring model consumes less energy than the Star model in the backhaul, because the former requires 3 steps while the latter needs 4 to 5 steps to accomplish one data exchange cycle. Moreover, in terms of link redundancy, the Ring protocol is more reliable than the Star protocol, because any broken or bad link in the former can be easily tolerated by the remaining two links, whereas the operation of the Star protocol can be delayed with a broken or bad link between any source node to the controlling unit. However, as described in Section II A, in a cellular distributed antenna system, the Star protocol can be used in the wireless backhaul to exchange information amongst a controlling BS and three distributed relay antenna systems.

In the following, backhaul transmission strategies that achieve maximum backhaul throughput for both Star and Ring protocols are summarised. First, time sharing factors in the MAC phases are adjusted based on the SNR conditions between the nodes as described in theorems 5.1 and 5.2. As a result, the bit imbalance in the controlling unit is minimised in step 1 for both protocols. Furthermore, in the third step of the Star model, the third node is allowed to transmit to the controlling unit at its highest rate, i.e., $C(\gamma_3)$. Second, in the BC phases, the controlling unit transmits at the lowest rate, i.e., $C(\gamma_1)$, so that the broadcast data is decodable at all the other nodes.

5.6 Performance evaluation of the proposed beamforming schemes

In this section, the performance of MBF, UPA-MBF and CBF are investigated and compared under an ideal backhaul, i.e., delay-less, error-free and high speed with no power consumption at channels interconnecting BSs, and an imperfect backhaul, i.e., with latency, power consumption and limited capacity. Like chapters 3 and 4, an isolated 3-cell scenario is considered with 3 randomly dropped users in the critical areas, i.e., areas 2 and 3 shown in Fig. 3.3. The locations of 3 random users are referred to as one user distribution. Monte Carlo simulations are carried out over 100 independent distributions. In the following, the power consumption of the Ring protocol is characterised followed by the introduction of an effective sum rate to capture the backhaul effects. Finally, performance comparisons of different beamforming schemes are presented.

5.6.1 Power analysis for the Ring protocol

The required transmitting power to achieve a given BS-to-BS SNR of γ can be expressed as

$$P(\gamma) = \gamma \frac{N_0}{|h|^2}, \tag{5.21}$$

where h is the channel coefficient between the two BSs. The average power required by the Ring backhaul protocol is denoted by $\overline{P} = E/T$, where E is the overall energy spent by the Ring protocol over a time duration of T seconds. We introduce the following lemma.

Lemma 5.4. *The average power required by the Ring backhaul protocol is calculated as follows:*

1. *If* $\gamma_1 \leq \gamma_2 < \gamma_1 + \gamma_1^2$,

$$\overline{P} = P(\gamma_1) + \frac{2C(\gamma_1)}{4C(\gamma_1) + C(\gamma_1+\gamma_2)} P(\gamma_2). \tag{5.22}$$

2. *If* $\gamma_2 > \gamma_1 + \gamma_1^2$,

$$\overline{P} = P(\gamma_1) + \frac{C(\gamma_1)}{C(\gamma_1) + C(\gamma_1+\gamma_2)} P(\gamma_2). \tag{5.23}$$

Proof. If $\gamma_1 \leq \gamma_2 < \gamma_1 + \gamma_1^2$, as shown in the appendix D, the minimum overall time delay in the Ring protocol is

$$T = \underbrace{T_o}_{\text{step 1}} + \underbrace{T_o \frac{C(\gamma_1+\gamma_2)}{2C(\gamma_1)}}_{\text{step 2}} + \underbrace{T_o}_{\text{step 3}} = T_o \frac{4C(\gamma_1) + C(\gamma_1+\gamma_2)}{2C(\gamma_1)},$$

where T_o is the time duration of an information block transmitted in steps 1 and 3. The overall energy spent by the Ring protocol is calculated as

$$\begin{aligned} E = \; & T_o \left[\underbrace{(P(\gamma_1) + P(\gamma_2))}_{\text{step 1}} + \underbrace{\frac{C(\gamma_1+\gamma_2)}{2C(\gamma_1)} P(\gamma_1)}_{\text{step 2}} + \underbrace{P(\gamma_1)}_{\text{step 3}} \right] \\ = \; & P(\gamma_1)\, T_o \tfrac{4C(\gamma_1)+C(\gamma_1+\gamma_2)}{2C(\gamma_1)} + T_o P(\gamma_2). \end{aligned} \tag{5.24}$$

Using (5.24), (5.24) and $\overline{P} = E/T$, one can arrive at (5.22).

If $\gamma_2 > \gamma_1 + \gamma_1^2$, the minimum overall time delay of the Ring protocol is

$$T = \underbrace{T_o}_{\text{step 1}} + \underbrace{T_o \frac{C(\gamma_1+\gamma_2) - C(\gamma_1)}{C(\gamma_1)}}_{\text{step 2}} + \underbrace{T_o}_{\text{step 3}}. \tag{5.25}$$

Following similar steps as the previous case, one can arrive at (5.23). □

5.6.2 An effective sum rate

Referring to the classification of areas in Fig. 3.3, coordination among two and three BSs in areas 2 and 3 are allowed with the corresponding backhaul rates of R_{bh2} and R_{bh3}, respectively. Let V_{csi}, V_2 and V_3 denote the total number of CSIT bits corresponding to a number of simultaneous multiple users in the network, the total number of data bits to be circulated in areas 2 and 3, respectively. The time duration to circulate information in the backhaul is

$$T_1 = \psi \left(\frac{V_2}{R_{\text{bh2}}} + \frac{V_3}{R_{\text{bh3}}} \right) + \frac{V_{\text{csi}}}{R_{\text{bh3}}}, \tag{5.26}$$

where $\psi = 1$ for MBF, i.e., signal level coordination, and $\psi = 0$ for CBF, i.e., beamforming level coordination.

Let R_i be the downlink rate excluding the backhaul latency effect for user i and v_i be the corresponding number of data bits delivered in a time span of v_i/R_i seconds. Assume, user m requires the longest time span among the other $U-1$ users, i.e., $T_2 = \max_i(\frac{v_i}{R_i}) = \frac{v_m}{R_m}$. Then, an overall duration of $T = T_1 + T_2$ seconds is required to exchange information, i.e., users' data and CSIT, in the backhaul and, then, deliver a total number of $V = V_2 + V_3$ bits to U simultaneous users. Note that, here, the processing time and power have been ignored from the calculations. One can write

$$T = V \frac{\chi R_{\text{bh3}} + R_m \left[\varphi + \psi\{1 + \rho\,(\beta - 1)\}\right]}{R_{\text{bh3}} R_m}, \tag{5.27}$$

where $\varphi = V_{\text{csi}}/V$, $\chi = v_m/V$, $\rho = V_2/V$ and $\beta = R_{\text{bh3}}/R_{\text{bh2}}$.
Let $R_{\text{eff}} = \frac{V}{T}$ define the effective sum rate, i.e., including the downlink and the backhaul latency, of U simultaneous users. Then

$$R_{\text{eff}} = \frac{R_{\text{bh3}} R_m}{\chi R_{\text{bh3}} + R_m \left[\varphi + \psi\{1 + \rho\,(\beta - 1)\}\right]}. \tag{5.28}$$

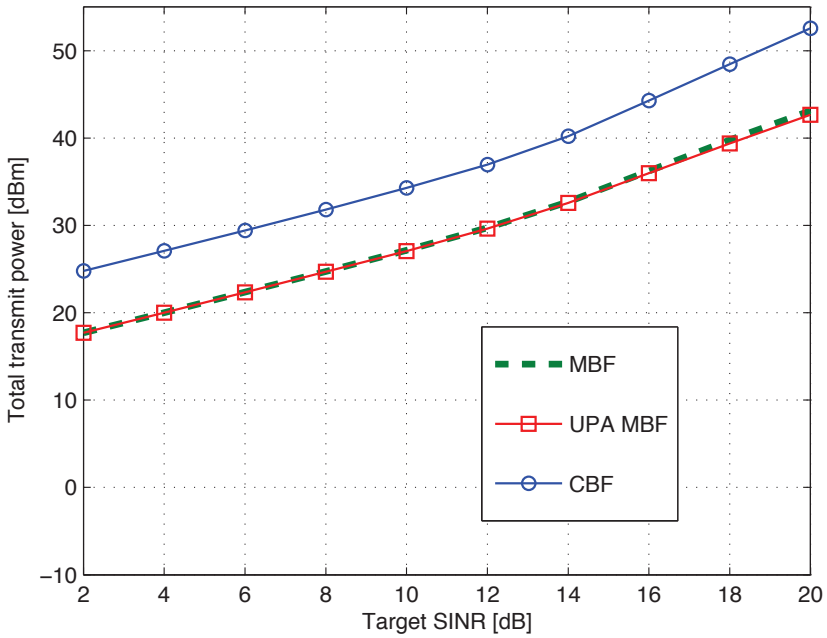

Figure 5.11: Total transmit power against targeted SINR per user.

5.6.3 Performance evaluation under an ideal backhaul

The simulation setup uses 6 antenna elements per sector with antenna spacing of a half of a wavelength and a downlink carrier frequencies of 2 GHz. A standard deviation of 2° for the angular spread due to 5 random scatterers around each user terminal is assumed. The setup assumes $N = 512$ Gaussian parallel MISO subchannels between a base station and a user terminal, where the fading coefficients for each subchannel is a 1×6 randomly generated ZMCSCG variables with unit variance. The noise power spectral density for all users is -174 dBm/Hz, the noise figure is 5 dB and a subchannel bandwidth is 15 kHz wide. The array antenna gain at BSs is set at 15dBi. The setup uses $128.1 + 37.6\log_{10}(l)$, where l is in km, as the path loss model. A standard deviation of 8 dB is assumed for log-normal shadowing. Also, any two neighbouring BSs are located 3 km apart from one another.

Fig. 5.11 shows the variation of the sum-transmit power of BSs against targeted SINR levels at user terminals for different beamforming strategies. In the MBF scheme, all users are assigned to 3 BSs while algorithm 3.1 is employed to assign users in the UPA MBF scheme. Then algorithm 3.2 is used to find the optimal solutions for the MBF and the UPA MBF. Interestingly, the performance of the UPA MBF is almost the same as that of the MBF. Although each user is allocated to 3 BSs in the MBF

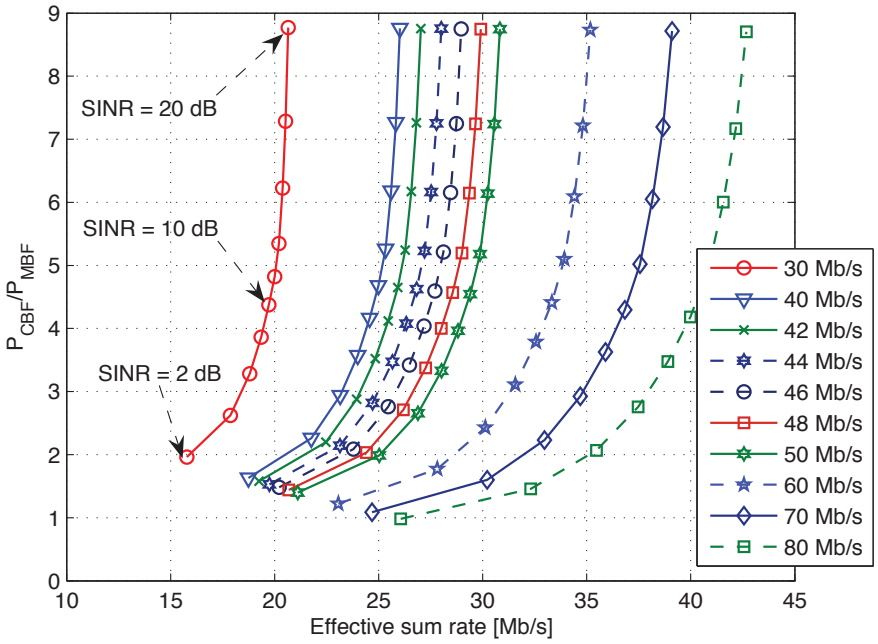

Figure 5.12: Illustration of total power consumption ratios of the CBF over the MBF schemes versus the effective sum rate with various MBF backhaul rate constraints.

scheme, it is effectively supported only by nearby BS. This is due to the total power minimising objective function and the fact that the constraints take into account the path loss. Also note that, an equal targeted SINR per user is assumed. This motivates the proposed UPA strategy which results in almost equal transmit power but imposes less backhaul burden than the MBF. Fig. 5.11 also shows that the MBF is more power efficient than the CBF. The advantage of MBF in being more power efficient is due to more effective co-channel interference management by the MBF strategies than the CBF. However, the MBF demands heavier backhaul than the CBF for user data circulation. In the following, the performance of the MBF and the CBF under the effect of backhaul are compared.

5.6.4 Performance evaluation under limited backhaul

In this section, the ratio $\frac{P_{\text{CBF}}}{P_{\text{MBF}}}$, where P_{CBF} and P_{MBF} are the total power consumptions by the CBF and the MBF schemes, respectively, versus the effective sum rate, i.e.,(5.28), at various MBF backhaul rate constraints is drawn in Fig. 5.12 using the following steps.

1. Assuming equal target SINRs for all users, find the corresponding transmit power

and maximum rate for each scheme using Fig. 5.11 and $R_m = B\log_2(1+\text{SINR}_m)$, respectively, where B indicates the transmission bandwidth.

2. Given a limited backhaul rate for MBF, i.e., $R_{\text{bh3}}(\text{MBF})$, and R_m from step 1, set $\psi = 1$, $\varphi = 0.2$, $\chi = 1/3$, $\rho = 0$, $\beta = 2/3$ and use (5.28) to find R_{eff}.

3. Given R_m and R_{eff} from steps 1 and 2, use (5.28) with $\psi = 0$ to find the backhaul rate for CBF, i.e., $R_{\text{bh3}}(\text{CBF})$.

4. Using $R_{\text{bh3}}(\text{MBF})$ and $R_{\text{bh3}}(\text{CBF})$ and B, find the SNR values, i.e., γ_1 and γ_2, for the backhaul channels of each scheme from Fig. 5.13.

5. For each sheme, use the corresponding values of γ_1 and γ_2 in (5.22) or (5.23) to find the backhaul power required for the MBF and the CBF schemes. Then, the total power of each scheme is the sum of their corresponding transmit power, i.e., calculated in step 1, and the backhaul power.

The downlink bandwidth for data transmission is 7.68 MHz wide. Backhaul bandwidths of 7.5, 10, 10.5, 11, 11.5, 12, 12.5, 15, 17.5, and 20 MHz with a backhaul spectral efficiency of 4 bits/s/Hz are used. An equal noise power spectral density of -174 dBm/Hz is assumed at all BSs and a carrier frequency of 2.4 GHz is used for the backhaul links.

The results shown in Fig. 5.12 confirm that the MBF is more power efficient than the CBF even when the backhaul effects are taken into consideration.

5.7 Conclusion

In this chapter, a possible power-saving gain by dividing a cell into tiers of smaller cells has been derived as a function of the number of tiers and pass loss exponent. In an infrastructure arisen from cell splitting, unoccupied UHF frequency bands with very good propagation characteristics can be used to establish robust wireless links amongst the neighbouring BSs. Network coding enabled wireless Star and Ring backhaul protocols for the cellular distributed antenna systems have been introduced. Exploiting network coding, time sharing factors have been derived to control the bit imbalance due to the SNR gap between two channels with different link qualities, so that the backhaul throughput is maximised. Upper bound expressions on the achievable throughputs of the proposed protocols have also been obtained. It has been concluded that, in general, the Ring protocol is more efficient and more tolerant than the Star protocol in terms of overall energy consumption and link redundancy. However, the Star model is an

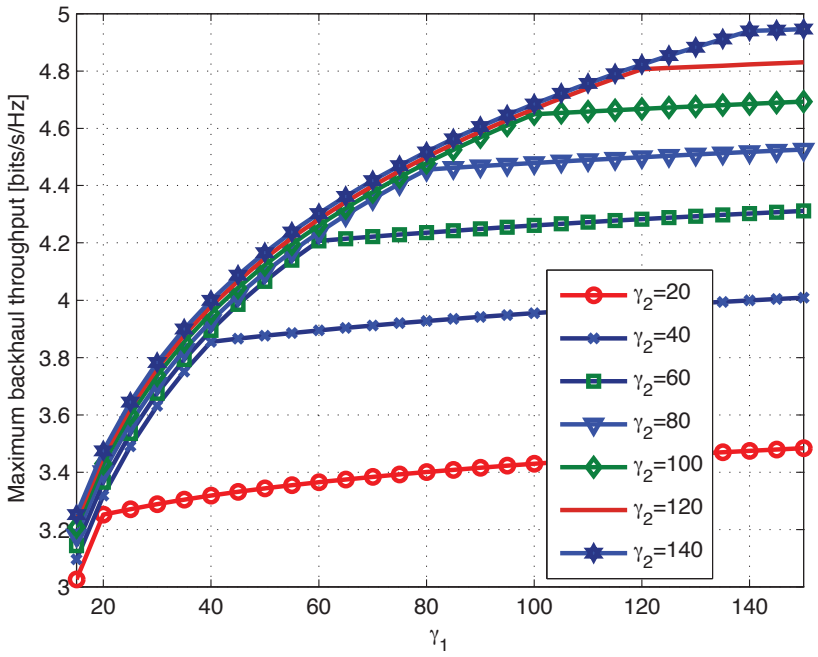

Figure 5.13: Achievable maximum backhaul spectral efficiency for the Ring model against γ_1 with different values of γ_2 in linear scale.

efficient wireless backhaul solution for exchanging information within a cellular sector, where three fixed relay stations are deployed to save an extra energy consumption in the BS by opening interference free dimensions and avoiding long range transmissions. Using the Ring protocol, a framework has been introduced to evaluate the overall performance of MBF and CBF schemes that include backhaul effects on both latency and power consumption. Simulation results have indicated that the MBF approach is more power efficient than the CBF scheme even when the backhaul effects are taken into consideration.

Chapter 6

Decentralised beamforming

The deployments of MBF, UPA-MBF and CBF schemes require a central unit for a group of coordinating BSs as well as backhaul links amongst them. In fact, a central unit may not always be available, e.g., in femtocell and self-organising networks, while backhaul links may be limited. This chapter proposes a downlink transmission strategy and an iterative algorithm that enables each BS to design locally its own beamforming vectors without relying on data or downlink channel state information of links from other BSs to the users. This algorithm is the solution to an optimisation problem that minimises a linear combination of data transmission power and the resulting inter-cell interference power with pricing factors at each BS and maintains the required signal-to-interference-plus-noise ratios required by the users. Two pricing strategies are introduced to calculate the interference pricing factors. The convergence of the proposed algorithm in cellular systems is proven and the impact of the pricing factors in saving power at BSs is characterised. A feasibility condition for the existence of such an iterative algorithm is derived. This condition can be used as a scheduling algorithm to choose a set of active users within each cell. Simulation results show that the proposed algorithm converges to a network-wide equilibrium point by balancing and stabilising the mutual inter-cell interference levels and assigning power optimal beamforming vectors to the BSs. The results also confirm the effectiveness of the proposed algorithm in closely following the performance limits of its centralised coordinated beamforming counterpart.

6.1 Introduction

Demand for enhancing spectrum reusability and uniform-capacity coverage in cellular networks is growing fast. This is due to the emerging applications of mobile internet in different areas such as education and healthcare. Although exploiting spatial dimension

in multiple antenna wireless systems improves spectrum reuse, inter-cell interference (ICI) remains a major drawback in uniform improvement of capacity across the cells, particularly at cell boarders. Network MIMO technique that exploits the ICI via baseband signal cooperation for joint encoding and decoding at base stations (BSs) has been a focal point for research community and an emphasis of LTE-Advanced and beyond systems. Although network MIMO technique shows promising theoretical performance [27], it requires the baseband time synchronisation and message sharing among different BSs, which are currently challenging issues in terms of implementation and imposing a heavy overhead on the backbone network. On the other hand, in the absence of message sharing, the cellular channel becomes an interference channel if time and spectral resources are to be extensively reused in the network.

Centralised interference coordination which avoids message sharing but coordinates multi-cell channel state information (CSI) mitigates ICI via coordinated spatial resource allocation across the BSs, e.g., [32] and [30]. In [32], where multiple BSs jointly optimise their respective beamforming vectors, it is shown that the overall network performance in terms of total power saving can be improved compared to the conventional method of independent beamforming in each cell. Authors in [30] maximise the instantaneous sum-rate in the network subject to per-BS-power constraints in two multi-cell scenarios identified as fully-connected cluster, where both message and CSI are shared among a group of BSs, and partially-connected cluster, where only CSI are shared among a group of BSs. In the developments reported in [32] and [30], it is assumed that the instantaneous global CSI are available at all BSs.

In [77], a set of soft-shaping constraints is used in designing the downlink beamforming vectors at individual BSs to ensure that the ICI leakages of each BS on the other users are kept under some tolerable thresholds. Authors in [96] assume perfect CSI knowledge and show that for the two-cell multiple-input single-output (MISO) downlink scenario with one user per cell, the Pareto optimal beamforming vector for each user can be obtained in the form of a linear combination of two vectors designed using a purely selfish and a purely altruistic strategies and a single real-valued parameter. In purely selfish strategy, i.e., maximum-ratio transmission (MRT) in [96], each BS chooses its beamforming vectors to maximise the data rate to its intended local users, while ignoring the ICI effects on the other users. In purely altruistic strategy, i.e., zero-forcing (ZF) in [96], the BS designs its beamforming vectors to cause absolutely no ICI on other users. This work is extended by [97] to the case where only partial CSI is available in the same two-cell scenario as in [96]. Authors in [98] have generalised the work in [96] to the multiple-input multiple-output (MIMO) case using

Bayesian games and derived semi-distributed beamforming solutions.

The authors in [99] consider a cellular network with only one active user per cell and propose a decentralised algorithm for rate maximization within each cell while satisfying a set of interference-temperature constraints on the users of the other cells. In [100], the authors study a distributed network MIMO where the cooperating BSs share users' data but only have local CSI. They characterize the outer boundary of the achievable rate region for the BSs with either instantaneous or statistical CSI and propose a distributed virtual SINR beamforming scheme that achieves the optimal multiplexing gain. The work in [101] proposes a robust monotonic optimisation framework for general multi-cell scenarios with imperfect CSI. In [102], the authors introduce an approach for computing the jointly optimal beamforming, user selection and scheduling strategy for each BS under an arbitrary utility objective, i.e., weighted sum-rate, max-min fairness and proportional fairness.

In this chapter, a decentralised inter-cell interference balancing strategy that can be simultaneously operated by the multiple cells of a cellular network at the same frequency band is developed. Specifically, the strategy minimises a linear combination of two utility functions, characterizing each BS's weighted sum of transmitted power to the intra-cell users and its resulting weighted sum of interference power inflicted upon the users of the other cells, subject to maintaining a set of desired SINR levels at the intra-cell users. While the first utility function attempts to maintain the local users' SINR demands in a power efficient way, the second utility function tries to balance and stabilise the multi-cell network at an equilibrium point. Exploiting the uplink-downlink duality of wireless channels, an iterative algorithm based on the second order statistical CSI, locally attainable by each BS, for designing the beamforming vectors at each BS is developed. The major significance of this work is the distributiveness of the resulting solutions that are applicable to large cellular networks with highly efficient reusability of spectral resources. The proposed approach gains this advantage as a result of the following key consideration. The approach embeds a balance between the power consumption of each BS for data transmission to its intra-cell users and the resulting inevitable inter-cell interference in a unifying objective function of an optimisation problem, so that users' demands are met and an optimal equilibrium point is reached across the multi-cell network. Furthermore, the users within a cell obtain their data signals only from their dedicated local BS, hence data sharing amongst the BSs is not required.

The rest of this chapter is organized as follows. Section 6.2 describes the system model and proposes an optimisation for multi-cell networks. Section 6.3 develops an

iterative solution to the proposed problem, based on the second order statistical CSI and finds a feasibility condition for the existence of the solution. Section 6.5 presents and discusses the simulation results. Finally, the concluding remarks are given in Section 6.6.

6.2 System model and problem formulation

Consider a cellular scenario of N BSs, where each BS forms power-efficient beams toward its locally active users to deliver their desired levels of SINR and simultaneously controls the resulting interference on the other users of the adjacent cells. Without loss of generality, assuming that each cell has U users. Let $\mathcal{S}_b = \{1, \cdots, N\}$ and $\mathcal{S}_l = \{1, \cdots, U\}$ be, respectively, the set of indices of BSs and locally active users in each cell. We assume that each BS is equipped with M antenna elements and each user has one antenna element. Let the index $i(q)$, $i \in \mathcal{S}_l$ and $q \in \mathcal{S}_b$, indicate the ith user in cell q. Then, the overall received signal at user i in cell q is given by

$$\mathrm{y}_{i(q)} = \mathbf{h}_{i(q)}(q)\mathbf{w}_{i(q)}s_{i(q)} + \sum_{j\in\mathcal{S}_l, j\neq i} \mathbf{h}_{i(q)}(q)\mathbf{w}_{j(q)}s_{j(q)} + v_{i(q)} + n_{i(q)} \tag{6.1}$$

where $\mathbf{h}_{i(q)}(q) \in \mathcal{C}^{1\times M}$ is the channel of user $i(q)$ as seen by the BS of cell q, $\mathbf{w}_{i(q)} \in \mathcal{C}^{M\times 1}$ and $s_{i(q)}$ are, respectively, the beamforming vector and the data symbol associated to user $i(q)$, $n_{i(q)}$ is a zero mean circularly symmetric complex Gaussian noise with variance σ^2, i.e., $n_{i(q)} \sim \mathcal{CN}(0, \sigma^2)$, at user $i(q)$ and $v_{i(q)}$ is the overall inter-cell interference received by user $i(q)$ from the BSs of the other cells, i.e., other than cell q. Let $\mathbf{R}_{i(q)}(q) = \mathbb{E}\left(\mathbf{h}^H_{i(q)}(q)\mathbf{h}_{i(q)}(q)\right)$ denote the downlink channel covariance matrix of user $i(q)$, as seen by the BS in cell q [1]. Letting the average energy in transmitting a symbol to the user $i(q)$, i.e., denoted as $s_{i(q)}$, be normalised to unity, i.e., $\mathbb{E}\left(\left|s_{i(q)}\right|^2\right) = 1$, one can write the SINR at any local user $i(q)$ as

$$\mathrm{SINR}_{i(q)} = \frac{\mathbf{w}^H_{i(q)}\mathbf{R}_{i(q)}(q)\mathbf{w}_{i(q)}}{\sum_{j\in\mathcal{S}_l, j\neq i}\mathbf{w}^H_{j(q)}\mathbf{R}_{i(q)}(q)\mathbf{w}_{j(q)} + \xi_{i(q)} + \sigma^2}, \tag{6.2}$$

where $\xi_{i(q)} = \mathbb{E}\left(\left|v_{i(q)}\right|^2\right)$ is the total inter-cell interference power imposed on user $i(q)$. It is assumed that the inter-cell interference is an ergodic process, i.e., the statistical average can be estimated by averaging over time, and any user $i(q)$ can estimate the induced outer-cell interference power $\xi_{i(q)}$ and report it to its local BS. For a detailed

[1] Note that $\mathbf{R}_{t(k)}(q)$ represents the cross channel covariance matrix of user t of cell k, as seen by the BS in cell q.

discussion on inter-cell interference modeling, the interested readers are referred to [103]. The optimisation problem to calculate the downlink beamforming vectors for all users in the network is introduced as

$$\begin{aligned} \min_{\mathbf{w}_{i(q)}} \quad & \sum_{q\in\mathcal{S}_b}\left(\sum_{i\in\mathcal{S}_l}\mathbf{w}_{i(q)}^H\mathbf{w}_{i(q)}+\sum_{k\in\mathcal{S}_b,k\neq q}\sum_{t\in\mathcal{S}_l}\sum_{i\in\mathcal{S}_l}\mu_{t(k)}\mathbf{w}_{i(q)}^H\mathbf{R}_{t(k)}(q)\mathbf{w}_{i(q)}\right) \\ \text{s. t.} \quad & \frac{\mathbf{w}_{i(q)}^H\mathbf{R}_{i(q)}(q)\mathbf{w}_{i(q)}}{\sum_{j\in\mathcal{S}_l,j\neq i}\mathbf{w}_{j(q)}^H\mathbf{R}_{i(q)}(q)\mathbf{w}_{j(q)}+\xi_{i(q)}+\sigma^2}\geq\gamma_{i(q)}, \quad \forall i\in\mathcal{S}_l, q\in\mathcal{S}_b \end{aligned} \tag{6.3}$$

where $\gamma_{i(q)}$ is the SINR target required by an active user $i(q)$ and $\mu_{t(k)}$ is the pricing factor for user t in cell k. In the objective function of (6.3), the term $\sum_{i\in\mathcal{S}_l}\mathbf{w}_{i(q)}^H\mathbf{w}_{i(q)}$ indicates the total signal power transmitted to the locally active users within a cell q, while the term $\sum_{k\in\mathcal{S}_b,k\neq q}\sum_{t\in\mathcal{S}_l}\sum_{i\in\mathcal{S}_l}\mu_{t(k)}\mathbf{w}_{i(q)}^H\mathbf{R}_{t(k)}(q)\mathbf{w}_{i(q)}$ represents the aggregate weighted interference power induced on the users of the other cells by the BS in cell q.

6.3 An iterative algorithm for decentralised beamforming

In this section, an iterative solution for the optimisation problem in (6.3) for any fixed pricing factors is proposed. Rearranging the constraints in problem (6.3), one can form the Lagrangian as

$$\begin{aligned} L(\mathbf{w}_{i(q)},\lambda_{i(q)}) &= \sum_{q\in\mathcal{S}_b}\sum_{i\in\mathcal{S}_l}\mathbf{w}_{i(q)}^H\mathbf{w}_{i(q)}+\sum_{q\in\mathcal{S}_b}\sum_{k\in\mathcal{S}_b,k\neq q}\sum_{t\in\mathcal{S}_l}\sum_{i\in\mathcal{S}_l}\mu_{t(k)}\mathbf{w}_{i(q)}^H\mathbf{R}_{t(k)}(q)\mathbf{w}_{i(q)} \\ &+\sum_{q\in\mathcal{S}_b}\sum_{i\in\mathcal{S}_l}\lambda_{i(q)}\left[\sum_{j\in\mathcal{S}_l}\mathbf{w}_{j(q)}^H\mathbf{R}_{i(q)}(q)\mathbf{w}_{j(q)}+\xi_{i(q)}+\sigma^2-\mathbf{w}_{i(q)}^H\mathbf{R}_{i(q)}(q)\mathbf{w}_{i(q)}\left(1+\frac{1}{\gamma_{i(q)}}\right)\right], \end{aligned}$$

where $\lambda_{i(q)}$ is the Lagrange multiplier associated with the $i(q)$-th user constraint in (6.3). Equivalently,

$$L(\mathbf{w}_{i(q)},\lambda_{i(q)})=\sum_{q\in\mathcal{S}_b}\sum_{i\in\mathcal{S}_l}\lambda_{i(q)}\left(\xi_{i(q)}+\sigma^2\right)+\sum_{q\in\mathcal{S}_b}\sum_{i\in\mathcal{S}_l}\mathbf{w}_{i(q)}^H\mathbf{A}_{i(q)}\mathbf{w}_{i(q)}, \tag{6.4}$$

where

$$\mathbf{A}_{i(q)}=\sum_{k\in\mathcal{S}_b,k\neq q}\sum_{t\in\mathcal{S}_l}\mu_{t(k)}\mathbf{R}_{t(k)}(q)+\mathbf{I}+\sum_{j\in\mathcal{S}_l}\lambda_{j(q)}\mathbf{R}_{j(q)}(q)-\lambda_{i(q)}\left(1+\frac{1}{\gamma_{i(q)}}\right)\mathbf{R}_{i(q)}(q). \tag{6.5}$$

Hence, the Lagrange dual function can be written as

$$g\left(\lambda_{i(q)}\right) = \inf_{\mathbf{w}_{i(q)}} \left(L(\mathbf{w}_{i(q)}, \lambda_{i(q)})\right) = \begin{cases} \sum_{q\in\mathcal{S}_b}\sum_{i\in\mathcal{S}_l} \lambda_{i(q)}\left(\xi_{i(q)}+\sigma^2\right), & \text{if } \mathbf{A}_{i(q)} \succeq 0 \\ -\infty, & \text{otherwise .} \end{cases} \tag{6.6}$$

Therefore, the Lagrange dual of the primal optimisation problem (6.3) is

$$\begin{aligned} \max_{p_{i(q)}} \quad & \sum_{q\in\mathcal{S}_b}\sum_{i\in\mathcal{S}_l} p_{i(q)} \\ \text{s. t.} \quad & \mathbf{A}_{i(q)} \succeq 0,\ \forall i \in \mathcal{S}_l, q \in \mathcal{S}_b, \end{aligned} \tag{6.7}$$

where $p_{i(q)} = \lambda_{i(q)}\left(\xi_{i(q)}+\sigma^2\right)$. The following lemma is introduced to find the solution to problem (6.7).

Lemma 6.1. *The solution to the dual problem (6.7) can be found via the solution to the following dual-uplink problem.*

$$\begin{aligned} \min_{p_{i(q)}} \quad & \sum_{q\in\mathcal{S}_b}\sum_{i\in\mathcal{S}_l} p_{i(q)} \\ s.\ t. \quad & \max_{\left\|\hat{\mathbf{w}}_{i(q)}\right\|=1} \frac{p_{i(q)}\hat{\mathbf{w}}_{i(q)}^H \mathbf{R}_{i(q)}(q)\hat{\mathbf{w}}_{i(q)}}{\hat{\mathbf{w}}_{i(q)}^H \mathbf{G}_{i(q)}\left(\mathbf{p}\right)\hat{\mathbf{w}}_{i(q)}} \geq \gamma_{i(q)},\ \forall i \in \mathcal{S}_l, q \in \mathcal{S}_b, \end{aligned} \tag{6.8}$$

where $\hat{\mathbf{w}}_{i(q)}$ is the dual uplink beamforming vector for user i of cell q and

$$\mathbf{G}_{i(q)}\left(\mathbf{p}\right) = \sum_{j\in\mathcal{S}_l, j\neq i} p_{j(q)}\mathbf{R}_{j(q)}(q) + \left(\xi_{i(q)}+\sigma^2\right)\left(\sum_{k\in\mathcal{S}_b, k\neq q}\sum_{t\in\mathcal{S}_l}\mu_{t(k)}\mathbf{R}_{t(k)}(q) + \mathbf{I}\right). \tag{6.9}$$

Proof. Using (6.5), one can rewrite the problem (6.7) as

$$\begin{aligned} \max_{p_{i(q)}} \quad & \sum_{q\in\mathcal{S}_b}\sum_{i\in\mathcal{S}_l} p_{i(q)} \\ \text{s. t.} \quad & \sum_{k\in\mathcal{S}_b, k\neq q}\sum_{t\in\mathcal{S}_l}\mu_{t(k)}\mathbf{R}_{t(k)}(q) + \mathbf{I} + \sum_{j\in\mathcal{S}_l}\lambda_{j(q)}\mathbf{R}_{j(q)}(q) \succeq \lambda_{i(q)}\left(1+\frac{1}{\gamma_{i(q)}}\right)\mathbf{R}_{i(q)}(q), \\ & \forall i \in \mathcal{S}_l, q \in \mathcal{S}_b. \end{aligned} \tag{6.10}$$

Let $\hat{\mathbf{w}}_{i(q)}^{\star}$ be the optimal solution to the left-hand side of the constraint in problem (6.8). Plugging $\hat{\mathbf{w}}_{i(q)}^{\star}$ in the constraints in (6.8) and rearranging the terms using (6.9), one can write

$$\hat{\mathbf{w}}_{i(q)}^{\star H}\left(\sum_{k\in\mathcal{S}_b, k\neq q}\sum_{t\in\mathcal{S}_l}\mu_{t(k)}\mathbf{R}_{t(k)}(q) + \mathbf{I} + \sum_{j\in\mathcal{S}_l}\lambda_{j(q)}\mathbf{R}_{j(q)}(q) - \lambda_{i(q)}\left(1+\frac{1}{\gamma_{i(q)}}\right)\mathbf{R}_{i(q)}(q)\right)\hat{\mathbf{w}}_{i(q)}^{\star} \leq 0. \tag{6.11}$$

To arrive at (6.11), we have used the fact that $p_{i(q)} = \lambda_{i(q)}\left(\xi_{i(q)} + \sigma^2\right) > 0$. Hence,

$$\sum_{k\in\mathcal{S}_b, k\neq q}\sum_{t\in\mathcal{S}_l}\mu_{t(k)}\mathbf{R}_{t(k)}(q) + \mathbf{I} + \sum_{j\in\mathcal{S}_l}\lambda_{j(q)}\mathbf{R}_{j(q)}(q) \preceq \lambda_{i(q)}\left(1+\frac{1}{\gamma_{i(q)}}\right)\mathbf{R}_{i(q)}(q). \quad (6.12)$$

Therefore, the problem (6.8) can be rewritten as

$$\begin{aligned}\min_{p_{i(q)}} \quad & \sum_{q\in\mathcal{S}_b}\sum_{i\in\mathcal{S}_l} p_{i(q)} \\ \text{s. t.} \quad & \sum_{k\in\mathcal{S}_b, k\neq q}\sum_{t\in\mathcal{S}_l}\mu_{t(k)}\mathbf{R}_{t(k)}(q) + \mathbf{I} + \sum_{j\in\mathcal{S}_l}\lambda_{j(q)}\mathbf{R}_{j(q)}(q) \preceq \lambda_{i(q)}\left(1+\frac{1}{\gamma_{i(q)}}\right)\mathbf{R}_{i(q)}(q), \\ & \forall i \in \mathcal{S}_l, q \in \mathcal{S}_b.\end{aligned} \quad (6.13)$$

Comparing the problems in (6.10) and (6.13), one can see that except the replacement of the minimisation and the maximisation in the objective functions and the reversal of the inequality direction of the constraints, these two problems are the same. It can also be verified that the constraints in the both problems hold with equality at the optimal solutions. Therefore (6.10) and (6.13) have the same solutions. This concludes the proof. □

In order to solve the problem (6.8), let $\mathbf{p} = \begin{bmatrix}\mathbf{p}_1^T & \mathbf{p}_2^T & \cdots & \mathbf{p}_N^T\end{bmatrix}^T$, where $\mathbf{p}_q = \begin{bmatrix}p_{1(q)} & p_{2(q)} & \cdots & p_{U(q)}\end{bmatrix}^T, \forall q \in \mathcal{S}_b$. Furthermore, let

$$\mathbf{k}(\mathbf{p}) = \begin{bmatrix}\mathbf{k}_1(\mathbf{p})^T & \mathbf{k}_2(\mathbf{p})^T & \cdots & \mathbf{k}_N(\mathbf{p})^T\end{bmatrix}^T, \quad (6.14)$$

where $\mathbf{k}_q(\mathbf{p}) = \begin{bmatrix}k_{1(q)}(\mathbf{p}) & k_{2(q)}(\mathbf{p}) & \cdots & k_{U(q)}(\mathbf{p})\end{bmatrix}^T$ with

$$k_{i(q)}(\mathbf{p}) = \min_{\|\hat{\mathbf{w}}_{i(q)}\|=1} \gamma_{i(q)}\frac{\hat{\mathbf{w}}_{i(q)}^H\mathbf{G}_{i(q)}(\mathbf{p})\,\hat{\mathbf{w}}_{i(q)}}{\hat{\mathbf{w}}_{i(q)}^H\mathbf{R}_{i(q)}(q)\hat{\mathbf{w}}_{i(q)}}, \ \forall q \in \mathcal{S}_b. \quad (6.15)$$

The optimal solution to (6.15), denoted as $\hat{\mathbf{w}}_{i(q)}^\star$, is the dominant eigenvector, i.e., the eigenvector associated with the maximum eigenvalue, of matrix $\mathbf{G}_{i(q)}^{-1}(\mathbf{p})\,\mathbf{R}_{i(q)}(q)$. It can be easily verified that the constraint in (6.8) can be rewritten as follows

$$\mathbf{p} \succeq \mathbf{k}(\mathbf{p}). \quad (6.16)$$

Therefore, the problem (6.8) can be restated in the following equivalent form

$$\begin{aligned}\min_{p_{i(q)}} \quad & \sum_{q\in\mathcal{S}_b}\sum_{i\in\mathcal{S}_l} p_{i(q)} \\ \text{s. t.} \quad & \mathbf{p} \succeq \mathbf{k}(\mathbf{p}).\end{aligned} \quad (6.17)$$

The work in [74] has formed an elegant power-control framework for the class of standard functions. A function is called standard if it satisfies the positivity, monotonicity and scalability criteria. The key results of the standard power control framework are stated in the following from [74]. If (6.16) has a fixed point, i.e., a feasible solution, and $\mathbf{k}(\mathbf{p})$ is standard, then that fixed point is unique. Furthermore, if (6.16) has a fixed point $\mathbf{p}^\star$ and $\mathbf{k}(\mathbf{p})$ is standard, then from any initial power vector $\mathbf{p}$, the following iterative power control algorithm

$$\mathbf{p}\left(n+1\right) = \mathbf{k}\left(\mathbf{p}\left(n\right)\right) \tag{6.18}$$

converges both synchronously and asynchronously to the fixed point $\mathbf{p}^\star$. In an asynchronous case, some BSs can perform power adjustments faster and use more iterations than the others. Furthermore, the asynchronous case allows the BSs to execute these power updates using the outdated information on the interference, caused by the other BSs.

It has been shown in the Appendix G that $\mathbf{k}(\mathbf{p})$ is standard. Therefore, the solution to (6.17) can be generated using the iterative power control algorithm (6.18). Moreover, the multi-cell wise convergence is guaranteed for both synchronous and asynchronous implementations. Interestingly, by observing the structures of $\mathbf{p}$ and $\mathbf{k}(\mathbf{p})$, it can be stated that the iterative power control algorithm (6.18) is an element-wise operation, i.e., each element of $\mathbf{p}$ is updated using the corresponding element of $\mathbf{k}(\mathbf{p})$. Notice that the qth element of $\mathbf{k}(\mathbf{p})$, i.e., $\mathbf{k}_q(\mathbf{p})$, is linked to the BSs other than the BS q through the cross-channel covariance matrices $\mathbf{R}_{t(k)}(q)$, $k \in \mathcal{S}_b$ and $k \neq q$ according to (6.9). Since, we assume that each BS can obtain these cross-channel covariance matrices, the equivalent dual-uplink problem (6.17) can be restated as N individual optimisation problems at N individual BSs. Hence, without loss of generality, the dual-uplink problem at an individual BS $q \in \mathcal{S}_b$ can be written as

$$\begin{aligned} \min_{p_{i(q)}} \quad & \sum_{i \in \mathcal{S}_l} p_{i(q)} \\ \text{s. t.} \quad & \mathbf{p}_q \succeq \mathbf{k}_q(\mathbf{p}). \end{aligned} \tag{6.19}$$

Following the similar steps as in Appendix G, one can easily show that $\mathbf{k}_q(\mathbf{p})$ is also standard. Hence, the problem in (6.19) can be iteratively solved by

$$\mathbf{p}_q\left(n+1\right) = \mathbf{k}_q\left(\mathbf{p}_q\left(n\right)\right). \tag{6.20}$$

In Appendix H, it is shown that the optimum downlink beamforming vector for user i in cell q, i.e., $\mathbf{w}^\star_{i(q)}$, can be obtained from the corresponding optimum dual

uplink beamforming vector $\hat{\mathbf{w}}^{\star}_{i(q)}$ as

$$\mathbf{w}^{\star}_{i(q)} = \alpha_{i(q)}\hat{\mathbf{w}}^{\star}_{i(q)}, \tag{6.21}$$

where $\alpha_{i(q)}$ is the dual-uplink/downlink scaling factor associated with the user i in cell q, i.e., $i(q)$. In the following, we find the scaling factor $\alpha_{i(q)}$ for any user $i \in \mathcal{S}_l$ in any cell $q \in \mathcal{S}_b$.

Applying the complementary slackness condition with $\lambda_{i(q)} > 0$ to the primal downlink problem (6.3) leads to

$$\sum_{j\in\mathcal{S}_l, j\neq i} \gamma_{i(q)}\mathbf{w}^{\star H}_{j(q)}\mathbf{R}_{i(q)}(q)\mathbf{w}^{\star}_{j(q)} + \gamma_{i(q)}\left(\xi_{i(q)} + \sigma^2\right) - \mathbf{w}^{\star H}_{i(q)}\mathbf{R}_{i(q)}(q)\mathbf{w}^{\star}_{i(q)} = 0. \tag{6.22}$$

Then, substituting for $\mathbf{w}^{\star}_{i(q)}$ from (6.21) into (6.22) yields

$$\alpha^2_{i(q)}\hat{\mathbf{w}}^{\star H}_{i(q)}\mathbf{R}_{i(q)}(q)\hat{\mathbf{w}}^{\star}_{i(q)} - \sum_{j\in\mathcal{S}_l, j\neq i} \gamma_{i(q)}\alpha^2_{j(q)}\hat{\mathbf{w}}^{\star H}_{j(q)}\mathbf{R}_{i(q)}(q)\hat{\mathbf{w}}^{\star}_{j(q)} = \gamma_{i(q)}\left(\xi_{i(q)} + \sigma^2\right). \tag{6.23}$$

Let us denote $\mathbf{m}_q = \left[\gamma_{1(q)}\left(\xi_{1(q)} + \sigma^2\right) \quad \gamma_{2(q)}\left(\xi_{2(q)} + \sigma^2\right) \quad \cdots \quad \gamma_{U(q)}\left(\xi_{U(q)} + \sigma^2\right)\right]^T$, $\mathbf{t}_q = \left[\alpha^2_{1(q)} \quad \alpha^2_{2(q)} \quad \cdots \quad \alpha^2_{U(q)}\right]^T$ and define the $U \times U$ matrix $\mathbf{D}_q$ with the $(i(q), j(q))$th entry as

$$[\mathbf{D}_q]_{i(q),j(q)} = \begin{cases} \hat{\mathbf{w}}^{\star H}_{i(q)}\mathbf{R}_{i(q)}(q)\hat{\mathbf{w}}^{\star}_{i(q)}, & \text{if} \quad i = j \\ -\gamma_{i(q)}\hat{\mathbf{w}}^{\star H}_{j(q)}\mathbf{R}_{i(q)}(q)\hat{\mathbf{w}}^{\star}_{j(q)}, & \text{if} \quad i \neq j \end{cases} \tag{6.24}$$

for all $i, j \in \mathcal{S}_l$. One can rewrite (6.23) as

$$\mathbf{D}_q\mathbf{t}_q = \mathbf{m}_q. \tag{6.25}$$

The scaling factors $\alpha_{i(q)}, i \in \mathcal{S}_l$, can be determined by finding $\mathbf{t}_q$ from (6.25). Since all elements of $\mathbf{t}_q$ have to be nonnegative and $\mathbf{m}_q$ is a vector with nonnegative values on all dimensions, the existence of a feasible solution for $\mathbf{t}_q$ depends on the structure of $\mathbf{D}_q$. The condition for the existence of a feasible solution to (6.25) is stated in the following lemma.

Lemma 6.2. *There exists a unique feasible solution to the problem (6.25) in the form of* $\mathbf{t}_q = \mathbf{D}_q^{-1}\mathbf{m}_q$*, if Z-matrix* $\mathbf{D}_q$*, given in (6.24), satisfies*

$$\hat{\mathbf{w}}^{\star H}_{i(q)}\mathbf{R}_{i(q)}(q)\hat{\mathbf{w}}^{\star}_{i(q)} > \gamma_{i(q)} \sum_{j\in\mathcal{S}_l, j\neq i} \hat{\mathbf{w}}^{\star H}_{j(q)}\mathbf{R}_{i(q)}(q)\hat{\mathbf{w}}^{\star}_{j(q)}, \quad \forall i \in \mathcal{S}_l. \tag{6.26}$$

Proof. First, we outline the following definitions:

Definition 1 [104], [105], [106]: A matrix $\mathbf{A} \in \mathcal{R}^{K\times K}$ is called a Z-matrix if all of its off-diagonal elements are non-positive. A matrix $\mathbf{A} \in \mathcal{R}^{K\times K}$ is a P-matrix if its all

principal minors are positive.

Definition 2 [105, Definition 2.2.19]: A matrix $\mathbf{A} \in \mathcal{R}^{K\times K}$ is strictly row diagonally dominant if

$$|a_{ii}| > \sum_{j=1, j\neq i}^{K} |a_{ij}|, \quad i = 1, \cdots, K, \tag{6.27}$$

where a_{ii} denotes the (i,i)th entry of matrix $\mathbf{A}$ and $|\cdot|$ represents the absolute value operator. It is clear from (6.24) that $\mathbf{D}_q$ is a Z-matrix.

If the Z-matrix $\mathbf{D}_q$ satisfies the conditions in (6.26), then it is a strictly row diagonally dominant matrix. Therefore according to [106, Theorem 6.2.3], the Z-matrix $\mathbf{D}_q$ is also a P-matrix. Furthermore, the inverse of a matrix that is Z and P is nonnegative [105, Theorem 3.11.10]. By a nonnegative matrix, we mean that all elements of that matrix are real and nonnegative. Since all elements of the vector $\mathbf{m}_q$ in (6.25) are non-negative, then

$$\mathbf{t}_q = \mathbf{D}_q^{-1}\mathbf{m}_q \succeq 0. \tag{6.28}$$

□

A trivial consequence of (6.19) implies the following remark.

Remark: The optimisation problem in (6.3) can be reformulated as a set of N individual optimisation problems that can be solved by the N BSs in N individual cells. The resulting optimisation problem for any BS $q \in \mathcal{S}_b$ is given by

$$\begin{aligned} \min_{\mathbf{w}_{i(q)}} \quad & \sum_{i\in\mathcal{S}_l} \mathbf{w}_{i(q)}^H \mathbf{w}_{i(q)} + \sum_{k\in\mathcal{S}_b, k\neq q} \sum_{t\in\mathcal{S}_l} \sum_{i\in\mathcal{S}_l} \mu_{t(k)} \mathbf{w}_{i(q)}^H \mathbf{R}_{t(k)}(q) \mathbf{w}_{i(q)} \\ \text{s. t.} \quad & \mathrm{SINR}_{i(q)} \geq \gamma_{i(q)}, \quad \forall i \in \mathcal{S}_l. \end{aligned} \tag{6.29}$$

Proof. Using the similar steps of proof lemma 6.1, it is straightforward to show that the Lagrange dual of the problem (6.29) has the same solution as the problem (6.19). □

The downlink beamforming scheme described by the problem (6.29) can be considered as distributed in a sense that each BS designs its beamforming vectors independently, using the direct and the cross channel statistical information. In cellular systems, each BS may capture the cross channel information of the adjacent cell's cell-edge users who are close enough to the cell borders via overhearing and exploiting the channel reciprocity in the time division duplex (TDD) systems [21] or through a direct feedback channel initiated by the cell-edge users in the frequency division duplex (FDD) systems. Otherwise, the cross channel information of the users of the neighboring cells are attained from their corresponding BSs via backhaul. The steps of the proposed iterative scheme are summarized in Algorithm 6.1 where the iterations in step 5 converge to an optimal point for any initialized values in step 3. The scheduling routine from step 9 to step 13 in Algorithm 6.1 is executed to ensure the existence of

the optimal downlink beamforming vectors.

Algorithm 6.1 Iterative algorithm for the BS q, $q \in \mathcal{S}_b$

1: Define a set of locally active users $\mathcal{S}_l$ with their corresponding SINR requirements and a stopping point ϵ of the algorithm.
2: $n = 1$.
3: Initialize $\mathbf{p}_q(n) \succeq 0$.
4: For all $i \in \mathcal{S}_l$, find $\hat{\mathbf{w}}_{i(q)}(n)$ as the dominant eigenvector of the matrix $\mathbf{G}_{i(q)}^{-1}(\mathbf{p}_q(n))\mathbf{R}_{i(q)}(q)$ and calculate $k_{i(q)}(\mathbf{p}_q(n)) = \gamma_{i(q)} \frac{\hat{\mathbf{w}}_{i(q)}^H(n)\mathbf{G}_{i(q)}(\mathbf{p}_q(n))\hat{\mathbf{w}}_{i(q)}(n)}{\hat{\mathbf{w}}_{i(q)}^H(n)\mathbf{R}_{i(q)}(q)\hat{\mathbf{w}}_{i(q)}(n)}$.
5: Update $\mathbf{p}_q(n+1) = \mathbf{k}(\mathbf{p}_q(n))$.
6: $n = n + 1$.
7: Repeat lines 4 to 6 until $\| \mathbf{p}_q(n+1) - \mathbf{p}_q(n) \| \leq \epsilon$.
8: $\hat{\mathbf{w}}_{i(q)}^{\star} = \hat{\mathbf{w}}_{i(q)}(n+1)$.
9: **if** condition (6.26) is satisfied for all i **then**
10: go to line 14
11: **else if** condition (6.26) is not satisfied for a user i **then**
12: either reduce its required SINR so that (6.26) holds or remove that user from $\mathcal{S}_l$. Then go to line 2.
13: **end if**
14: The optimal downlink beamforming vector for user i is given as $\mathbf{w}_{i(q)}^{\star} = \alpha_{i(q)}\hat{\mathbf{w}}_{i(q)}^{\star}$ where $\alpha_{i(q)}$ is found as the square root of the i-th entry of the vector $\mathbf{t}_q = \mathbf{D}_q^{-1}\mathbf{m}_q$.

6.4 Choice of the pricing factors

This section deals with finding the pricing factors for the optimisation problem (6.3), or equivalently (6.29) for all individual BSs $q \in \mathcal{S}_b$, to expand the operational range of SINR constraints via pricing. It will be shown in Section 6.5.2, with trivial choice of unity for the pricing factors, the required total transmit power to attain larger SINR targets, i.e, beyond some certain levels, can rise to higher values that may not be affordable in practical scenarios. In this section, an additional outer-loop search for finding the prices to achieve these higher targets of SINR with lower increases in the total transmit power of the network is introduced. In the following, two pricing strategies are proposed.

6.4.1 Pricing-per-user strategy

Consider the price tuple $\mathbf{r} \triangleq (\mathbf{r}_k)_{k=1}^N = \begin{bmatrix} \mathbf{r}_1^T & \mathbf{r}_2^T & \cdots & \mathbf{r}_N^T \end{bmatrix}^T$, where $\mathbf{r}_q = \begin{bmatrix} \mu_{1(q)} & \mu_{2(q)} & \cdots & \mu_{U(q)} \end{bmatrix}^T$, $q \in \mathcal{S}_b$. Let P_q be the transmitted power of a BS q at a critical SINR target of its local user i, i.e., $i(q)$. Here, the critical refers to

a SINR target beyond which a sharp rise in the BS transmitted power is inevitable. On the other hand, achieving such a power-hungry SINR target may be essential for the user, but may not be sustainable by the BS due to the limited power constraint. In order to come up with an efficient compromise between the power and the SINR demand, this section proposes to update the current price of user $i(q)$ and broadcast it to the other BSs, so that the induced inter-cell interference power on user $i(q)$ is reduced and, hence, further increase in its SINR target is achievable with an affordable transmit power at the BS q. Let us also define $g_{i(q)}\left(\mathbf{r}_{-q}\right) = P_{i(q)} - \mathbf{w}_{i(q)}^H \mathbf{w}_{i(q)}$, where $\mathbf{r}_{-q} \triangleq (\mathbf{r}_k)_{k=1,k\neq q}^N$, and $\mathbf{g}(\mathbf{r}) = \left[\mathbf{g}_1^T(\mathbf{r}_{-1}) \quad \mathbf{g}_2^T(\mathbf{r}_{-2}) \quad \cdots \quad \mathbf{g}_N^T(\mathbf{r}_{-N})\right]^T$, where $\mathbf{g}_q(\mathbf{r}_{-q}) = \left[g_{1(q)}\left(\mathbf{r}_{-q}\right) \quad g_{2(q)}\left(\mathbf{r}_{-q}\right) \quad \cdots \quad g_{U(q)}\left(\mathbf{r}_{-q}\right)\right]^T$, $q \in \mathcal{S}_b$. Then, the prices for the users of BS q can be updated using the iterative Projection Algorithm with constant step size according to

$$\mathbf{r}_q\left(n+1\right) = \left[\mathbf{r}_q\left(n\right) - \tau \mathbf{g}_q\left(\mathbf{r}_{-\mathbf{q}}\left(n\right)\right)\right]^+, \tag{6.30}$$

where $[a]^+ = \max(0, a)$, τ is a positive step size and n is the iteration index. Each BS updates its users' prices at each iteration and broadcasts these prices to the other BSs. Then, each BS uses the received prices for its outer-cell users to update the beamforming vectors towards its local users via the proposed iterations in Algorithm 6.1. Notice that broadcasting the pricing factors requires inter-BS cooperation via a backhaul link. The detailed steps of the proposed pricing scheme are summarized in Algorithm 6.2. Here, the iterations in Algorithms 6.1 and 6.2 are referred to as the inner and the outer iterations, respectively.

Algorithm 6.2 Pricing-per-user algorithm

1: Define the stopping point ϵ_q for the algorithm.
2: $n = 1$.
3: Initialize $\mathbf{r}\left(n\right) \succeq 0$ and chose the step size $\tau > 0$.
4: Each BS executes Algorithm 6.1 with the weighting factors for its outer-cell users obtained from the price tuple $\mathbf{r}\left(n\right)$.
5: Each BS $q \in \mathcal{S}_b$ updates its price vector: $\mathbf{r}_q\left(n+1\right) = \left[\mathbf{r}_q\left(n\right) - \tau \mathbf{g}_q\left(\mathbf{r}_{\mathbf{q}}\left(n\right)\right)\right]^+$ then broadcasts the updated price vector $\mathbf{r}_q\left(n+1\right)$.
6: $n = n + 1$.
7: Repeat lines 4 and 6 until $\| \mathbf{g}_q\left(\mathbf{r}_{-q}\left(n\right)\right) - \mathbf{g}_q\left(\mathbf{r}_{-q}\left(n-1\right)\right) \| \leq \epsilon_q$.

Algorithm 6.2 converges to an equilibrium as long as the increased pricing factors lead to further decrease in inter-cell interference by the inner iterations, i.e., the proposed optimisation problem in (6.3), at any given BS q. At a current iteration n of (6.30), a larger gap between the actually transmitted power by the BS q to the local user $i(q)$, i.e., $\mathbf{w}_{i(q)}^H(n)\mathbf{w}_{i(q)}(n)$, and the minimum desired power level for that user,

i.e,, $P_{i(q)}$, leads to a larger pricing factor for the user $i(q)$ in the following iteration $n+1$, i.e., $\mu_{i(q)}(n+1) > \mu_{i(q)}(n)$. Hence, the increased price of user $i(q)$ enforces the other BSs, through the inter-cell interference controlling term of the proposed objective function in (6.3), to reduce $\xi_{i(q)}$, i.e., other BSs aggregate interference power on user $i(q)$. It can be verified from the proof of Lemma 6.2 and the result (6.28), therein, that since the qth element of $\mathbf{m}_q$ decreases as $\xi_{i(q)}$ decreases and $\mathbf{D}_q^{-1}$ is a non-negative matrix, i.e., all of its elements are non-negative and real, all dimensions of $\mathbf{t}_q$ including the qth dimension decreases at iteration $n+1$. On the other hand the element on dimension q of $\mathbf{t}_q$ is the scaling factor $\alpha_{i(q)}^2$ that determines the transmit power level of BS q towards the user $i(q)$, i.e., see (6.21). Therefore, $\mu_{i(q)}(n+1) > \mu_{i(q)}(n)$ leads to $\mathbf{w}_{i(q)}^H(n+1)\mathbf{w}_{i(q)}(n+1) < \mathbf{w}_{i(q)}^H(n)\mathbf{w}_{i(q)}(n)$. However, the limited number of antenna elements at BSs imposes a restriction on the minimum power transmitted by the BS q towards its ith user, i.e., user $i(q)$. This, in turn, ultimately leads to some minor changes in transmitted powers, i.e., within a prescribed limit specified as ϵ_q in Algorithm 6.2, between any two successive iterations, i.e., $\mathbf{w}_{i(q)}^H(n+1)\mathbf{w}_{i(q)}(n+1) \approx \mathbf{w}_{i(q)}^H(n)\mathbf{w}_{i(q)}(n)$. At this point, $g_{i(q)}\left(\mathbf{r}_{-q}(n+1)\right) \approx g_{i(q)}\left(\mathbf{r}_{-q}(n)\right)$ leads to the stabilization of the pricing factor $\mu_{i(q)}$ at an equilibrium, i.e., $\mu_{i(q)}(n+1) \approx \mu_{i(q)}(n)$. Without loss of generality, the convergence analysis given for any user $i(q)$ can be applied to justify the convergence of a collection of simultaneous users in the network.

6.4.2 Pricing-per-BS strategy

In order to avoid the circulation of prices amongst BSs, a single pricing factor μ_q is locally calculated and used at each BS q, $q \in \mathcal{S}_b$, in this strategy. In fact, the objective function in the original optimisation problem (6.3) is amended by using μ_q instead of $\mu_{t(k)}$. Let P_q be the total transmitted power of a BS q at some critical SINR targets of its local users. Here, the critical refers to those SINR targets beyond which a sharp rise in the transmitted power is required. On the other hand, achieving such power-hungry SINR demands may be essential, but may not be sustainable by the BS q due to the limited power constraint. Hence, this strategy aims at reaching a power-efficient compromise by updating the current pricing factor of the induced interference levels of the BS q on the other users of the other cells, so that further increases in SINR targets are achievable with an affordable transmit power at the BS q. In the sequel, the proposed Pricing-per-BS strategy is described. Defining $\tilde{g}_q\left(\mu_q\right) = P_q - \sum_{i \in \mathcal{S}_l} \mathbf{w}_{i(q)}^H \mathbf{w}_{i(q)}$, the pricing factor of BS q is updated as

$$\mu_q\left(n+1\right) = \left[\mu_q\left(n\right) - \tau \tilde{g}_q\left(\mu_q\left(n\right)\right)\right]^+, \tag{6.31}$$

where τ is a positive step size. Algorithm 6.3 outlines the steps of the proposed Pricing-per-BS strategy. The convergence of Algorithm 6.3 can be verified using the similar steps described for verifying the convergence of the Pricing-per-user strategy in Section 6.4.1. Here, a larger aggregate transmit power of a BS q at a current iteration n, i.e., $\sum_{i\in\mathcal{S}_l} \mathbf{w}_{i(q)}^H(n)\mathbf{w}_{i(q)}(n)$, results in a higher pricing factor for the next iteration $n+1$, i.e., $\mu_q(n+1) > \mu_q(n)$. This, in turn, enforces lower induced interference by the BS q on the users of the other cells. Similarly, applying the results from the proof of lemma 6.2, one can verify that decreased inter-cell interference by the BS q on the users of the other BSs decreases the transmitted power of the other BSs and this, in turn, lowers their induced interference on the local users of the BS q. Therefore, it can be concluded that $\mu_q(n+1) > \mu_q(n)$ leads to $\sum_{i\in\mathcal{S}_l} \mathbf{w}_{i(q)}^H(n+1)\mathbf{w}_{i(q)}(n+1) < \sum_{i\in\mathcal{S}_l} \mathbf{w}_{i(q)}^H(n)\mathbf{w}_{i(q)}(n)$ and ultimately the Algorithm 6.3 converges to an equilibrium.

Algorithm 6.3 Pricing-per-BS algorithm

1: Define the stopping point ϵ_q for the algorithm.
2: $n = 1$.
3: Initialize $\mu_q(n) \geq 0$ and chose the step size $\tau > 0$.
4: BS q executes Algorithm 6.1 with the price $\mu_q(n)$.
5: BS q updates its price vector: $\mu_q(n+1) = [\mu_q(n) - \tau\tilde{g}_q(\mu_q(n))]^+$.
6: $n = n + 1$.
7: Repeat lines 4 and 6 until $\tilde{g}_q(\mu_q(n)) - \tilde{g}_q(\mu_q(n-1)) \leq \epsilon_q$.

In the following, the proposed pricing strategies are intuitively described and compared. In the Pricing-per-user strategy, when any user $i(q)$ requires a significantly higher transmit power to obtain a higher SINR, the corresponding local BS allocates a higher price for that user and broadcasts it to other BSs. In response, the other BSs design their beamforming vectors for their local users such that their induced interference on that user $i(q)$ is reduced. Whereas, in a similar situation in the Pricing-per-BS strategy, the local BS q allocates a higher pricing factor on its own induced interference on the other users of the other cells. In return, the other BSs reduce their induced interference on the local users of BS q, since the other BSs also follow the same strategy as the BS q. Pricing-per-user is a cooperative strategy and can be viewed as a passive pricing strategy whereas the Pricing-per-BS strategy is a decentralised mechanism and can be regarded as an active pricing strategy.

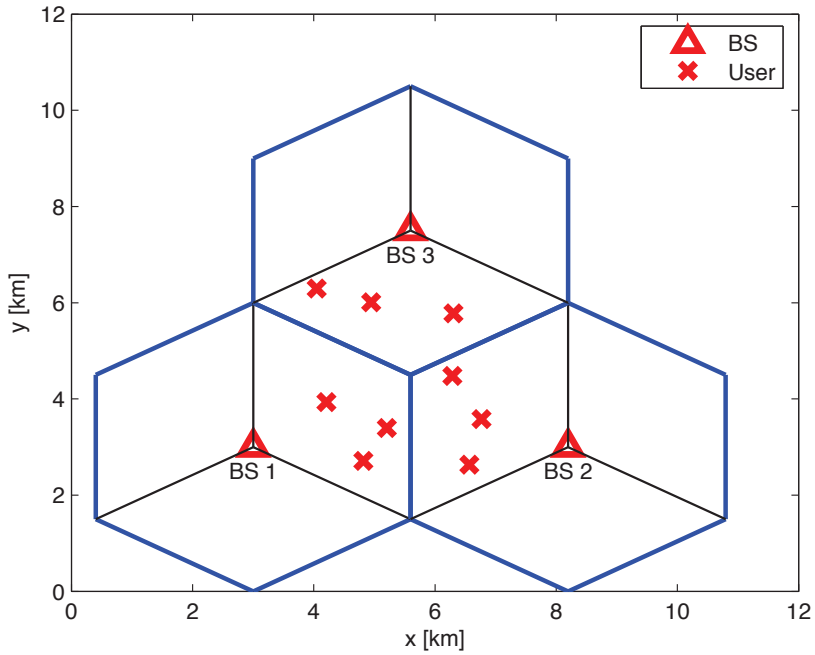

Figure 6.1: An example of random 3-user distribution per sector.

6.5 Simulation results

6.5.1 Simulation setup

In this section, the performance of the proposed algorithms are demonstrated within a cellular network composed of 3 cells, as shown in Fig. 6.1. In particular, either 2 or 3 users per sector are randomly distributed such that they are located within the 3 adjacent sectors of 3 neighbouring cells, i.e., either 6 or 9 users per 3 adjacent sectors. With this set up, a critical scenario is considerd in terms of severeness of ICI and the convergence behavior of the distributed BSs in reaching to an equilibrium point. Monte-Carlo simulations have been carried out over 30 independent sets of 2 users per sector and 30 independent sets of 3 users per sector. Fig. 6.1 shows an example of one of these distributions. It is also assumed that any two neighboring BSs are located 3 km apart from one another.

The channel covariance matrix from BS q to user i in cell k, i.e., $\mathbf{R}_{i(k)}(q)$, is modeled as

$$\mathbf{R}_{i(k)}(q) = \vartheta_{i(k)}(q)\,\mathbf{R}\left(\theta_{i(k)}(q), \sigma_a\right), \tag{6.32}$$

where $\vartheta_{i(k)}(q)$ is the channel gain coefficient, $\theta_{i(k)}(q)$ is the nominal azimuth angle, σ_a is the standard deviation of the angular spread and the (m,n)th element of

$\mathbf{R}\left(\theta_{i(k)}(q), \sigma_a\right)$ is [33, 56],

$$e^{\frac{j2\pi\Delta}{\lambda}\left[(n-m)\sin\theta_{i(k)}(q)\right]} e^{-2\left[\frac{\pi\Delta\sigma_a}{\lambda}\left\{(n-m)\cos\theta_{i(k)}(q)\right\}\right]^2}. \tag{6.33}$$

In (6.33), λ is the carrier wavelength and Δ is the antenna spacing at BSs. We have set $\Delta = \lambda/2$ and $\sigma_a = 2^\circ$. In (6.32), $\vartheta_{i(k)}(q)$ captures the distance-dependent path-loss according to $34.5 + 35\log_{10}(l)$, where l is the distance in meters with $l \geq 35m$, a log-normal shadow fading with 8dB standard deviation and a Rayleigh component for the fading channel. The distance between neighboring BSs is assumed to be 3km. The noise power spectral density is set to -174 dBm/Hz. An antenna gain of 15dBi is assumed. Either 4, 8 or 12 antenna elements per sector have been used in simulations.

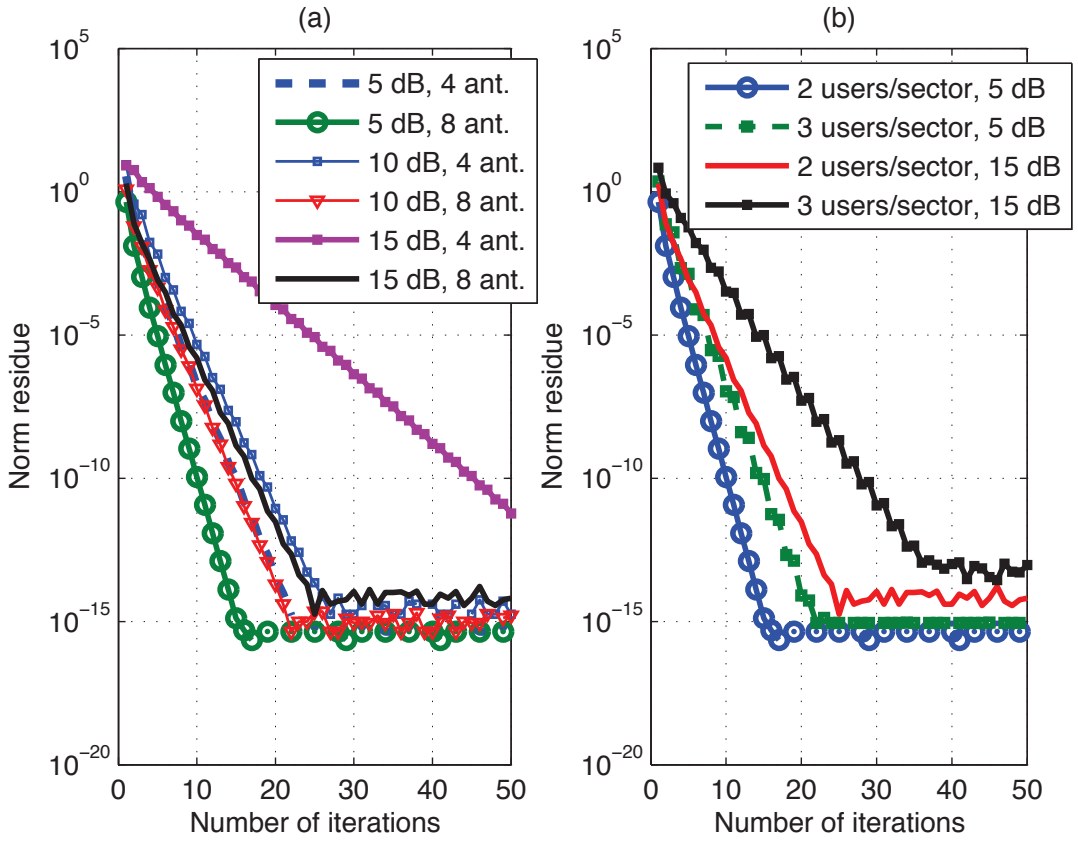

Figure 6.2: Residual norm versus number of iterations of the proposed iterative Algorithm 6.1 with equal pricing factors of one for all users and: (a) with different number of antenna elements and SINR targets for 2 users per sector, (b) with 8 antenna elements for 2 and 3 users per sector.

6.5.2 Simulation results

In Fig. 6.2 (a), the residual norm of $\| \mathbf{p}(n) - \mathbf{p}^\star \|$, where $\mathbf{p}^\star$ is the optimal solution to problem (6.17), has been drawn versus the number of iterations to demonstrate the speed of convergence of Algorithm 6.1 to $\mathbf{p}^\star$ for 2 users per sector. The results show that with the same number of users per sector, the speed of convergence increases either with a higher number of antenna elements at BSs or with a lower SINR target at user terminals. Moreover, the convergence speed of the proposed algorithm also depends on the number of active users per sector. It is shown in Fig. 6.2 (b) that more users per sector results in a slower convergence speed.

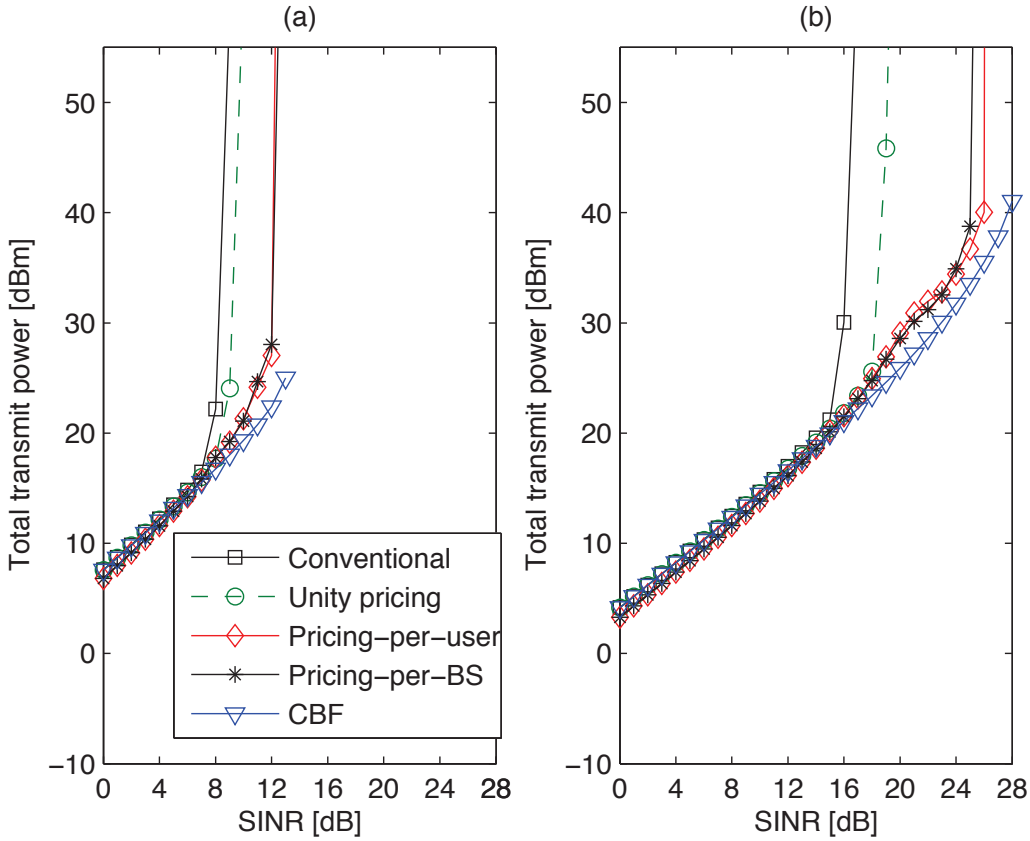

Figure 6.3: Sum-power consumption of all BSs for the proposed, conventional and centralised schemes versus SINR targets with 2 users per sector and: (a) 4 antenna elements per sector, (b) 8 antenna elements per sector.

In Figs. 6.3 and 6.4, the proposed algorithm has been compared against the conventional scheme and a centralised coordinated beamforming technique, i.e., CBF [37], in terms of sum-power consumption by all BSs versus equal SINR targets at user terminals. In the conventional scheme, each BS selfishly minimises its own total transmit

power subject to maintaining a set of SINR requirements for its local users, i.e., without accounting for the induced inter-cell interference on the users who are operating on the same frequency band. The CBF technique jointly optimises and designs the beamforming vectors of all BSs in a centralised unit as described in [37]. The proposed scheme optimises the downlink beamforming vectors at individual BSs in a distributive fashion, as described in Algorithms 6.1, 6.2 and 6.3. Figs. 6.3(a) and 6.3(b) show the results for 4 and 8 antenna elements per sector, respectively, and for 2 users per sector of the adjacent cells. Whereas, Figs. 6.4(a) and 6.4(b) illustrate the results for 8 and 12 antenna elements per sector, respectively, and for 3 users per sector of the adjacent cells, as depicted in Fig. 6.1. A step size of $\tau = 10^{-4}$ has been used for both of the proposed pricing strategies. In trying to obtain as closer performance as possible to the centralised CBF solutions, i.e., for the sake of comparison, the reference power levels of $P_{i(q)}$ and P_q in the proposed Pricing-per-user and Pricing-per-BS strategies, respectively, have been set as the power levels required by the centralised CBF scheme for the same SINR demands.

The results shown in Figs. 6.3 and 6.4 confirm that the proposed scheme outperforms the conventional one in terms of power efficiency in supporting relatively larger SINR targets, even with a trivial setting of all pricing factors to unity. However, by activating the pricing mechanisms in the proposed scheme, one can extend the power-efficient coverage of SINR targets to higher figures. For instance, the results in Figs. 6.3(a) and 6.3(b) show extensions of 3 dB and 8 dB in power-efficient SINR coverage for 4 and 8 antenna elements, respectively, with 2 users per sector. The drawback of the conventional scheme is due to the so-called ping-pong effect in a multi-cell environment, where each BS keeps increasing its transmit power to maintain its users' SINR requirements and, inevitably, keeps increasing its interference on the users' of the other cells. Whereas the second term of the objective function of the proposed optimization problem in (6.3) controls the inflicted inter-cell interference by each BS and stabilizes the egoistic dynamic of the conventional network in an equilibrium point, agreed by all BSs. As a result of this stabilization, the proposed algorithm can effectively extend the operational range of SINR. Although, both pricing strategies show almost the same performance in terms of power requirements over the most power-efficient range of SINR targets they tend to depart gradually at higher SINR targets, e.g., considerably at 14 dB in Fig. 6.4 (a) and at 17 dB in Fig. 6.4 (b). This observation shows that the Pricing-per-user strategy is more sensitive than the Pricing-per-BS strategy at higher SINR targets to the balance between the number of antenna elements and the total number of active users in all of the adjacent sectors. For instance, in Fig. 6.4 (a),

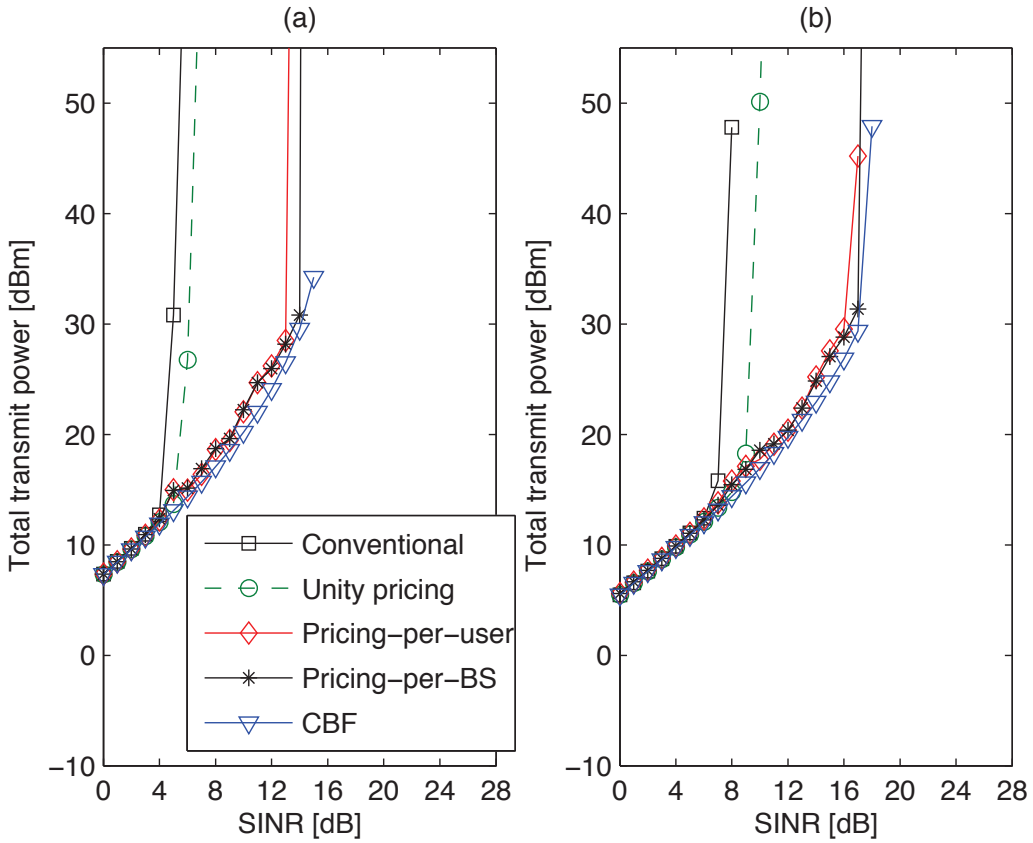

Figure 6.4: Sum-power consumption of all BSs for the proposed, conventional and centralised schemes versus SINR targets with 3 users per sector and: (a) 8 antenna elements per sector, (b) 12 antenna elements per sector.

the total number of 9 active users exceeds the available 8 antenna elements per sector, whereas, in Fig. 6.4 (b), this imbalance reverses to 9 active users versus 12 antenna elements per sector. Furthermore, results shown in Figs. 6.3 and 6.4 indicate that our proposed algorithm with pricing strategies can closely follow the performance of the centralised CBF [37] scheme.

Fig. 6.5 shows the convergence dynamic of total as well as per BS transmit power and inter-cell interference induced on each user versus the number of pricing iterations at 22 dB SINR target for the proposed pricing strategies. Comparing Figs. 6.5(a) and 6.5(b), one can see that the transmit power at BSs as well as the inter-cell interference levels settle faster at their corresponding equilibrium points in the Pricing-per-BS strategy. This is because of more pricing factors to be adjusted by the proposed algorithm for the Pricing-per-user strategy than the Pricing-per-BS strategy. Fig. 6.6 shows the convergence dynamic of the pricing factors in both of the pricing strategies for the same scenario as in Fig. 6.5. A comparison of the depicted results in Figs.

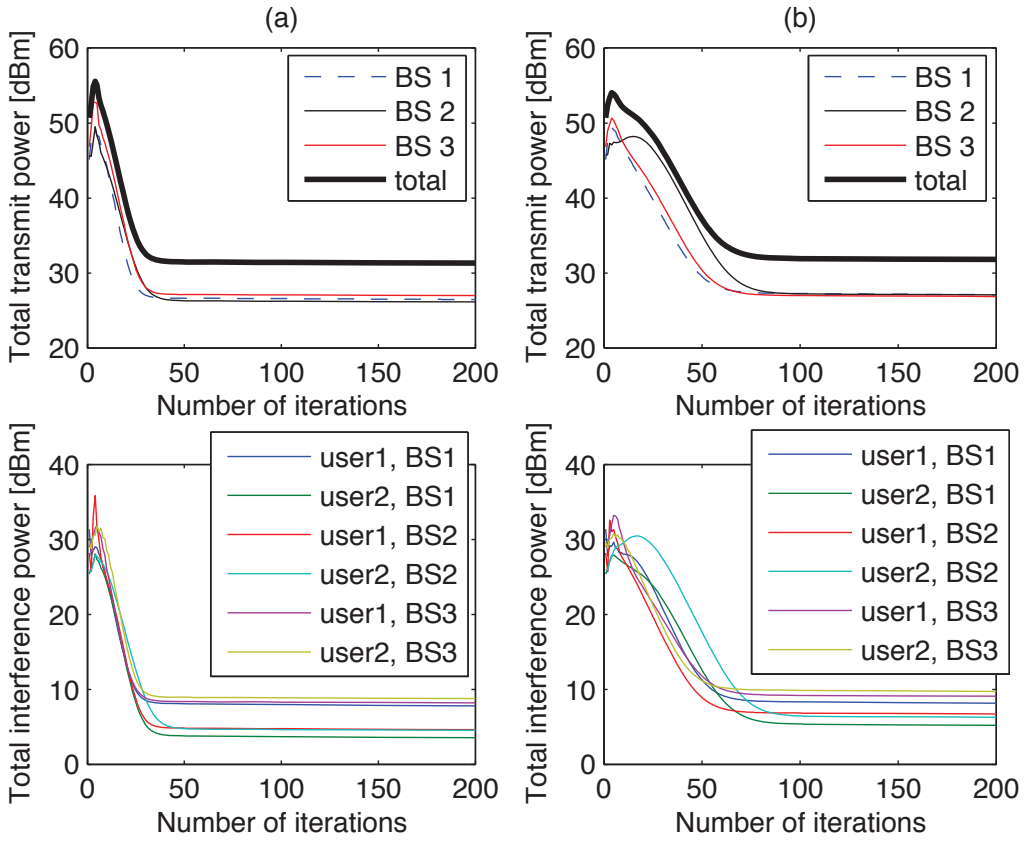

Figure 6.5: Convergence and transient behavior of transmit power and inter-cell interference versus the number of pricing iterations for 2 users per sector and 22 dB SINR target in: (a) Pricing-per-BS strategy and (b) Pricing-per-user strategy.

6.6(a) and 6.6(b) also confirms that the pricing factors in the Pricing-per-BS strategy converge faster than those of the Pricing-per-user strategy to their equilibrium points. Furthermore, the Pricing-per-BS strategy is suitable for distributed implementation at individual BSs, whereas the Pricing-per-user strategy requires the exchange of prices amongst BSs.

6.6 Conclusion

In this chapter, a decentralised beamforming strategy for downlink transmission in multi-cell processing networks has been introduced with two interference pricing strategies. In terms of flexibility, the proposed optimisation approach allows each BS to reach a balance between minimising the total interference leakage and minimising the total transmit power while assuring the desired SINR targets for its local user terminals. The Pricing-per-user and Pricing-per-BS strategies have been introduced to widen the

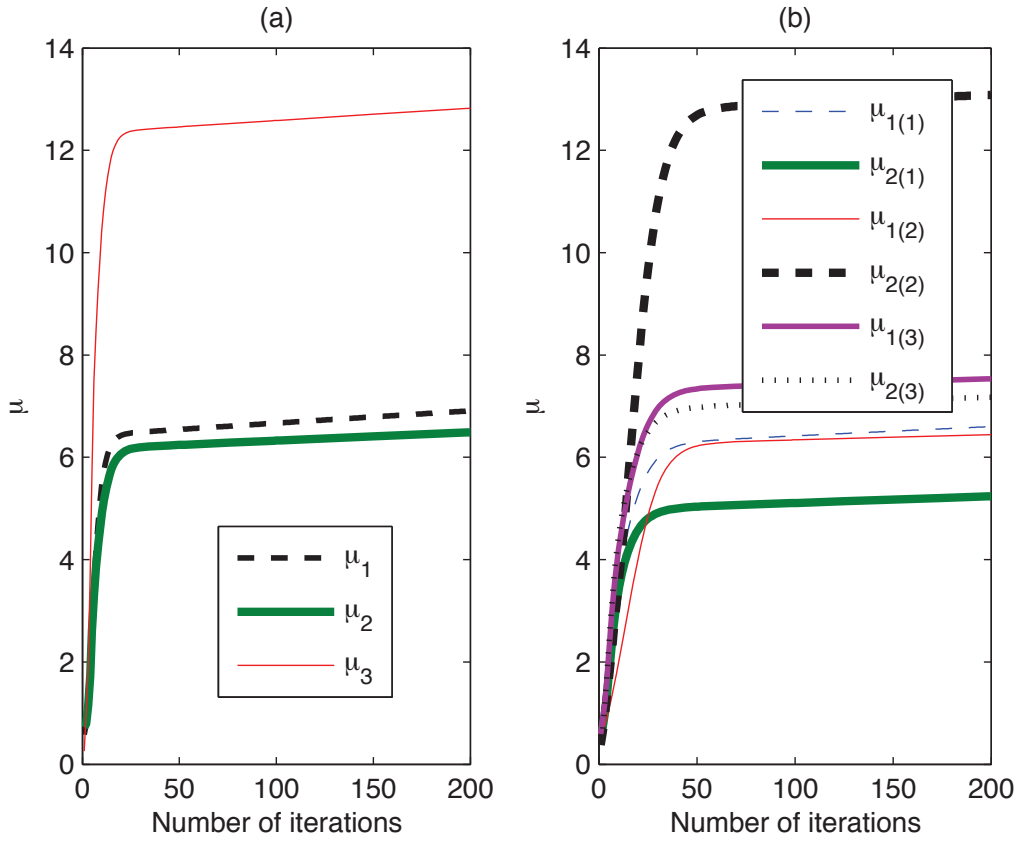

Figure 6.6: Convergence and transient behavior of pricing factors versus the number of pricing iterations for 2 users per sector and 22 dB SINR target in: (a) Pricing-per-BS strategy and (b) Pricing-per-user strategy.

range of SINR demands that can be supported by the BSs efficiently in terms of total power consumption. In the former, the BS allocates a higher price for a corresponding local user whose target SINR requires a high transmit power and broadcasts it to the other BSs. In return, the other BSs design their beamforming vectors for their local users such that their induced interference on that user is reduced. Whereas, in the latter and in a similar situation, the local BS allocates a higher pricing factor on its own induced interference on the other users of the other cells. In return, the other BSs reduce their induced inter-cell interference on the vulnerable users of the original BS. It has been shown that the proposed algorithms converge to an equilibrium in a multi-cell scenario where the same bandwidth is used across the adjacent cells. The simulation results show that the proposed approach not only outperforms the conventional scheme but it also closely follows the performance of a centralised coordinated beamforming scheme in terms of power-efficient transmission.

Chapter 7

Conclusions and future work

The aim of this thesis is to reduce the overall power consumption of the cellular network while ensuring required levels of signal-to-interference-plus-noise ratios for all active user terminals. Interference has been identified as a challenge to be tackled in order to achieve this goal. To this end, this thesis exploited cooperation amongst base stations and proposed several interference management techniques based on beamforming. Three beamforming schemes with different levels of cooperation amongst base station were proposed to meet flexible requirements and backhaul availabilities. Multi-cell beamforming scheme was introduced at a signal-cooperative level where all users' data are circulated amongst BSs for a joint transmission. Coordinated beamforming scheme was developed at a beamforming-cooperative level where data is kept locally at each base station. User position aware multi-cell beamforming approach was proposed at a hybrid-level of the two aforementioned ones to take advantages of both multi-cell and coordinated beamforming schemes. Fast wireless backhaul protocols were introduced using network coding concept to establish interconnections amongst cooperating base stations. A framework was developed to evaluate the overall performance, including backhaul effects on power consumption and latency of the proposed beamforming schemes. In order to overcome the single-point-of-failure drawback caused by the centralised implementation of the aforementioned beamforming schemes, a decentralised beamforming scheme is introduced. In the decentralised beamforming scheme, individual BS can independently perform signal processing tasks using either locally attained channel state information or with limited exchange of channel state information amongst base stations.

This chapter summarises the findings of previous chapters and outlines possible future research directions.

7.1 Thesis summary

7.1.1 Summary of Chapter 1

The introductory chapter outlined the motivation of this thesis and defined the open issues regarding interference management in multi-cell networks. The contributions of this thesis were also stated.

7.1.2 Summary of Chapter 2

This chapter reviewed principles of beamforming using linear antenna array along with concepts of second order cone programming and semidefinite programming. An optimisation problem was presented to calculate transmit beamformers for multiple active users in a single-cell scenario. Different approaches to solve the optimisation problem were outlined.

7.1.3 Summary of Chapter 3

In this chapter, a multi-cell beamforming (MBF) scheme was proposed at the signal-cooperative level. Downlink beamforming vectors for all users of the network were jointly designed as if all coordinating BSs were a single BS. As a result of joint transmission each user's data was circulated amongst BSs. In order to reduce backhaul burden, a user position aware algorithm was introduced to allocate any user to the nearby BSs based on the information of the user's location. An iterative algorithm was developed to find optimal solution to the optimisation problem of the MBF scheme using uplink-downlink duality. The convergence of the algorithm depended on the number of antenna elements, the targeted SINRs, and the number of active users. Monte-Carlo simulation results confirmed that the proposed algorithm attained the optimal solution with the accuracy of 10^{-7} for the worst case, after just 50 iterations.

7.1.4 Summary of Chapter 4

In this chapter, a coordinated beamforming (CBF) scheme was developed at the beamforming-cooperative level to reduce backhaul burden. Beamforming vectors were jointly designed for coordinating BSs in a manner that each BS only transmits to its own users. The optimisation problem for the CBF scheme using instantaneous CSI

was formulated in standard semidefinite programming (SDP) form. In order to reduce signaling overhead in attaining instantaneous CSI, the optimisation problem for CBF was also cast in SDP form using second order statistical CSI, i.e., channel covariance matrix. The scheme was designed to tolerate a certain level of error in the estimation of the covariance matrix. Simulation results revealed that although the robustness came at the cost of increased transmit power, there was an opportunity to achieve a significant reduction in signaling overhead with a minor increase in total transmit power at moderately low SINRs. The results also showed that the performance of two proposed CBF schemes tended to converge at the moderately low region of SINR disregarding the level of uncertainty/error in CSI estimation.

7.1.5 Summary of Chapter 5

In this chapter, a possible power-saving gain offered by dividing a cell into tiers of smaller cells was derived as a function of the number of tiers and pass loss exponent. Network coding enabled wireless Star and Ring backhaul protocols were introduced to establish interconnection amongst BSs. Upper bound expressions on the achievable throughputs of the proposed protocols were derived. Using the Ring protocol, a framework was introduced to evaluate the overall performance of MBF and CBF schemes that include backhaul effects on both latency and power consumption. Interestingly, simulation results indicated that although the multi-cell beamforming scheme requires heavier backhaul than the coordinated beamforming scheme, the former outperformed the latter in terms of lower overall power consumption, including backhaul effects, when supporting cell-edge users. The results revealed a tradeoff between the power consumption gain and the complexity of backhaul.

7.1.6 Summary of Chapter 6

In this chapter, a decentralised beamforming (DBF) strategy for downlink transmission in multi-cell processing networks was proposed. Like the CBF scheme, users within a cell only obtained their data signals from their dedicated local BS. However, DBF differed from CBF in the fact that each BS locally designed its own beamforming vectors without relying on data or downlink CSI of links from other BSs to the users. Moreover, the iterative algorithm proposed for DBF was the solution to an inter-cell interference balancing optimisation problem. This problem minimises a linear combination of data transmission power and the resulting inter-cell interference power at each BS, while

maintaining the required SINRs by the local users. The Pricing-per-user and Pricing-per-BS strategies were introduced to widen the range of SINR demands that can be supported by the BSs efficiently in terms of total power consumption. It was shown that the proposed algorithm converges to an equilibrium in a multi-cell scenario where the same bandwidth is used across the adjacent cells. The simulation results indicated that the proposed approach not only outperforms the conventional scheme but it also closely follows the performance of a centralised coordinated beamforming scheme in terms of power-efficient transmission.

7.2 Future research directions

The contributions of this thesis suggest the following future research directions related to beamforming techniques for multi-cell processing (MCP).

7.2.1 Joint optimisation of downlink and backhaul

Backhaul link is an essential part in MCP. In practical scenarios, the backhaul has limited capacity. Therefore, the first effect of a non ideal backhaul on MPC is latency. In MCP, an additional phase of communications amongst coordinating BSs is required to jointly design transmitting parameters and/or exchange users' data. As a result, the delivered sum rate to end users depends on both backhaul rates and forward link rates (i.e., from BSs to users). An effective sum rate was introduced in Section 5.6.4 to capture the delay effect of the backhaul. The effective sum rate is a function of the backhaul rate and the smallest value of users' forward link rates, which is related to the smallest user's SINR. The second effect of the backhaul on MCP is the additional power required for circulating information among coordinating BSs. In Section 5.6.1, the Ring protocol was characterised in terms of power consumption. The power consumption of the protocol is a function of SNRs of inter-BS links with the assumption that the link between any two BSs is single-input-single-output and line-of-sight.

The framework introduced in Section 5.6.4 can be considered as a combination of two independent tasks, i.e. forward-link-design and backhaul-parameter-selection tasks, in order to gain a required effective sum rate. Although the framework provides a fair comparison for various beamforming schemes with different backhaul requirements, the combination of two independent tasks is not optimal in terms of neither the overall power consumption nor the effective sum rate. Therefore, joint optimising for both

downlink beamforming and backhaul parameters is a challenging problem for future research.

7.2.2 Robust beamforming

In downlink MCP, channel state information is required to design transmit beamforming/precoding vectors for all users terminals. This increases the burden on signaling overhead between BSs and their user terminals, especially for a large size of coordinating BSs. For this reason, algorithms that demand less signaling overhead are desirable for MCP. Furthermore, the obtained channel state information at the BS, i.e., the CSIT, may not be accurate due to the channel estimation error. As the system design based on corrupt CSIT may not function as expected in the realistic channel conditions, robust schemes to the uncertainties in CSIT are also of interests.

A worst-case robust beamforming for CBF presented in Chapter 4 is based on the assumption that channel uncertainty matrices are norm-bounded. This conservative approximation may decrease the performance of the robust beamforming schemes due to having too many protections for errors in channel estimation. Flexible approaches that avoid the conservative approximation and worst-case design are desirable. A possible approach is to use a probabilistic model to capture the randomness of the wireless channel. Furthermore, robust designs for the novel DBF scheme, introduced in Chapter 6, remain open.

7.2.3 Rate maximisation under power constraint

The focus of this thesis is on energy efficiency. Therefore, the objective functions defined in Chapters 3 and 4 are to minimise total transmit power across coordinating BSs. On the other hand, the objective function introduced in Chapter 6 is to minimise a linear combination of two utility functions, characterising each BS's weighted sum of transmitted power to the intra-cell users and its resulting weighted sum of interference power inflicted upon the users of the other cells. The constraints of all optimisation problems introduced in this thesis are on users' signal-to-interference-plus-noise ratios (SINRs). In other words, beamforming schemes proposed in this thesis ensure all users' quality of services above requirement levels with minimum total transmit power. A possible extension for the work in this thesis is to maximise the effective sum rate under transmit-power and backhaul-power constraints.

7.2.4 Multi-antenna users

An assumption used to develop beamforming schemes in this thesis is that user terminals are equipped with single antenna. When user terminals and base stations both have multiple antennas, there are more degree of freedom to effectively control interference. However, transmit and receive beamforming should be jointly designed. A question arising here is whether global optimality can be achieved by iteratively optimising transmit and receive beamforming. Complexity and signaling overhead are expected to significantly increase. Therefore, practical solutions to the optimal beamforming and tradeoff between optimality and complexity are open problems for research.

Appendix A: Proof for the mean of a log-normal random variable

In order to find $\mathbb{E}(10^{\frac{-x}{10}})$ where $x \sim \mathcal{N}(0, \sigma_S^2)$, let's consider a random variable $y = 10^{\frac{x}{10}}$. In the following we first find $\mathbb{E}(y)$. We have

$$\Pr(y < k) = \Pr\left(10^{\frac{x}{10}} < k\right) = \Pr(x < 10log_{10}k) = \int_{-\infty}^{10log_{10}k} \frac{1}{\sqrt{2\pi}\sigma} e^{-\frac{x^2}{2\sigma^2}} dx. \tag{1}$$

From $y = 10^{\frac{x}{10}}$, one can write

$$x = 10\frac{lny}{ln10} = \frac{lny}{a} \tag{2}$$

where $a = \frac{ln10}{10}$. Furthermore

$$dx = \frac{1}{ay} dy. \tag{3}$$

Substituting for x and dx from (2) and (3) into (1) we arrive at

$$\Pr(y < k) = \int_{-\infty}^{k} \frac{1}{\sqrt{2\pi}\sigma ay} e^{-\frac{ln^2 y}{2a^2\sigma^2}} dy. \tag{4}$$

Therefore, the pdf of y can be written as

$$f(y) = \frac{1}{\sqrt{2\pi}\sigma ay} e^{-\frac{ln^2 y}{2a^2\sigma^2}}. \tag{5}$$

We proceed to calculate $\mathbb{E}(y)$ as

$$\mathbb{E}(y) = \int_{-\infty}^{\infty} yf(y)dy = \int_{-\infty}^{\infty} \frac{y}{ay\sigma\sqrt{2\pi}} e^{-\frac{ln^2 y}{2a^2\sigma^2}} dy. \tag{6}$$

Let $z = lny$ then one can write $y = e^z$ and $dy = e^z dz$. Therefore

$$\begin{aligned}
\mathbb{E}(y) &= \int_{-\infty}^{\infty} \frac{1}{a\sigma\sqrt{2\pi}} e^z e^{-\frac{z^2}{2a^2\sigma^2}} dz & (7)\\
&= \int_{-\infty}^{\infty} \frac{1}{a\sigma\sqrt{2\pi}} e^{\frac{(-z^2+2za^2\sigma^2-a^4\sigma^4)+a^4\sigma^4}{2a^2\sigma^2}} dz & (8)\\
&= e^{\frac{a^2\sigma^2}{2}} \int_{-\infty}^{\infty} \frac{1}{a\sigma\sqrt{2\pi}} e^{-\frac{(z-a^2\sigma^2)^2}{2a^2\sigma^2}} dz & (9)\\
&= e^{\frac{a^2\sigma^2}{2}}. & (10)
\end{aligned}$$

Since $\mathbb{E}(10^{\frac{x}{10}}) = e^{\frac{a^2\sigma^2}{2}}$, $\mathbb{E}(10^{\frac{-x}{10}}) = e^{-\frac{a^2\sigma^2}{2}}$. This concludes the proof.

Appendix B: Extension of the UPA algorithm for sectoral cells

Consider a distributed antenna system (DAS) consisting of 7 cells depicted in Fig. 3.4, i.e., 2 tiers of cells [38]. This model can be extended for a DAS with more than 2 tiers of cells. Each cell is divided into 3 sectors with a linear antenna array of M elements per sector. The central cell, i.e., cell 1, acts as the controlling unit to assign users to different zones and to design beamforming vectors. The antenna arrays of 7 geographically separated BSs form a distributed-arrays antenna (DAA). We study the scenario where the DAA simultaneously supports K single-antenna users under the same carrier frequency.

Let $1\times 21M$ vector $\mathbf{h}_i$ be the global channel of user i as seen by the DAA and finally $1\times 3M$ vector $\overline{\mathbf{h}}_i(p)$ as the local channel of user i within the p^{th} cell, i.e., $i \in \{1, 2, \cdots K\}$ and $p \in \{1, 2, \cdots 7\}$. As the DAA comprises of arrays of 7 coordinating cells, one can write $\mathbf{h}_i = \left[\overline{\mathbf{h}}_i(1) \quad \overline{\mathbf{h}}_i(2) \cdots \quad \overline{\mathbf{h}}_i(7)\right]$ where

$$\begin{aligned} \overline{\mathbf{h}}_i(p) &= \left[a_i(p,1)\mathbf{h}_i(p,1) \quad a_i(p,2)\mathbf{h}_i(p,2) \quad a_i(p,3)\mathbf{h}_i(p,3)\right] \\ \mathbf{h}_i(p,q) &= \left[h_i\,(p,q,1) \quad h_i\,(p,q,2) \cdots h_i\,(p,q,M)\right], \end{aligned}$$

$q \in \{1, 2, 3\}$ indicates the sector index within a cell, $h_i\,(p, q, k)$ is the channel of user i as seen by the k^{th} element, i.e., $k \in \{1, 2 \cdots M\}$, of the array in sector q of cell p, and finally the controlling coefficient $a_i(p, q)$ is either 1 if user i is allocated to be served by sector q of cell p or 0 otherwise. In the following, we introduce the modification of UPA algorithm.

The radius Ω of the QoS guarantee circle for a cell is determined by path-loss exponent, user's targeted SINR and transmit power at BS. The QoS circles are shown as the outer-cell circles in Fig. 3.4. An intersection of two QoS circles and the nearest

BS defines the radius Ω_o of the inner-cell circle in Fig. 3.4. We distinguish two types of triangle within a DAS shown in Fig. 3.4 as follows. First, upward triangles comprise $\triangle$(2,3,1), $\triangle$(1,4,5), and $\triangle$(7,1,6). Second, downward triangles include $\triangledown$(3,4,1), $\triangledown$(1,5,6), and $\triangledown$(2,1,7). We define 3 kinds of zone for both upward and downward triangles as follows. Zone 1 is the area within the inner-cell circle, e.g., Z_1, Z_2 and Z_3. Users in zone 1 are supported by 1 or 2 nearest arrays. Zone 2 is the area bounded by a line connecting 2 BSs, their inner-cell circles and the outer-cell circle of the third cell, e.g., Z_{12}, Z_{13} and Z_{23}. Users in zone 2 are supported by 2 nearest arrays. Zone 3 is the common area of 3 outer-cell circles, e.g., Z_{123}. Users in zone 3 are supported by 3 or 6 arrays.

Let D denote the radius of cell, $A_i(p)$ be an angle of user i and BS p in 360^o coordinate, we first introduce algorithms to allocate users within the areas of the upward and downward triangles in Algorithms .1 and .2, respectively, then we propose the UPA algorithm to allocate user within the DAS in Algorithm .3.

Algorithm .1 Upward triangle(x, y, z, i)

$\Omega_o \triangleq \frac{3D}{2} - \sqrt{\Omega^2 - \frac{3D^2}{4}}$
if $l_{i,}(x) \leq \Omega_o$ **then**
  $a_i(x, 2) = 1\{$Assign user i to $Z_x\}$
else if $l_i(y) \leq \Omega_o$ **then**
  $a_i(y, 3) = 1\{$Assign user i to $Z_y\}$
else if $l_i(z) \leq \Omega_o$ **then**
  $a_i(z, 1) = 1\{$Assign user i to $Z_z\}$
else if $(\Omega_o < l_i(x) \leq \Omega)$ **and** $(\Omega_o < l_i(y) \leq \Omega)$ **and** $(l_i(z) > \Omega)$ **then**
  $a_i(x, 2) = 1$, $a_i(y, 3) = 1\{$Assign user i to $Z_{xy}\}$
else if $(\Omega_o < l_i(x) \leq \Omega)$ **and** $(\Omega_o < l_i(z) \leq \Omega)$ **and** $(l_i(y) > \Omega)$ **then**
  $a_i(x, 2) = 1$, $a_i(z, 1) = 1\{$Assign user i to $Z_{xz}\}$
else if $(\Omega_o < l_i(y) \leq \Omega)$ **and** $(\Omega_o < l_i(z) \leq \Omega)$ **and** $(l_i(x) > \Omega)$ **then**
  $a_i(y, 3) = 1$, $a_i(z, 1) = 1\{$Assign user i to $Z_{yz}\}$
else if $(\Omega_o < l_i(x) \leq \Omega)$ **and** $(\Omega_o < l_i(y) \leq \Omega)$ **and** $(\Omega_o < l_i(z) \leq \Omega)$ **then**
  $a_i(x, 2) = 1$, $a_i(y, 3) = 1$, $a_i(z, 1) = 1\{$Assign user i to $Z_{xyz}\}$
end if

Algorithm .2 Downward triangle(x, y, z, i)

$\Omega_o \triangleq \frac{3D}{2} - \sqrt{\Omega^2 - \frac{3D^2}{4}}$
if $l_i(x) \leq \Omega_o$ **then**
  if $l_i(y) = l_i(z)$ **then**
    $a_i(x, 2) = 1$, $a_i(x, 3) = 1\{$Assign user i to $Z_x\}$
  else if $l_i(y) > l_i(z)$ **then**
    $a_i(x, 3) = 1$ $\{$Assign user i to $Z_x\}$
  else if $l_i(y) < l_i(z)$ **then**
    $a_i(x, 2) = 1\{$Assign user i to $Z_x\}$
  end if
else if $l_i(y) \leq \Omega_o$ **then**
  if $l_i(x) = l_i(z)$ **then**
    $a_i(y, 1) = 1$, $a_i(y, 3) = 1\{$Assign user i to $Z_y\}$
  else if $l_i(x) > l_i(z)$ **then**
    $a_i(y, 3) = 1$ $\{$Assign user i to $Z_y\}$
  else if $l_i(x) < l_i(z)$ **then**
    $a_i(y, 1) = 1\{$Assign user i to $Z_y\}$
  end if
else if $l_i(z) \leq \Omega_o$ **then**
  if $l_i(x) = l_i(y)$ **then**
    $a_i(z, 1) = 1$, $a_i(z, 2) = 1\{$Assign user i to $Z_z\}$
  else if $l_i(x) > l_i(y)$ **then**
    $a_i(z, 2) = 1$ $\{$Assign user i to $Z_z\}$
  else if $l_i(x) < l_i(y)$ **then**
    $a_i(z, 1) = 1\{$Assign user i to $Z_z\}$
  end if
else if $(\Omega_o < l_i(x) \leq \Omega)$ **and** $(\Omega_o < l_i(y) \leq \Omega)$ **and** $(l_i(z) > \Omega)$ **then**
  $a_i(x, 2) = 1$, $a_i(y, 1) = 1\{$Assign user i to $Z_{xy}\}$
else if $(\Omega_o < l_i(x) \leq \Omega)$ **and** $(\Omega_o < l_i(z) \leq \Omega)$ **and** $(l_i(y) > \Omega)$ **then**
  $a_i(x, 3) = 1$, $a_i(z, 1) = 1\{$Assign user i to $Z_{xz}\}$
else if $(\Omega_o < l_i(y) \leq \Omega)$ **and** $(\Omega_o < l_i(z) \leq \Omega)$ **and** $(l_i(x) > \Omega)$ **then**
  $a_i(y, 3) = 1$, $a_i(z, 2) = 1\{$Assign user i to $Z_{yz}\}$
else if $(\Omega_o < l_i(x) \leq \Omega)$ **and** $(\Omega_o < l_i(y) \leq \Omega)$ **and** $(\Omega_o < l_i(z) \leq \Omega)$ **then**
  $a_i(x, 2) = 1$, $a_i(x, 3) = 1$, $a_i(y, 1) = 1$, $a_i(y, 3) = 1$, $a_i(z, 1) = 1$, $a_i(z, 2) = 1\{$Assign user i to $Z_{xyz}\}$
end if

Algorithm .3 User Position Aware

Set $a_i(p,q) = 0$, $\forall i, p, q$
for $i = 1$ **to** K **do**
  if $(l_i(p) \leq D)$ **and** $(210 \leq A_i(p) \leq 330)$ **then**
    $a_i(p,1) = 1$, for $p \in \{2,3\}$
  else if $((l_i(p) \leq D)$ **and** $(0 \leq A_i(p) \leq 90))$ **or** $((l_i(p) \leq D)$ **and** $(330 \leq A_i(p) \leq 360))$ **then**
    $a_i(p,2) = 1$, for $p \in \{4,5\}$
  else if $(l_i(p) \leq D)$ **and** $(90 \leq A_i(p) \leq 210)$ **then**
    $a_i(p,3) = 1$, for $p \in \{6,7\}$
  else if $(0 \leq A_i(1) < 60)$ **then**
    Upward triangle$(1,4,5,i)$
  else if $(60 \leq A_i(1) < 120)$ **then**
    Downward triangle$(1,5,6,i)$
  else if $(120 \leq A_i(1) < 180)$ **then**
    Upward triangle$(7,1,6,i)$
  else if $(180 \leq A_i(1) < 240)$ **then**
    Downward triangle$(2,1,7,i)$
  else if $(240 \leq A_i(1) < 300)$ **then**
    Upward triangle$(2,3,1,i)$
  else if $(300 \leq A_i(1) < 360)$ **then**
    Downward triangle$(3,4,1,i)$
  end if
end for
return $\forall a_i(p,q)$

Appendix C: Proof of Lemma 5.1

Proof. Let r be the radius of each small cell. One can easily verify that the overlapping area between every 2 cells, i.e., s in Fig. 5.1, are equal and can be calculated as $s = (\frac{\pi}{3} - \frac{\sqrt{3}}{2})r^2$. The number of small cells of the N-Tier system, i.e., m, is given as:

$$m = 1 + 6\sum_{i=1}^{N-1} i = 3N^2 - 3N + 1. \tag{11}$$

Denoting the number of overlapping areas in N-Tier architecture by n and noting that every cell in Tier $N-1$ always has 6 neighbouring cells, we distinguish two cases of N as follows.

Case 1: N is even, i.e., $N = 2k$, where $k \in \{1, 2, 3 \ldots\}$. One can easily verify from Fig. 5.1 the following facts. The central cell, i.e., Tier 1, has 6 overlapping areas. Apart from the Tier 1, each cell at an odd tier has 5 overlapping areas while each cell at an even tier has 1 overlapping area. Therefore, we can write

$$n = 6 + \underbrace{1 \times \sum_{i=1, i:odd}^{2k-1} 6i}_{\text{even tiers}} + \underbrace{5 \times \sum_{i=2, i:even}^{2k-2} 6i}_{\text{odd tiers}}. \tag{12}$$

Using $\sum_{i=1,i:odd}^{2k-1} i = k^2$, $\sum_{i=2,i:even}^{2k-2} i = k(k-1)$ and $k = N/2$, we can rewrite (12) as:

$$n = 6 + 6k^2 + 30k(k-1) = 9N^2 - 15N + 6. \tag{13}$$

Case 2: N is odd, i.e., $N = 2k + 1$, where $k \in \{1, 2, 3 \ldots\}$. In this case, non overlapping area is counted for the central cell, i.e., Tier 1. Each cell at an even tier has 5 overlapping areas while apart from Tier 1, each cell at an odd tier has 1 overlapping area. Therefore, we have

$$n = \underbrace{5 \times \sum_{i=1,i:odd}^{2k-1} 6i}_{\text{even tiers}} + \underbrace{1 \times \sum_{i=2,i:even}^{2k} 6i}_{\text{odd tiers}} = 30k^2 + 6k(k+1) = 36k^2 + 6k. \tag{14}$$

Substituting for $k = (N-1)/2$ into (14) , we also arrive at (13). Using (11), (13) and algebra, the area covered by m cells in N Tiers, i.e., S, is calculated as:

$$S = m\pi r^2 - ns = r^2 \left[\frac{9\sqrt{3}}{2} N^2 + \left(2\pi - \frac{15\sqrt{3}}{2} \right) N + 3\sqrt{3} - \pi \right]. \tag{15}$$

Denoting R as the radius of an equivalent cell having the same covering area S, i.e., $S = \pi R^2$, and using (15), one can show that

$$R = r \left[2.481N^2 - 2.135N + 0.654 \right]^{\frac{1}{2}}. \tag{16}$$

Let us recall a simplified path loss model from [4] as follows:

$$P_r = P_t K \left(\frac{d_0}{d} \right)^{\alpha}, \tag{17}$$

where P_r and P_t are received and transmitted power, respectively; K is a constant factor; d_0 is a reference distance; d is the distance between transmitter and receiver; and α is the path loss exponent. Using (17), the received power at the cell edge of the N-Tier system, i.e., P_r^N, can be written as:

$$P_r^N = P_0 K \left(\frac{d_0}{r} \right)^{\alpha}. \tag{18}$$

Similarly, the received power at the cell edge of the equivalent cell having the same covering area S, i.e., P_r^S, is given as:

$$P_r^S = P_{\text{eq}}^m K \left(\frac{d_0}{R}\right)^{\alpha}. \tag{19}$$

The received power at the cell edge of the N-Tier system should equal to the received power at the cell edge of the equivalent cell, i.e., $P_r^N = P_r^S$. Therefore, using (18) and (19) we attain

$$P_{\text{eq}}^m = P_0 \frac{R^{\alpha}}{r^{\alpha}}. \tag{20}$$

Substituting for R from (16) into (20), one can write

$$P_{\text{eq}}^m = P_0 \left[2.481N^2 - 2.135N + 0.654\right]^{\frac{\alpha}{2}}. \tag{21}$$

Therefore, using (5.1), (11) and (21), we arrive at (5.2). □

Appendix D: Proof of lemma 5.2

Proof. Expanding (5.9), we can write

$$R_{2C}(\lambda) = \lambda log_2 \frac{1+\gamma_1+\gamma_2}{(1+\gamma_1)(1+\gamma_2)} + log_2(1+\gamma_2). \tag{22}$$

One can easily verify from (22) that $R_{2C}(\lambda)$ is a monotonically decreasing function of λ. Since $R_{1C}(\lambda)+R_{2C}(\lambda) = C(\gamma_1+\gamma_2)$, i.e., (5.7), $R_{1C}(\lambda)$ is a monotonically increasing function of λ.

Now, let us consider $F(\lambda) = R_{2C}(\lambda) - R_{1C}(\lambda)$. Substituting for $R_{1C}(\lambda)$ and $R_{2C}(\lambda)$ from (5.8) and (5.9), respectively, one can write

$$F(\lambda) = \lambda log_2 \frac{(1+\gamma_1+\gamma_2)^2}{(1+\gamma_1)^2(1+\gamma_2)^2} + log_2 \frac{(1+\gamma_2)^2}{1+\gamma_1+\gamma_2}. \tag{23}$$

Clearly, $F(\lambda)$ is a monotonically decreasing function of λ. We distinguish the following possible cases.

1. $F(\lambda) > 0$, i.e., $R_{2C}(\lambda) > R_{1C}(\lambda)$ for $\forall\lambda \in [0,1]$: The largest value of $F(\lambda)$ is obtained by setting $\lambda = 0$, i.e., $F(0) = log_2 \frac{1+2\gamma_2+\gamma_2^2}{1+\gamma_1+\gamma_2}$ which is always positive if $\gamma_2 \geq \gamma_1$. Node that $\gamma_2 \geq \gamma_1$ always holds according to (5.5). The lowest value of $F(\lambda)$ occurs at $\lambda = 1$. Hence, by setting $F(1) > 0$, i.e., $F(1) = log_2 \frac{(1+\gamma_1+\gamma_2)}{(1+\gamma_1)^2} > 0$, we conclude $\frac{(1+\gamma_1+\gamma_2)}{(1+\gamma_1)^2} > 1$, which holds if $\gamma_2 > \gamma_1 + \gamma_1^2$.

2. $F(\lambda) = 0$ occurs when $\gamma_1 \leq \gamma_2 < \gamma_1 + \gamma_1^2$. In particular, $F(\lambda) = 0$ at $\lambda = \lambda_0$ and

$R_{1C}(\lambda_0) = R_{2C}(\lambda_0) = \frac{C(\gamma_1+\gamma_2)}{2}$. Furthermore, using (23), we find λ_0 as follows,

$$\begin{aligned}\lambda_0 = & \frac{log_2(1+\gamma_2)-log_2\left(1+\frac{\gamma_1}{1+\gamma 2}\right)}{log_2(1+\gamma_1)(1+\gamma_2)-log_2\left(1+\frac{\gamma_1}{1+\gamma 2}\right)\left(1+\frac{\gamma 2}{1+\gamma_1}\right)} = \frac{log_2(1+\gamma_2)^2-log_2(1+\gamma_1+\gamma_2)}{log_2\left(\frac{(1+\gamma_1)(1+\gamma_2)}{1+\gamma_1+\gamma_2}\right)^2} \\ = & \frac{2log_2(1+\gamma_2)-log_2(1+\gamma_1+\gamma 2)}{2log_2(1+\gamma_1)(1+\gamma_2)-2log_2(1+\gamma_1+\gamma_2)} = \frac{2C(\gamma_2)-C(\gamma_1+\gamma_2)}{2C(\gamma_1)+2C(\gamma_2)-2C(\gamma_1+\gamma_2)}.\end{aligned}$$

Since $R_{2C}(\lambda)$ and $R_{1C}(\lambda)$ are monotonically decreasing and increasing functions of λ, respectively, and intersect each other at $\lambda = \lambda_0$. Moreover, taking into account that $F(\lambda)$ is a monotonically decreasing function of λ, we can conclude the following results:

- $F(\lambda) > 0$, i.e., $R_{2C}(\lambda) > R_{1C}(\lambda)$, for $\lambda < \lambda_0$.
- $F(\lambda) < 0$, i.e., $R_{2C}(\lambda) < R_{1C}(\lambda)$, for $\lambda > \lambda_0$.

□

Appendix E: Proof of theorem 5.1

Proof. Let K denote the time duration of an information block transmitted by a node to the controlling unit. Note that in 5-step protocol, i.e., when controlling unit acts as a source node, an additional block of information with time duration K is broadcast by the controlling unit to three source nodes. Let $M^{\mathrm{s},4}$ and $M^{\mathrm{s},5}$ denote the total number of exchanged bits in 4-step and 5-step protocols, respectively. We can write

$$M^{\mathrm{s},4} = KR_{1C}(\lambda) + KR_{2C}(\lambda) + KR_{3C}(\beta) = K\left(C(\gamma_1+\gamma_2) + R_{3C}\right). \quad (24)$$

$$M^{\mathrm{s},5} = M^{\mathrm{s},4} + KC(\gamma_1) = K\left(C(\gamma_1+\gamma_2) + R_{3C} + C(\gamma_1)\right). \quad (25)$$

In order to calculate the maximum backhaul throughput, in sequel, we will study four cases of the Star model, as described in Section III. We first find λ that minimises the time duration for the controlling unit to broadcast the combined message in step 2. Then, we calculate R_{3C} such that the backhaul throughput is maximised.

1. Case 1 [$R_{1C}(\lambda) > R_{2C}(\lambda)$]: According to *Lemma 1*, this case occurs if $\lambda > \lambda_0$ and $\gamma_1 \leq \gamma_2 < \gamma_1 + \gamma_1^2$. In step 2 of Case 1, the controlling unit broadcasts $KR_{2C}(\lambda)$ bits with rate $C(\gamma_1)$ and $K(R_{1C}(\lambda) - R_{2C}(\lambda))$ bits with a higher rate $C(\gamma_2)$. Let T_{case1} denote the total time duration required by the controlling unit for this broadcast. We can write:

$$T_{\mathrm{case1}} = K\frac{R_{2C}(\lambda)}{C(\gamma_1)} + K\frac{R_{1C}(\lambda) - R_{2C}(\lambda)}{C(\gamma_2)}. \quad (26)$$

Now, define $G(\lambda)$ as follows

$$\begin{aligned} G(\lambda) &= \frac{R_{2C}(\lambda)}{C(\gamma_1)} + \frac{R_{1C}(\lambda) - R_{2C}(\lambda)}{C(\gamma_2)} = \frac{R_{2C}(\lambda)}{C(\gamma_1)} + \frac{C(\gamma_1+\gamma_2) - 2R_{2C}(\lambda)}{C(\gamma_2)} \\ &= \frac{C(\gamma_1)C(\gamma_1+\gamma_2) + R_{2C}(\lambda)(C(\gamma_2) - 2C(\gamma_1))}{C(\gamma_1)C(\gamma_2)}. \end{aligned} \tag{27}$$

Note also that in this case, $1+\gamma_2 < 1+2\gamma_1+\gamma_1^2 = (1+\gamma_1)^2$. Hence, $log_2(1+\gamma_2) < log_2(1+\gamma_1)^2$ and consequently, $C(\gamma_2) < 2C(\gamma_1)$ or $C(\gamma_2) - 2C(\gamma_1) < 0$. Furthermore, since $R_{2C}(\lambda)$ is a monotonically decreasing function of λ, see Appendix A, it can be verified from (27) that $G(\lambda)$ is a monotonically increasing function of λ. Hence, $G(\lambda)$ and consequently T_{case1} are minimised when $\lambda \to \lambda_0$ and $R_{1C}(\lambda \to \lambda_0) \to R_{2C}(\lambda \to \lambda_0) \to \frac{C(\gamma_1+\gamma_2)}{2}$, i.e., see *Lemma 1*. Note that when $\lambda \to \lambda_0$, the imbalance in number of bits received by controlling unit in step 1 of Case 1 is diminished, i.e., $K(R_{1C}(\lambda) - R_{2C}(\lambda)) \to 0$. Hence, from (26), the minimum value of T_{case1}, i.e., $T_{\text{case1,min}}$, is calculated as follows

$$T_{\text{case1,min}} = K\frac{C(\gamma_1+\gamma_2)}{2C(\gamma_1)}. \tag{28}$$

2. Case 2 $[R_{1C}(\lambda) \leq R_{2C}(\lambda)]$: According to *Lemma 1*, this case occurs if $\gamma_2 > \gamma_1+\gamma_1^2$ or if $\lambda \leq \lambda_0$ and $\gamma_1 \leq \gamma_2 < \gamma_1+\gamma_1^2$. In step 2 of Case 2, the controlling unit broadcasts $KR_{2C}(\lambda)$ bits with rate $C(\gamma_1)$. Let T_{case2} be the total time duration required by the controlling unit for this broadcast. We have:

$$T_{\text{case2}} = K\frac{R_{2C}(\lambda)}{C(\gamma_1)}. \tag{29}$$

As proven in Appendix A, $R_{2C}(\lambda)$ is a monotonically decreasing function of λ. Therefore,

- If $\gamma_2 > \gamma_1+\gamma_1^2$, then, T_{case2} is minimum when $\lambda = 1$, i.e., vertex B in Fig.

5.6 with $R_{1C}(1) = C(\gamma_1)$ and $R_{2C}(1) = C(\frac{\gamma_2}{1+\gamma_1})$. Hence, the minimum value of T_{case2}, i.e., $T_{\text{case2,min}}$, is calculated as follows

$$T_{\text{case2,min}} = K\frac{C\left(\frac{\gamma_2}{1+\gamma_1}\right)}{C(\gamma_1)} = K\frac{C(\gamma_1+\gamma_2)-C(\gamma_1)}{C(\gamma_1)}. \tag{30}$$

- If $\lambda \leq \lambda_0$ and $\gamma_1 \leq \gamma_2 < \gamma_1 + \gamma_1^2$, then, T_{case2} is minimum when $\lambda = \lambda_0$, i.e., $R_{2C}(\lambda) = R_{2C}(\lambda_0) = \frac{C(\gamma_1+\gamma_2)}{2}$. Therefore, the minimum value of T_{case2}, i.e., $T_{\text{case2,min}}$, is calculated as follows

$$T_{\text{case2,min}} = K\frac{C(\gamma_1+\gamma_2)}{2C(\gamma_1)}. \tag{31}$$

  Note that with this setting the data rates of the source pairs involved in the underlying MAC phase in step 1 are balanced, i.e., $R_{1C}(\lambda_0) = R_{2C}(\lambda_0)$.

For the simplicity of notations, let denote the total broadcast time in step 2 of Case 1 or Case 2 by $T_{2,\text{min}}$ which equals either $T_{\text{case1,min}}$ or $T_{\text{case2,min}}$, respectively.

3. Case 3 [$R_{2C}(\lambda) \geq R_{3C}$]: In step 4, the controlling unit broadcasts $KR_{2C}(\lambda)$ with rate $C(\gamma_1)$. Let $T_{\text{case3}}^{\text{s},4}$ denote the total time duration required by the controlling unit to exchange information in four steps of Case 3. Noting that the time duration required by step 1 or step 3 is K, we can write

$$T_{\text{case3}}^{\text{s},4} = K + T_{2,\text{min}} + K + K\frac{R_{2C}(\lambda)}{C(\gamma_1)}. \tag{32}$$

Let $R_{\text{case3}}^{\text{s},4}$ define the backhaul throughput of the 4-step protocol in this case. Using (5.6), (24) and (32), we can calculate as follows

$$R_{\text{case3}}^{\text{s},4} = \frac{K\left(C(\gamma_1+\gamma_2)+R_{3C}\right)}{K\left(2+\frac{T_{2,\text{min}}}{K}+\frac{R_{2C}(\lambda)}{C(\gamma_1)}\right)}. \tag{33}$$

For the value of λ that minimises the time duration for broadcasting in step 2, $R_{2C}(\lambda)$ is fixed. One can easily show that $R^{\mathrm{s},4}_{\mathrm{case3}}$ is a monotonically increasing function of R_{3C}. Therefore, $R^{\mathrm{s},4}_{\mathrm{case3}}$ is maximised when $R_{3C} = R_{2C}(\lambda)$, and its maximum value, i.e., $R^{\mathrm{s},4}_{\mathrm{case3,max}}$, is calculated as follows

$$R^{\mathrm{s},4}_{\mathrm{case3,max}} = \frac{C(\gamma_1+\gamma_2)+R_{2C}(\lambda)}{2+\frac{T_{2,\min}}{K}+\frac{R_{2C}(\lambda)}{C(\gamma_1)}}. \tag{34}$$

4. Case 4 [$R_{3C} > R_{2C}(\lambda)$]: In step 4, the controlling unit broadcasts KR_{3C} bits with rate $C(\gamma_1)$. Let $T^{\mathrm{s},4}_{\mathrm{case4}}$ be the total time duration required by the controlling unit to exchange information in four steps of Case 4. We can write

$$T^{\mathrm{s},4}_{\mathrm{case4}} = K + T_{2,\min} + K + K\frac{R_{3C}}{C(\gamma_1)}. \tag{35}$$

Let $R^{\mathrm{s},4}_{\mathrm{case4}}$ denote the backhaul throughput of 4-step protocol in this case. Using (5.6), (24) and (35), we calculate

$$R^{\mathrm{s},4}_{\mathrm{case4}} = \frac{C(\gamma_1)\left[C(\gamma_1+\gamma_2)+R_{3C}\right]}{2C(\gamma_1)+\frac{C(\gamma_1)T_{2,\min}}{K}+R_{3C}}. \tag{36}$$

In the following, we rewrite $R^{\mathrm{s},4}_{\mathrm{case4}}$ in (36) as a function of R_{3C}:

$$R^{\mathrm{s},4}_{\mathrm{case4}} = \frac{AR_{3C}+B}{DR_{3C}+E} \triangleq R(R_{3C}), \tag{37}$$

where

$$A = C(\gamma_1), \tag{38}$$

$$B = C(\gamma_1)C(\gamma_1+\gamma_2), \tag{39}$$

$$D = 1, \tag{40}$$

$$E = 2C(\gamma_1)+\frac{C(\gamma_1)T_{2,\min}}{K}. \tag{41}$$

By direct substitution, one can easily verify that

$$-\frac{E}{D} = -2C(\gamma_1) - \frac{C(\gamma_1)T_{2,\min}}{K} < 0, \quad (42)$$

$$\frac{A}{D} = C(\gamma_1) > 0, \quad (43)$$

$$\frac{dR(R_{3C})}{dR_{3C}} = \frac{AE - BD}{(D\beta + E)^2}, \quad (44)$$

$$AE - BD = 2C^2(\gamma_1) + \frac{C^2(\gamma_1)T_{2,\min}}{K} - C(\gamma_1)C(\gamma_1 + \gamma_2). \quad (45)$$

It is clear that the graph of $R(R_{3C})$ has a vertical asymptote $R_{3C} = -\frac{E}{D} < 0$, i.e., (42), and a horizontal asymptote $R(R_{3C}) = \frac{A}{D} = C(\gamma_1) > 0$, i.e., (43). To see whether $R(R_{3C})$ is a decreasing or an increasing function of R_{3C}, we examine its derivative versus R_{3C}, i.e., (44), and, in particular, the sign of $(AE - BD)$ in (45).

From (28), (30) and (31), $T_{2,\min}$ is either $K\frac{C(\gamma_1+\gamma_2)}{2C(\gamma_1)}$ or $K\frac{C(\gamma_1+\gamma_2)-C(\gamma_1)}{C(\gamma_1)}$. One can easily verify that $(AE - BD) > 0$ for either $T_{2,\min} = K\frac{C(\gamma_1+\gamma_2)}{2C(\gamma_1)}$ or $T_{2,\min} = K\frac{C(\gamma_1+\gamma_2)-C(\gamma_1)}{C(\gamma_1)}$. Therefore, $R(R_{3C})$ is an increasing function of R_{3C}. Consequently, $R^{\mathrm{s},4}_{\mathrm{case4}}$ is maximum when $R_{3C} = C(\gamma_3)$. Let $R^{\mathrm{s},4}_{\mathrm{case4,max}}$ be the maximum value of $R^{\mathrm{s},4}_{\mathrm{case4}}$. Substituting for $R_{3C} = C(\gamma_3)$ into (36), we can write

$$R^{\mathrm{s},4}_{\mathrm{case4,max}} = \frac{C(\gamma_1)\left[C(\gamma_1 + \gamma_2) + C(\gamma_3)\right]}{2C(\gamma_1) + \frac{C(\gamma_1)T_{2,\min}}{K} + C(\gamma_3)}. \quad (46)$$

Based on the values of γ_1 and γ_2, we distinguish two regions to calculate the backhaul throughput as follows:

I. Region 1 $[\gamma_1 \leq \gamma_2 < \gamma_1 + \gamma_1^2]$:

According to (28) and (31), the minimum time duration in step 2 is $T_{2,\min} = K\frac{C(\gamma_1+\gamma_2)}{2C(\gamma_1)}$. This value is attained when $\lambda = \lambda_0$, i.e., $R_{1C}(\lambda_0) = R_{2C}(\lambda_0) = \frac{C(\gamma_1+\gamma_2)}{2}$. We also distinguish two cases of R_{3C} as follows

- Case 3 $[R_{2C}(\lambda) \geq R_{3C}]$: Plugging $T_{2,\min} = K\frac{C(\gamma_1+\gamma_2)}{2C(\gamma_1)}$ and $R_{2C}(\lambda_0) = \frac{C(\gamma_1+\gamma_2)}{2}$ into

(34), we get

$$R^{\mathrm{s},4}_{\mathrm{case3,max}} = \frac{3C(\gamma_1)C(\gamma_1+\gamma_2)}{4C(\gamma_1)+2C(\gamma_1+\gamma_2)}. \tag{47}$$

- Case 4 [$R_{3C} > R_{2C}(\lambda)$]: Plugging $T_{2,\min} = K\frac{C(\gamma_1+\gamma_2)}{2C(\gamma_1)}$ into (46), we get

$$R^{\mathrm{s},4}_{\mathrm{case4,max}} = \frac{2C(\gamma_1)\left[C(\gamma_1+\gamma_2)+C(\gamma_3)\right]}{4C(\gamma_1)+C(\gamma_1+\gamma_2)+2C(\gamma_3)}. \tag{48}$$

By direct substitution from (47) and (48), one can show that

$$R^{\mathrm{s},4}_{\mathrm{case4,max}} - R^{\mathrm{s},4}_{\mathrm{case3,max}} = \frac{C(\gamma_1)\log_2\frac{1+2\gamma_3+\gamma_3^2}{1+\gamma_1+\gamma_2}\log_2\frac{\left(1+2\gamma_1+\gamma_1^2\right)^2}{1+\gamma_1+\gamma_2}}{\left[4C(\gamma_1)+C(\gamma_1+\gamma_2)+2C(\gamma_3)\right]\left[4C(\gamma_1)+2C(\gamma_1+\gamma_2)\right]}. \tag{49}$$

Since $\gamma_1 \leq \gamma_2 \leq \gamma_3$ and $\gamma_2 < \gamma_1+\gamma_1^2$ in region 1, it can be easily verified that $\log_2\frac{1+2\gamma_3+\gamma_3^2}{1+\gamma_1+\gamma_2}\log_2\frac{\left(1+2\gamma_1+\gamma_1^2\right)^2}{1+\gamma_1+\gamma_2} > 0$ and, hence, $R^{\mathrm{s},4}_{\mathrm{case4,max}} > R^{\mathrm{s},4}_{\mathrm{case3,max}}$. Therefore, the maximum backhaul throughput in region 1 of the 4-step protocol, denoted by $R^{\mathrm{s},4}_{1,\max}$, is obtained with $R_{3C} = C(\gamma_3)$ as

$$R^{\mathrm{s},4}_{1,\max} = R^{\mathrm{s},4}_{\mathrm{case4,max}} = \frac{2C(\gamma_1)\left[C(\gamma_1+\gamma_2)+C(\gamma_3)\right]}{4C(\gamma_1)+C(\gamma_1+\gamma_2)+2C(\gamma_3)}. \tag{50}$$

Let $T_1^{\mathrm{s},5}$ denote the total time required by 5-step protocol to exchange information. Using (35), we have

$$T_1^{\mathrm{s},5} = T^{\mathrm{s},4}_{\mathrm{case4}} + K = K\left(3+\frac{T_{2,\min}}{K}+\frac{R_{3C}}{C(\gamma_1)}\right). \tag{51}$$

The addition of K in (51) is due to the time duration of the data block broadcast by the controlling unit (or the 4^{th} source node) to the other three source nodes. Let $R^{\mathrm{s},5}_{1,\max}$ represent the maximum backhaul throughput in region 1 of 5-step protocol. Then,

using (25), (51), $T_{2,\min} = K\frac{C(\gamma_1+\gamma_2)}{2C(\gamma_1)}$, and $R_{3C} = C(\gamma_3)$, we calculate

$$R_{1,\max}^{\mathrm{s},5} = \frac{2C(\gamma_1)\left[C(\gamma_1+\gamma_2)+C(\gamma_3)+C(\gamma_1)\right]}{6C(\gamma_1)+C(\gamma_1+\gamma_2)+2C(\gamma_3)}. \tag{52}$$

II. Region 2 $[\gamma_2 > \gamma_1+\gamma_1^2]$:

According to (30), the minimum time duration in step 2 is $T_{2,\min} = K\frac{C(\gamma_1+\gamma_2)-C(\gamma_1)}{C(\gamma_1)}$. This value is attained when $\lambda = 1$, i.e., vertex B in Fig. 5.6 with $R_{1C}(1) = C(\gamma_1)$ and $R_{2C}(1) = C(\frac{\gamma_2}{1+\gamma_1})$. Similarly, We distinguish two cases of R_{3C} as follows

- Case 3 $[R_{2C}(\lambda) \geq R_{3C}]$: Plugging $T_{2,\min} = K\frac{C(\gamma_1+\gamma_2)-C(\gamma_1)}{C(\gamma_1)}$ and $R_{2C}(1) = C(\frac{\gamma_2}{1+\gamma_1}) = C(\gamma_1+\gamma_2) - C(\gamma_1)$ into (34), we get

$$R_{\mathrm{case3,max}}^{\mathrm{s},4} = \frac{C(\gamma_1)\left[2C(\gamma_1+\gamma_2)-C(\gamma_1)\right]}{2C(\gamma_1+\gamma_2)}. \tag{53}$$

- Case 4 $[R_{3C} > R_{2C}(\lambda)]$: Plugging $T_{2,\min} = K\frac{C(\gamma_1+\gamma_2)-C(\gamma_1)}{C(\gamma_1)}$ into (46), we get

$$R_{\mathrm{case4,max}}^{\mathrm{s},4} = \frac{C(\gamma_1)\left[C(\gamma_1+\gamma_2)+C(\gamma_3)\right]}{C(\gamma_1)+C(\gamma_1+\gamma_2)+C(\gamma_3)}. \tag{54}$$

By direct substitution from (53) and (54), one can show that

$$R_{\mathrm{case4,max}}^{\mathrm{s},4} - R_{\mathrm{case3,max}}^{\mathrm{s},4} = \frac{C^2(\gamma_1)\log_2\frac{1+\gamma_1+\gamma_3+\gamma_1\gamma_3}{1+\gamma_1+\gamma_2}}{2C(\gamma_1+\gamma_2)\left[C(\gamma_1)+C(\gamma_1+\gamma_2)+C(\gamma_3)\right]}. \tag{55}$$

Since $\gamma_1 \leq \gamma_2 \leq \gamma_3$, it can be easily verified that $\log_2\frac{1+\gamma_1+\gamma_3+\gamma_1\gamma_3}{1+\gamma_1+\gamma_2} > 0$ and, hence, $R_{\mathrm{case4,max}}^{\mathrm{s},4} > R_{\mathrm{case3,max}}^{\mathrm{s},4}$. Therefore, the maximum backhaul throughput in region 1 of the 4-step protocol, denoted by $R_{2,\max}^{\mathrm{s},4}$, is obtained with $R_{3C} = C(\gamma_3)$ as

$$R_{2,\max}^{\mathrm{s},4} = R_{\mathrm{case4,max}}^{\mathrm{s},4} = \frac{C(\gamma_1)\left[C(\gamma_1+\gamma_2)+C(\gamma_3)\right]}{C(\gamma_1)+C(\gamma_1+\gamma_2)+C(\gamma_3)}. \tag{56}$$

Let $R_{2,\max}^{\mathrm{s},5}$ represent the maximum backhaul throughput in region 2 of 5-step pro-

tocol. Using (25), (51), $R_{3C} = C(\gamma_3)$ and $T_{2,\min} = K\frac{C(\gamma_1+\gamma_2)-C(\gamma_1)}{C(\gamma_1)}$, we can write

$$R_{2,\max}^{\mathrm{s},5} = \frac{C(\gamma_1)\left[C(\gamma_1+\gamma_2)+C(\gamma_3)+C(\gamma_1)\right]}{2C(\gamma_1)+C(\gamma_1+\gamma_2)+C(\gamma_3)}. \tag{57}$$

As an intuitive result, we conclude that the resulting time sharing factors try to reduce the imbalance of the received bits by the controlling unit in the MAC phase in order to maximise the backhaul throughput. □

Appendix F: Proof of theorem 5.2

Proof. Because of the similarity between the Star and Ring model, proof for the Ring model is briefly sketched here.

The total number of exchanged information bits, i.e., M^{r}, during the 3 steps of the Ring model can be written as

$$M^{\mathrm{r}} = KR_{13}(\lambda) + KR_{23}(\lambda) + KC(\gamma_1) = K\left(C(\gamma_1+\gamma_2) + C(\gamma_1)\right), \tag{58}$$

where K is the duration on an information block in a source node.

Depending upon the value of γ_2, we distinguish two regions as follows:

I. Region 1 $[\gamma_1 \leq \gamma_2 < \gamma_1 + \gamma_1^2]$:

Similar to the proof of Theorem 5.1, i.e., Case 1 and Case 2, one can show that the total time duration to exchange information bits, i.e., T_1^{r}, is given by

$$T_1^{\mathrm{r}} = K + K\frac{R_{13}(\lambda)}{C(\gamma_1)} + K, \quad \text{if} \quad \lambda \leq \lambda_0 \tag{59}$$

$$T_1^{\mathrm{r}} = K + K\frac{R_{13}(\lambda)}{C(\gamma_1)} + K\frac{R_{23}(\lambda) - R_{13}(\lambda)}{C(\gamma_2)} + K, \quad \text{if} \quad \lambda > \lambda_0. \tag{60}$$

Let $T_{1,\min}^{\mathrm{r}}$ be the minimum time duration required to exchange information in region 1. It is clear from (59) and (60), that $T_{1,\min}^{\mathrm{r}}$ is achieved when $\lambda = \lambda_0$, i.e., $R_{13}(\lambda_0) = R_{23}(\lambda_0) = \frac{C(\gamma_1+\gamma_2)}{2}$, and is given by

$$T_{1,\min}^{\mathrm{r}} = K\frac{4C(\gamma_1) + C(\gamma_1+\gamma_2)}{2C(\gamma_1)}. \tag{61}$$

Therefore, the maximum backhaul throughput of the Ring protocol in region 1, denoted by $R^{\mathrm{r}}_{1,\max}$, can be calculated using (58) and (61) as follows

$$R^{\mathrm{r}}_{1,\max} = \frac{M^{\mathrm{r}}}{T^{\mathrm{r}}_{1,\min}} = \frac{2C(\gamma_1)[C(\gamma_1) + C(\gamma_1 + \gamma_2)]}{4C(\gamma_1) + C(\gamma_1 + \gamma_2)}. \tag{62}$$

II. Region 2 $[\gamma_2 > \gamma_1 + \gamma_1^2]$:

Let T^{r}_2 be the total time duration required by the Ring protocol to exchange information in region 2. We can write

$$T^{\mathrm{r}}_2 = K + K\frac{R_{13}(\lambda)}{C(\gamma_1)} + K. \tag{63}$$

Following the same steps of the proof of Theorem 5.1, Case 2, one can verify that T^{r}_2 is minimum when the MAC phase involving S_1 and S_2 is allowed to operate at time sharing factor $\lambda = 1$ with $R_{23}(1) = C(\gamma_1)$ and $R_{13}(1) = C(\frac{\gamma_2}{1+\gamma_1})$. Hence, from (63), the minimum value of T^{r}_2, i.e., $T^{\mathrm{r}}_{2,\min}$, is calculated as

$$T^{\mathrm{r}}_{2,\min} = K\frac{C(\gamma_1 + \gamma_2) + C(\gamma_1)}{C(\gamma_1)}. \tag{64}$$

Finally, the maximum backhaul throughput in region 2, i.e., $R^{r}_{2,max}$, is calculated using (58) and (64) as

$$R^{\mathrm{r}}_{2,\max} = \frac{M^{\mathrm{r}}}{T^{\mathrm{r}}_{2,\min}} = C(\gamma_1). \tag{65}$$

As an intuitive result, we also conclude that the resulting time sharing factors try to reduce the imbalance of the received bits by the controlling unit to maximise the backhaul throughput. □

Appendix G: Proof that $\mathbf{k}(\mathbf{p})$ in (6.14) is standard

Proof. The function $\mathbf{k}(\mathbf{p})$ is standard because it satisfies the following criteria for all $\mathbf{p} \succeq 0$:

- *Positivity*: Since $\mathbf{R}_{i(q)}(k) \succeq 0$ and $\mathbf{G}_{i(q)}(\mathbf{p})$ is positive definite, $\forall i \in \mathcal{S}_l,\ q, k \in \mathcal{S}_b$, one can easily verify from (6.15) that $\mathbf{k}(\mathbf{p}) \succ 0$, i.e., all elements of vector $\mathbf{k}(\mathbf{p})$ are non-negative, for all $\mathbf{p} \succeq 0$.

- *Monotonicity*: If $\mathbf{p} \succeq \mathbf{p}'$, i.e., element-wise inequality, then, using (6.15), one can easily check that

$$k_{i(q)}(\mathbf{p}) - k_{i(q)}(\mathbf{p}') = \frac{\sum_{j \in \mathcal{S}_l, j \neq i} \left(p_{j(q)} - p'_{j(q)} \right) \hat{\mathbf{w}}_{i(q)}^{\star H} \mathbf{R}_{j(q)}(q) \hat{\mathbf{w}}_{i(q)}^{\star}}{\hat{\mathbf{w}}_{i(q)}^{\star H} \mathbf{R}_{i(q)}(q) \hat{\mathbf{w}}_{i(q)}^{\star}} \geq 0,$$

  for all $i \in \mathcal{S}_l$ and $q \in \mathcal{S}_b$. Therefore $\mathbf{k}(\mathbf{p}) \succeq \mathbf{k}(\mathbf{p}')$.

- *Scalability*: For all $\delta > 1$, $\delta k_{i(q)}(\mathbf{p})$ is calculated as

$$\delta k_{i(q)}(\mathbf{p}) = \frac{\sum_{j \in \mathcal{S}_l, j \neq i} \delta p_{j(q)} \hat{\mathbf{w}}_{i(q)}^{\star H} \mathbf{R}_{j(q)}(q) \hat{\mathbf{w}}_{i(q)}^{\star} + \delta \hat{\mathbf{w}}_{i(q)}^{\star H} \mathbf{C}_{i(q)} \hat{\mathbf{w}}_{i(q)}^{\star}}{\hat{\mathbf{w}}_{i(q)}^{\star H} \mathbf{R}_{i(q)}(q) \hat{\mathbf{w}}_{i(q)}^{\star}}, \tag{66}$$

  where $\mathbf{C}_{i(q)}$ is a positive definite matrix defined in (69). We can write

$$\delta \hat{\mathbf{w}}_{i(q)}^{\star H} \mathbf{C}_{i(q)} \hat{\mathbf{w}}_{i(q)}^{\star} > \hat{\mathbf{w}}_{i(q)}^{\star H} \mathbf{C}_{i(q)} \hat{\mathbf{w}}_{i(q)}^{\star}. \tag{67}$$

Using (66) and (67), one can verify

$$\delta k_{i(q)}(\mathbf{p}) > \frac{\sum_{j\in\mathcal{S}_l, j\neq i} \delta p_{j(q)} \hat{\mathbf{w}}_{i(q)}^{\star H} \mathbf{R}_{j(q)}(q) \hat{\mathbf{w}}_{i(q)}^{\star} + \hat{\mathbf{w}}_{i(q)}^{\star H} \mathbf{C}_{i(q)} \hat{\mathbf{w}}_{i(q)}^{\star}}{\hat{\mathbf{w}}_{i(q)}^{\star H} \mathbf{R}_{i(q)}(q) \hat{\mathbf{w}}_{i(q)}^{\star}},$$

which implies $\delta k_{i(q)}(\mathbf{p}) > k_{i(q)}(\delta\mathbf{p})$, for all $i \in \mathcal{S}_l$ and $q \in \mathcal{S}_b$. Therefore $\delta\mathbf{k}(\mathbf{p}) \succ \mathbf{k}(\delta\mathbf{p})$.

□

Appendix H: Proof for Equation (6.21)

Proof. Using the optimal solutions $p^{\star}_{i(q)}, i \in \mathcal{S}_l$, from (6.20) in $p_{i(q)} = \lambda_{i(q)} \left(\xi_{i(q)} + \sigma^2\right)$, one can calculate the optimal solutions $\lambda^{\star}_{i(q)}, i \in \mathcal{S}_l$, to the Lagrange dual problem (6.7). The gradient of $L(\mathbf{w}_{i(q)}, \lambda_{i(q)})$ in (6.4), i.e., the Lagrangian of the optimization problem (6.3), with respect to $\mathbf{w}_{i(q)}$ vanishes at the optimal points $\lambda^{\star}_{i(q)}$ and $\mathbf{w}^{\star}_{i(q)}$. Hence, after setting $L(\mathbf{w}^{\star}_{i(q)}, \lambda^{\star}_{i(q)}) = 0$, using algebra and the fact that $p^{\star}_{i(q)} = \lambda^{\star}_{i(q)} \left(\xi_{i(q)} + \sigma^2\right)$, we arrive at

$$\left(\mathbf{C}_{i(q)} + \sum_{j \in \mathcal{S}_l} p^{\star}_{j(q)} \mathbf{R}_{j(q)}(q) - p^{\star}_{i(q)} \left(1 + \frac{1}{\gamma_{i(q)}}\right) \mathbf{R}_{i(q)}(q)\right) \mathbf{w}^{\star}_{i(q)} = 0 \tag{68}$$

where

$$\mathbf{C}_{i(q)} = \left(\xi_{i(q)} + \sigma^2\right) \left(\sum_{k \in \mathcal{S}_b, k \neq q} \sum_{t \in \mathcal{S}_l} \mu_{t(k)} \mathbf{R}_{t(k)}(q) + \mathbf{I}\right). \tag{69}$$

Therefore,

$$\frac{\gamma_{i(q)}}{p^{\star}_{i(q)}} \mathbf{w}^{\star}_{i(q)} = \left(\mathbf{C}_{i(q)} + \sum_{j \in \mathcal{S}_l, j \neq i} p^{\star}_{j(q)} \mathbf{R}_{j(q)}(q)\right)^{-1} \mathbf{R}_{i(q)}(q) \mathbf{w}^{\star}_{i(q)}. \tag{70}$$

Since the optimal dual uplink-beamforming vector $\hat{\mathbf{w}}^{\star}_{i(q)}$ is obtained as the dominant

eigenvector of the matrix $\mathbf{G}_{i(q)}^{-1}(\mathbf{p})\,\mathbf{R}_{i(q)}(q)$, one can write

$$\mathbf{G}_{i(q)}^{-1}(\mathbf{p})\,\mathbf{R}_{i(q)}(q)\hat{\mathbf{w}}_{i(q)}^{\star} = \beta_{i(q)}\hat{\mathbf{w}}_{i(q)}^{\star}, \tag{71}$$

where $\beta_{i(q)}$ is the corresponding dominant eigenvalue. Using (6.9) and (69) in (71), we arrive at

$$\left(\mathbf{C}_{i(q)} + \sum_{j\in\mathcal{S}_l, j\neq i} p_{j(q)}^{\star}\mathbf{R}_{j(q)}(q)\right)^{-1}\mathbf{R}_{i(q)}(q)\hat{\mathbf{w}}_{i(q)}^{\star} = \beta_{i(q)}\hat{\mathbf{w}}_{i(q)}^{\star}. \tag{72}$$

From (70) and (72), one can express the i-th optimum downlink beamforming vector in terms of its optimum dual uplink counterpart as

$$\mathbf{w}_{i(q)}^{\star} = \alpha_{i(q)}\hat{\mathbf{w}}_{i(q)}^{\star}, \tag{73}$$

where $\alpha_{i(q)}$ is the dual-uplink/downlink scaling factor associated with the user i in cell q, i.e., $i(q)$. □

References

[1] Huawei Technologies Co., Ltd., "Improving energy efficiency, lower CO_2 emission and TCO," 2011. [Online]. Available: http://www.huawei.com/en/static/hw-076768.pdf

[2] C. Han, T. Harrold, S. Armour, I. Krikidis, S. Videv, P. M. Grant, H. Haas, J. S. Thompson, I. Ku, C.-X. Wang, T. A. Le, M. R. Nakhai, J. Zhang, and L. Hanzo, "Green radio: Radio techniques to enable energy-efficient wireless networks," *IEEE Wireless Communications Magazine*, vol. 49, no. 6, pp. 46–54, Jun. 2011.

[3] F. Rashid-Farrokhi, K. J. R. Liu, and L. Tassiulas, "Joint optimal power control and beamforming in wireless networks using antenna arrays," *IEEE Trans. Commun.*, vol. 46, no. 10, pp. 1313– 1324, Oct. 1998.

[4] A. Goldsmith, *Wireless Communications*. Cambridge University Press, 2005.

[5] M. R. Nakhai and A. K. Yousafzai, "Interference alignment with cyclic unidirectional cooperation in multicell networks," in *Proc. IEEE Global Telecommun. Conf. (GLOBECOM 2012)*, to appear.

[6] V. R. Cadambe and S. A. Jafar, "Interference alignment and degrees of freedom of the k-user interference channel," *IEEE Trans. Information Theory*, vol. 54, no. 8, pp. 3425–3441, Aug. 2008.

[7] R. Mudumbai, D. R. Brown, U. Madhow, and H. V. Poor, "Distributed transmit beamforming: Challenges and recent progress," *IEEE Commun. Magazine*, vol. 47, no. 2, pp. 102– 110, Feb. 2009.

[8] L. Hanzo and T. Keller, *OFDM and MC-CDMA A Primer*. John Wiley & Sons Inc., 2006.

[9] S. Isam and I. Darwazeh, "Robust channel estimation for spectrally efficient FDM system," *19th International Conference on Telecommunications (ICT 2012)*, pp. 1–6, Apr. 2012.

[10] J. Zhang, S. Chen, X. Mu, and L. Hanzo, "Joint channel estimation and multiuser detection for SDMA/OFDM based on dual repeated weighted boosting search," *IEEE Trans. Veh. Technol.*, vol. 60, no. 7, pp. 3265–3275, Sep. 2011.

[11] S. Vigneshwaran, N. Sundararajan, and P. Saratchandran, "Direction of arrival (DoA) estimation under array sensor failures using a minimal resource allocation neural network," *IEEE Trans. Antennas and Propagation*, vol. 55, no. 2, pp. 334–343, Feb. 2007.

[12] M. Jansson, B. Goransson, and B. Ottersten, "A subspace method for direction of arrival estimation of uncorrelated emitter signals," *IEEE Trans. Signal Processing*, vol. 47, no. 4, pp. 945–956, Apr. 1999.

[13] D. Astely, L. Swindlehurst, and B. Ottersten, "Spatial signature estimation for uniform linear arrays with unknown receiver gains and phases," *IEEE Trans. Signal Processing*, vol. 47, no. 8, pp. 2128–2138, Aug. 1999.

[14] T. Trump and B. Ottersten, "Estimation of normal direction of arrival and angular spreed using an array of sensors," *Elsevier Signal Processing*, vol. 50, no. 1-2, pp. 57–69, Apr. 1996.

[15] D. P. Palomar, J. M. Cioffi, and M. A. Lagunas, "Joint Tx-Rx beamforming design for multicarrier MIMO channels: a unified framework for convex optimization," *IEEE Trans. Signal Processing*, vol. 51, no. 9, pp. 2381–2401, Sep. 2003.

[16] M. Schubert and H. Boche, "Solution of the multiuser downlink beamforming problem with individual SINR constraints," *IEEE Trans. Veh. Technol.*, vol. 53, no. 1, pp. 18–28, Jan. 2004.

[17] ——, "Iterative multiuser uplink and downlink beamforming under SINR constraints," *IEEE Trans. Signal Process.*, vol. 53, no. 7, pp. 2324–2334, Jul. 2005.

[18] F. Rashid-Farrokhi, K. J. R. Liu, and L. Tassiulas, "Transmit beamforming and power control for cellular wireless systems," *IEEE JSAC*, vol. 16, no. 8, pp. 1437–1450, Oct. 1998.

[19] D. P. Palomar, J. M. Cioffi, and M. A. Lagunas, "Optimum linear joint transmit-receive processing for MIMO channels with QoS constraints," *IEEE Trans. Signal Processing*, vol. 52, no. 5, pp. 1179–1197, May 2004.

[20] E. Visotsky and U. Madhow, "Optimum beamforming using transmit antenna arrays," in *Proc. IEEE Veh. Technol. Conf.*, May 1999, pp. 851–856.

[21] A. Tolli, H. Pennanen, and P. Komulainen, "Decentralized minimum power multi-cell beamforming with limited backhaul signaling," *IEEE Trans. Wireless Comm.*, vol. 10, no. 2, pp. 570–580, Feb. 2011.

[22] A. Wiesel, Y. C. Eldar, and S. Shamai, "Linear precoding via Conic optimization for fixed MIMO receivers," *IEEE Trans. Signal Process.*, vol. 54, no. 1, pp. 161–176, Jan. 2006.

[23] O. Simeone, O. Somekh, H. Poor, and S. Shamai, "Local base station cooperation via finite-capacity links for the uplink of linear cellular networks," *IEEE Trans. Inform. Theory*, vol. 55, no. 1, pp. 190–204, Jan. 2009.

[24] O. Somekh, B. M. Zaidel, and S. Shamai, "Sum rate characterization of joint multiple cell-site processing," *IEEE Trans. Inform. Theory*, vol. 53, no. 12, pp. 4473–4497, Dec. 2007.

[25] S. Jing, D. N. Tse, J. B. Soriaga, J. Hou, J. E. Smee, and R. Padovani, "Downlink macro-diversity in cellular networks," *IEEE International Symposium on Information Theory*, pp. 1–5, Jun. 2007.

[26] B. L. Ng, J. S. Evans, S. V. Hanly, and D. Aktas, "Distributed downlink beamforming with cooperative base stations," *IEEE Trans. Inform. Theory*, vol. 54, no. 12, pp. 5491–5499, Dec. 2008.

[27] D. Gesbert, S. Hanly, H. Huang, S. Shamai, O. Simeone, and W. Yu, "Multi-cell MIMO cooperative networks: A new look at interference," *IEEE JSAC*, vol. 28, no. 9, pp. 1–29, Dec. 2010.

[28] W. Liu, S. X. Ng, and L. Hanzo, "Multicell cooperation based SVD assisted multi-user MIMO transmission," in *Proc. IEEE 69th Veh. Technol. Conf. (VTC Spring 2009)*, Apr. 2009, pp. 1–5.

[29] E. Bjornson, R. Zakhour, D. Gesbert, and B. Ottersten, "Cooperative multicell precoding: Rate region characterization and distributed strategies with instantaneous and statistical CSI," *IEEE Trans. Signal Processing*, vol. 58, no. 8, pp. 4298–4310, Aug. 2010.

[30] L. Venturino, N. Prasad, and X. Wang, "Coordinated linear beamforming in downlink multi-cell wireless networks," *IEEE Trans. Wireless Commun.*, vol. 9, no. 4, pp. 1451–1461, Apr. 2010.

[31] T. A. Le and M. R. Nakhai, "User position aware multicell beamforming for a distributed antenna system," in *Proc. IEEE 22nd International Symposium on PIMRC*, Sep. 2011, pp. 1398–1342.

[32] H. Dahrouj and W. Yu, "Coordinated beamforming for the multicell multi-antenna wireless system," *IEEE Trans. Wireless Commun.*, vol. 9, no. 5, pp. 1748–1759, May 2010.

[33] T. A. Le and M. R. Nakhai, "An iterative algorithm for downlink multi-cell beam-forming," in *Proc. IEEE Global Telecommun. Conf. (GLOBECOM 2011)*, Dec. 2011, pp. 1–6.

[34] T. A. Le, S. Nasseri, A. Zarrebin-Esfahani, A. Mills, and M. R. Nakhai, "Power-efficient downlink transmission in multicell networks with limited wireless backhaul," *IEEE Wireless Communications Magazine, Special Issue on Technologies for Green Radio Communication Networks*, vol. 18, no. 5, pp. 82–88, Oct. 2011.

[35] M. R. Nakhai, T. A. Le, A. M. Akhtar, and O. Holland, "Chapter: Cooperative multicell processing techniques for energy-efficient cellular wireless networks," in *E. Hossain, V. K. Bhargava and G. P. Fettweis, Green Radio Communication Networks*, Cambridge University Press, 2012.

[36] D. Gerlach and A. Paulraj, "Base station transmitting antenna arrays for multipath environments," *Signal Processing*, vol. 54, no. 1, pp. 59–73, Oct. 1996.

[37] T. A. Le and M. R. Nakhai, "Coordinated beamforming using semidefinite programming," in *Proc. IEEE Int. Conf. Commun. (ICC 2012)*, Jun. 2012, pp. 1–5.

[38] ——, "Possible power-saving gains by dividing a cell into tiers of smaller cells," *IET Electronics Letters*, vol. 46, no. 16, pp. 1163–1165, Aug. 2010.

[39] ——, "Throughput analysis of network coding enabled wireless backhauls," *IET Communications*, vol. 5, no. 10, pp. 1318–1327, Jul. 2011.

[40] ——, "A decentralized downlink beamforming algorithm for multicell processing," in *Proc. IEEE Global Telecommun. Conf. (GLOBECOM 2012)*, to appear.

[41] ——, "Intercell interference balancing in multicell processing networks," *IEEE Trans. Commun.*, under review.

[42] S. Boyd and L. Vandenberghe, *Convex Optimization*. Cambridge University Press, 2004.

[43] H. Hindi, "A tutorial on convex optimization," in *Proc. American Control Conf.*, vol. 4, Jul. 2004, pp. 3252–3265.

[44] Z.-Q. Luo and W. Yu, "An introduction to convex optimization for communications and signal processing," *IEEE JSAC*, vol. 24, no. 8, pp. 1426–1438, Aug. 2006.

[45] L. Vandenberghe and S. Boyd, "Semidefinite programming," *SIAM Review*, vol. 38, no. 1, pp. 49–95, Mar. 1996.

[46] J. F. Sturm, *Using SeDuMi 1.02, a MATLAB toolbox for optimization over symmetric cones*. Optimization Methods and Software, 1999, software availabe at http://sedumi.mcmaster.ca/.

[47] M. Grant and S. Boyd, *cvx Users' Guide for cvx version 1.2 (build 711)*, 2009, software availabe at http://www.stanford.edu/~boyd/cvx/download.html.

[48] F. Gross, *Smart Antennas for Wireless Communications*. McGraw-Hill, 2005.

[49] A. Paulraj, R. Nabar, and D. Gore, *Introduction to Space-Time Wireless Communications*. Cambridge University Press, 2006.

[50] J. D. Kraus and R. Marhefka, *Antennas for All Applications*. McGraw-Hill, 2002.

[51] C. A. Balanis, *Antenna Theory: Analysis and Design*. John Wiley & Sons, 2005.

[52] Z.-Q. Luo, W.-K. Ma, A. M.-C. So, Y. Ye, and S. Zhang, "Semidefinite relaxation of quadratic optimization problems," *IEEE Signal Process. Mag.*, vol. 27, no. 3, pp. 20–34, May 2010.

[53] A. B. Gershman, N. D. Sidiropoulos, Shahhazpanahi, M. Bengtsson, and B. Ottersten, "Convex optimization-based beamforming," *IEEE Signal Process. Mag.*, vol. 27, no. 3, pp. 62–75, May 2010.

[54] H. Dahrouj and W. Yu, "Multicell interference mitigation with joint beamforming and common message decoding," *IEEE Trans. Commun.*, vol. 59, no. 8, pp. 2264–2273, Aug. 2011.

[55] E. Karipidis, N. D. Sidiropoulos, and Z.-Q. Luo, "Quality of service and Max-Min fair transmit beamforming to multiple cochannel multicast groups," *IEEE Trans. Signal Processing*, vol. 56, no. 3, pp. 1268–1279, Mar. 2010.

[56] M. Bengtsson and B. Ottersten, "Optimal downlink beamforming using Semidefinite optimization," in *Proc. 37th Annu. Allerton Conf. Commun., Control, and Computing*, 1999, pp. 987 – 996.

[57] W. Yu and T. Lan, "Transmitter optimization for the multi-antenna downlink with per-antenna power constraints," *IEEE Trans. Signal Process.*, vol. 55, no. 6, pp. 2646–2660, Jun. 2007.

[58] J. Zhang, R. Chen, J. G. Andrews, A. Ghosh, and R. W. H. Jr., "Network MIMO with cluster linear precoding," *IEEE Trans. Wireless Commun.*, vol. 8, no. 4, pp. 1910–1921, Apr. 2009.

[59] A. K. Yousafzai and M. R. Nakhai, "Block QR decomposition and near-optimal ordering in intercell cooperative MIMO-OFDM," *IET Communications*, vol. 4, no. 12, pp. 1452–1462, Aug. 2010.

[60] X. Xu, R. Zhang, S. Ghafoor, and L. Hanzo, "Imperfect digital-fiber-optic-link-based cooperative distributed antennas with fractional frequency reuse in multicell multiuser networks," *IEEE Trans. Veh. Technol.*, vol. 60, no. 9, pp. 4439–4449, Nov. 2011.

[61] R. Zhang, K. Giridhar, and L. Hanzo, "Distributed downlink multi-cell processing required reduced-rate back-haul data exchange," in *Proc. IEEE Wireless Communications and Networking Conference*, Mar. 2011, pp. 1277 –1281.

[62] R. Zhang and L. Hanzo, "Cooperative downlink multicell processing relying on reduced-rate back-haul data exchange," *IEEE Trans. Veh. Technol.*, vol. 60, no. 2, pp. 539–545, Feb. 2011.

[63] J. Zhang, R. Zhang, G. Li, and L. Hanzo, "Remote coalition network elements for base station cooperation aided multicell processing," *IEEE Trans. Veh. Technol.*, vol. 61, no. 3, pp. 1406–1415, Mar. 2012.

[64] F. Boccardi and H. Huang, "Limited downlink network coordination in cellular networks," *IEEE 18th International Symposium on PIMRC*, Sep. 2007.

[65] S. Venkatesan, "Coordinating base stations for greater uplink spectral efficiency in a cellular network," *IEEE 18th International Symposium on PIMRC*, Sep. 2007.

[66] P. Marsch and G. Fettweis, "A framework for optimizing the downlink performance of distributed antenna systems under a constrained backhaul," *European Wireless Conference*, Apr. 2007.

[67] ——, "On multi-cell cooperative transmission in backhaul-constrained cellular systems," *Springer Annals of Telecommunications*, vol. 63, no. 5-6, pp. 253–269, May 2008.

[68] A. Papadogiannis, E. Hardouin, and D. Gesbert, "Decentralising multicell cooperative processing: A novel robust framework," *EURASIP Journal on Wireless Communications and Networking*, vol. 2009, Aug. 2009, article ID 890685, 10 pages.

[69] A. Papadogiannis, H. J. Bang, D. Gesbert, and E. Hardouin, "Efficient selective feedback design for multicell cooperative networks," *IEEE Trans. Veh. Technol.*, vol. 60, no. 1, pp. 196–205, Jan. 2011.

[70] R. Zakhour, Z. K. M. Ho, and D. Gesbert, "Distributed beamforming coordination in multicell MIMO channels," *IEEE Vehicular Technology Conference*, pp. 1–5, Apr. 2009.

[71] H. Dahrouj and W. Yu, "Coordianted beamforming for the multicell multi-antenna wireless system," *IEEE Trans. Wireless Commun.*, vol. 9, no. 5, pp. 1748–1759, May 2010.

[72] M. Sadek, A. Tarighat, and A. H. Sayed, "A leakage-based precoding scheme for downlink multi-user MIMO channels," *IEEE Trans. Wireless Commun.*, vol. 6, no. 5, pp. 1711–1721, May 2007.

[73] I. S. Gradshteyn and I. M. Ryzhik, *Table of Integrals, Series, and Products*. Academic Press, 2007, pp. 365.

[74] R. D. Yates, "A framework for uplink power control in cellular radio systems," *IEEE JSAC*, vol. 13, no. 7, pp. 1341–1348, Sep. 1995.

[75] C. Botella, G. Pinero, A. Gonzalez, and M. D. Diego, "Coordianted in a multi-cell multi-antenna multi-user W-CDMA system: A beamforming approach," *IEEE Trans. Wireless Commun.*, vol. 7, no. 11, pp. 4479–4485, Nov. 2008.

[76] J. Mattingley and S. Boyd, "Real-time convex optimisation in signal processing," *IEEE Signal Processing Magazine*, vol. 27, no. 3, pp. 50–61, May 2010.

[77] Y. Huang and D. P. Palomar, "Rank-constrained separable semidefinite programming with applications to optimal beamforming," *IEEE Trans. Signal Processing*, vol. 58, no. 2, pp. 664– 678, Feb. 2010.

[78] M. Bengtsson and B. Ottersten, *Optimal and Suboptimal Transmit Beamforming*. Chapter 18 in Handbook of Antennas in Wireless Communications ed. Lal Chand Godara: CRC Press, 2001.

[79] D. Castanheira and A. Gameiro, "Distributed antenna system capacity scaling," *IEEE Trans. Wireless Commun.*, vol. 17, no. 3, pp. 68–75, Jun. 2010.

[80] T. Mayer, H. Jenkac, and J. Hagenauer, "Turbo base- station cooperation for intercell interference cancellation," *IEEE International Conference Communications*, vol. 11, pp. 4977–4982, Jun. 2006.

[81] W. Choi and J. G. Andrews, "Downlink performance and capacity of distributed antenna systems in a multicell environment," *IEEE Trans. Wireless Commun.*, vol. 6, no. 1, pp. 69–73, Jan. 2007.

[82] O. Somekh, O. Simeone, A. Sanderovich, B. Zaidel, and S. Shamai, "On the impact of limited-capacity backhaul and inter-users links in cooperative multicell networks," *42nd IEEE Conference on Information Sciences and Systems*, pp. 776–780, Mar. 2008.

[83] H. Hu, Y. Zhang, and J. Luo, *Distributed Antenna Systems: Open Architecture for Future Wireless Communications*. Auerbach Publications, CRC Press, 2007.

[84] T. Wang, Y. Wang, K. Sun, and Z. Chen, "On the performance of downlink transmission for distributed antenna systems with multi-antenna arrays," *IEEE Vehicular Technology Conference*, pp. 1–5, Sep. 2009.

[85] R. Ahlswede, N. Cai, S.-Y. R. Li, and R. W. Yeung, "Network information flow," *IEEE Trans. Inform. Theory*, vol. 46, no. 4, pp. 1204–1216, Jul. 2000.

[86] S.-Y. R. Li, R. W. Yeung, and N. Cai, "Linear network coding," *IEEE Trans. Inform. Theory*, vol. 49, no. 2, pp. 371–381, Feb. 2003.

[87] S. Zhang, S.-C. Liew, and P. P.Lam, "Physical-layer network coding," *ACM MobiCom '06*, Sep. 2006.

[88] P. Popovski and H. Yomo, "Physical network coding in two-way wireless relay channels," *IEEE International Conference on Communications*, pp. 707–712, Jun. 2007.

[89] W. Nam, S.-Y. Chung, and Y. H. Lee, "Capacity bounds for two-way relay channels," *IEEE International Zurich Seminar on Communications*, pp. 144–147, Mar. 2008.

[90] A. S. Avestimehr, A. Sezgin, and D. N. Tse, "Approximate capacity of the two-way relay channel: A deterministic approach," *Arxiv preprint arXiv:0808.3145, 2008 - arxiv.org*, Aug. 2008.

[91] I.-J. Baik and S.-Y. Chung, "Network coding for two-way relay channels using lattices," *IEEE International Conference on Communications*, pp. 3898–3902, May 2008.

[92] S. J. Kim, P. Mitran, C. John, R. Ghanadan, and V. Tarokh, "Coded bi-directional relaying in combat scenarios," *IEEE Military Communications Conference*, pp. 1–7, Oct. 2007.

[93] I. Hammerstrom, M. Kuhn, C. Esli, J. Zhao, A. Wittneben, and G. Bauch, "Mimo two-way relaying with transmit csi at the relay," *IEEE Workshop on Signal Processing Advances in Wireless Communications*, pp. 1–5, Jun. 2007.

[94] P. Larsson, N. Johansson, and K.-E. Sunell, "Coded bi-directional relaying," *IEEE Vehicular Technology Conference*, vol. 2, pp. 851–855, 2006.

[95] T. M. Cover and J. A. Thomas, *Elements of Information Theory*. John Wiley & Sons Inc., 2006.

[96] E. A. Jorswieck, E. G. Larsson, and D. Danev, "Complete charaterization of Pareto boundary for the MISO interference channel," *IEEE Trans. Signal Processing*, vol. 56, no. 10, pp. 5292–5296, Oct. 2008.

[97] J. Lindblom, E. Karipidis, and E. G. Larsson, "Selfishness and altruism on the MISO interference channel: The case of partial transmitter CSI," *IEEE Commun. Letters*, vol. 13, no. 9, pp. 667–669, Sep. 2009.

[98] Z. K. M. Ho and D. Gesbert, "Balancing egoism and altruism on interference channel: The MIMO case," in *Proc. IEEE Int. Conf. Commun. (ICC 2010)*, May 2010, pp. 1–5.

[99] R. Zhang and S. Cui, "Cooperative interference management with MISO beamforming," *IEEE Trans. Signal Processing*, vol. 58, no. 10, pp. 5450–5458, Oct. 2010.

[100] E. Bjornson, R. Zakhour, D. Gesbert, and B. Ottersten, "Cooperative multicell precoding: Rate region characterization and distributed strategies with instantaneous and statistical CSI," *IEEE Trans. Signal Processing*, vol. 58, no. 8, pp. 4298–4310, Aug. 2010.

[101] E. Bjornson, G. Zheng, D. Gesbert, and B. Ottersten, "Robust monotonic optimization framework for multicell MISO systems," *IEEE Trans. Signal Processing*, vol. 60, no. 5, pp. 2508–2523, May 2012.

[102] J. Brehmer and W. Utschick, "Optimal interference management in multi-antenna, multi-cell systems," in *Proc. Zurich Seminar on Communications (IZS)*, Mar. 2010, pp. 134–137.

[103] T. Ren and R. J. La, "downlink beamforming algorithms with intercell interference in cellular networks," *IEEE Trans. Wireless Comm.*, vol. 5, no. 10, pp. 2814–2823, Oct. 2006.

[104] A. Attar, M. R. Nakhai, and A. H. Aghvami, "Cognitive radio game for secondary spectrum access problem," *IEEE Trans. Wireless Commun.*, vol. 8, no. 4, pp. 2121–2131, Apr. 2009.

[105] R. Cottle, J. S. Pang, and R. Stone, *The Linear Complimentarity Problem.* Society for Industrial and Applied Mathematics, 1992.

[106] A. Berman and R. Plemmons, *Nonnegative Matrices in Mathematical Sciences, 2nd ed.* SIAM Classics in Applied Mathematics, 1994.